PREPARATION AND CHARACTERIZATION OF BIOADSORBENT BEADS FOR REMOVING SELECTED HEAVY METAL IONS FROM WASTEWATER

A Dissertation

presented to

the Faculty of the Graduate School

at the University of Missouri-Columbia

In Partial Fulfillment

of the Requirements for the Degree

Doctor of Philosophy

---

by

Suhaib S. Salih

Dr. Tushar T. Ghosh, Dissertation Supervisor

July 2018

The undersigned, appointed by the dean of the Graduate School, have examined the dissertation entitled

PREPARATION AND CHARACTERIZATION OF BIOADSORBENT BEADS FOR REMOVING SELECTED HEAVY METAL IONS FROM WASTEWATER

presented by Suhaib S. Salih, a candidate for the degree of doctor of philosophy, of Chemical Engineering, and hereby certify that, in their opinion, it is worthy of acceptance.

Professor Tushar T. Ghosh

Professor David G. Retzloff

Professor Bret Ulery

Professor Sudarshan K. Loyalka

To my amazing and wonderful Dad, Shwish.

ACKNOWLEDGEMENTS

First and foremost, I would like to express my sincere gratitude to my advisor Dr. Tushar T. Ghosh for his heartfelt guidance, continuous motivation, distinctive perspective and endless supports during the research of my Ph.D. study. His encouragement and enthusiasm helped me in all the time of research. I could not have imagined having a better advisor and mentor for my Ph.D. study.

I am grateful as well to the rest of my outstanding committee members for their valuable input: Dr. David G. Retzloff, Dr. Bret Ulery, and Dr. Sudarsan K. Loyalka. for their insightful comments, guidance, and generosity.

I express my special thanks to the Chemical Engineering, and Nuclear Science and Engineering Institute at the University of Missouri-Columbia, the USA for financial support of the experimental studies and in the general help with other analyses.

I would also like to extend my thanks to the Higher Committee for Education Development (HCED) in Iraq for their financial support.

Last but not the least, I am very grateful to my father, Shwish Salih-God bless him, my mother, Allia Jasam, my brothers Mohammed and Saleh, and all my sisters for their support, encouragement, and love throughout the years.

This dissertation is dedicated to my big love….Iraq.

Suhaib S. Salih

TABLE OF CONTENTS

LIST OF FIGURES

LIST OF TABLES

ABSTRACT

Rapid industrialization is one of the major threats to water pollution worldwide, as discharge effluents contain large amounts of toxic metal ions. Heavy metals are highly toxic to the ecosystem and human even at very low concentrations. We focused on easily available, green and eco-friendly with low operational cost materials to remove heavy metals from industrial wastewater. Chitosan is considered an alternative and sustainable adsorbent due to its highly efficient adsorption capacities for heavy metals. In this particular study, chitosan was successfully modified by using diatomaceous earth and then fabricated as spherical beads using the drop-wise method. Pristine chitosan (CS) beads and chitosan coated diatomaceous earth (CSDE) beads were used to remove zinc, chromium, lead, and nickel ions from aqueous solutions in batch and continuous adsorption processes. The prepared adsorbents were characterized by using scanning electron microscopy (SEM), Brunauer−Emmett−Teller (BET), Fourier-transform infrared spectroscopy (FTIR), energy dispersive X-ray spectroscopy (EDS), X-ray diffraction (XRD), and zeta potential. The results showed that the prepared adsorbents were porous in nature and the total surface area were increased from 1.9 m^2/g for pristine chitosan to 14.4 m^2/g for chitosan coated diatomaceous earth.

The performance of prepared adsorbents was investigated at different temperatures, initial pH of the solution, contact times, initial metal concentrations. The pseudo-second-order kinetic model is more likely to predict the kinetic behavior of the metal ions adsorption process for the whole used contact time range, and the adsorption isotherm data of CS and CSDE beads were well fitted to Langmuir model.

The maximal adsorption capacities of prepared CSDE beads were found to be pH dependent as follows:

- Zinc ion – 127.4 mg/g at initial Zn(II) concentration 500 mg/L and pH 6.
- Chromium ion – 84.23 mg/g at initial Cr(VI) concentration 1000 mg/L and pH 3.
- Lead ion – 175.22 mg/g at initial Pb(II) concentration 400 mg/L and pH 7.
- Nickel ion – 149.64 mg/g at initial Ni(II) concentration 400 mg/L and pH 6.

Successful desorption and regeneration of prepared adsorbents were achieved (with common chemicals) and possessed excellent reusability (up to 10 cycles without a significant loss in adsorption capacity). The common anions and cations coexisting ions have insignificant impact on the removal capacity of prepared adsorbents.

Overall, these results suggest that the environmentally friendly materials might be recognized as effective adsorbent and sustainable means for the separation of heavy metals from wastewater streams. That will lead to a new solution to water pollution required in the modern industrial society.

CHAPTER 1. INTRODUCTION

1.1. Significance/Motivation

Heavy metal pollution has increasingly drawn much attention from all over the world, due to its strong diffusibility, high toxicity, nonbiodegradability, and bioaccumulation in ecosystem. The main source of heavy metal ions contamination is from different industrial activities, such as mining operations, metal plating, petroleum refinery, electric device manufacturing, and so on [1,2]. According to U.S. Environmental Protection Agency, the chromium, zinc, nickel, and lead appear in the list of the priority toxic heavy metals. Industrial wastewater typically contains high concentrations of heavy metals such as chromium ranging from 0.5 to 270 mg/L [3], zinc has been recorded over 620 mg/L in drainage from abandoned copper mines [4], the lead concentrations in different industrial wastewaters are up to 100 - 150 mg/L [5], and the Ni(II) concentration in wastewater from mine drainage and metal finishing has been reported up to 130 mg/L [6]. Accumulation of heavy metals in an aquatic organism, and further transferred to the human body through food chains, causing various physical diseases or disorders even at very low concentrations. According to U.S. Environmental Protection Agency (EPA), the maximum contaminant level (MCL) of chromium, zinc, lead, and nickel ions in drinking water has been set at a low level of 0.005, 5, 0.015, and 0.1 mg/L, respectively [7]. Therefore, efficient removal of heavy metal ions from wastewater streams is important in the protection of environmental quality and public health.

Numbers of technologies (physical or chemical) have been used to remove heavy metals over the years such as chemical precipitation, solvent extraction, filtration, ion exchange, evaporation, reverse osmosis, electrolysis, and adsorption. However, these

methods are either too costly or inefficient in removing trace levels of heavy metal ions from aqueous solutions. The more ordinarily used of these methods is ion exchange, chemical precipitation, solvent extraction, and adsorption [8]. Adsorption is an effective and economical separation process that can be employed for heavy metal ion removal from wastewater steams by using various traditional adsorbents such as activated carbon, zeolite, silica, and alumina. However, recently adsorbents of biological origin like seaweed, alginate, and chitosan have been more attracted for heavy metals removal. Among these adsorbents, chitosan has been received a great attention over the last few decades due to its excellent adsorption behavior of uptake various toxic heavy metals and its unique properties such as friendly environment, low cost, easy to reuse, and effective in trace and medium level removal of heavy metal ions from industrial wastewater [9,10].

Chitosan is partially soluble in dilute mineral and organic acids, such as nitric acid, hydrochloric acid, phosphoric acid, acetic acid, and formic acid. Pristine chitosan tends to agglomerate and forms a gel in acidic solutions. Also, chitosan has crystallized form, low surface area, inadequate mechanical strength, and low thermal stability. Therefore, most of its active hydroxyl and amino groups become inaccessible for metal binding [11]. To improve and enlarge the mechanical strength and thermal stability of chitosan beads, and increasing the total surface area of adsorption. In this work, chitosan is physically spread/coated on natural substances, diatomaceous earth.

1.2 Objectives and scopes of the study

As mentioned early, chitosan in its natural form is soft and has a tendency to agglomerate or form gels and has relatively poor mechanical properties. Often binding

sites of this polymer in its natural form are not readily available for adsorption. Therefore, it is necessary to provide a physical support to increase the accessibility of the metal binding sites for adsorption process applications.

The primary objective of this particular research is the development of a sustainable bio-adsorbent, a novel chitosan coated on natural and inert substances, diatomaceous earth, which is non-hazardous amorphous natural material formed from the remains of diatoms, and then formed into spherical beads by using drop-wise method to increase its surface area and enhance its mechanical properties. That leads to affordably implemented and maintained achievement of high simultaneous removal efficiency of contaminated heavy metal from aqueous waste streams.

The novel prepared chitosan-diatomaceous earth beads were evaluated for chromium, zinc, lead, and nickel removal from aqueous solution by obtaining equilibrium adsorption data at various temperatures, initial metal concentrations, contact times, and solutions-pH. The regeneration of prepared adsorbents was carried out using various solutions including acidic and alkaline solutions.

The specific scopes of the study included:

(1) Develop chitosan based bio-adsorbents for removal of heavy metal ions.

(2) Characterize the prepared adsorbents by scanning electron microscopy (SEM), Brunauer-Emmett-Teller (BET), energy dispersive spectroscopic (EDS), zeta potential analyzer, X-ray microanalyses, Fourier transform infrared spectroscopy (FTIR), thermogravimetric analyzer (TGA), X-ray diffraction (XRD). Characterization of the liquid phase (filtrate) was carried out using inductively coupled plasma mass spectrometry (ICP-MS).

(3) Evaluate the prepared adsorbent performance for removing selected heavy metal ions such as Cr(VI), Zn(II), Pb(II), and Ni(II) at different solutions-pH,

different initial concentrations, different temperatures, and different contact times.

(4) Evaluate the performance of prepared adsorbents in the presence of various foreign ions.

(5) Study the regeneration characteristics under batch and dynamic conditions by using ethylene di-amine tetra acetic acid (EDTA), NaOH, and HCl.

(6) Study the adsorption isotherms: to describe how adsorbates interact with adsorbents and determine the maximal adsorption capacities of prepared adsorbents. Moreover, adsorption isotherms are useful in demonstrating the extent of homogeneity of the adsorption sites and the affinity of these sites towards the adsorbed cations.

(7) Study the adsorption kinetics : to establish the time course of metals uptake on the adsorbents.

(8) Calculate the thermodynamic parameters, enthalpy (ΔH^o) , Gibbs free energy (ΔG^o), entropy (ΔS^o), and isosteric heat of adsorption (ΔH_x), for the adsorption process. They can help in testing whether or not the electrostatic binding forces are involved in adsorption process.

(9) Study of breakthrough characteristic of target metal ions under dynamic conditions.

1.3. Background

Among toxic substances, heavy metals pollution is one of the most dangerous pollution in the environment because they are stable and tend to persist and accumulate in the environment, and have extremely effect on human health. The major causes of water pollution include sewage, wastewater, industrial waste, marine dumping, radioactive waste, oil pollution, and atmospheric deposition. Heavy metals

are define as metals with a specific weight (density) usually more than 5 g/cm^3, which is five times than water. Most heavy metals are transition elements because they have incompletely filled the outer orbitals, these orbitals provide heavy metal cations in solution with the ability to form complex components which may or may not be redox active. Heavy metals play an important role as trace element in sophisticated biochemical reaction. The toxic metals, probably existing in high concentrations, must be effectively treated or removed from the wastewaters. When wastewaters were discharged directly into natural waters, they will constitute a significant risk for the aqueous ecosystem, whereas the direct discharge into the sewerage system may affect negatively on the next biological wastewater treatment. The proper management of global environment is increasingly becoming an important issue. In view of effective environmental protection, heavy metals are particularly of priority because of their important industrial roles and wide presence in various water or wastewater, and also their accumulation through food chain, which sustains toxic or restrained effect on living things [12, 13].

1.3.1 Heavy metals

Heavy metals are metallic elements and naturally occurring elements that have a high atomic weight between 63.5 and 200.6, and a specific gravity greater than 5.0 [14]. Heavy metals wastewaters are directly or indirectly discharged into the environment increasingly, especially in developing countries. They accumulate in soils, plants, and animals due to their affinity for binding to solids and organisms. The presence of heavy metal ions in water causes adverse effects on ecosystems and results in human health issues such as cancer and other chronic diseases [15]

1.3.1.1. Chromium (Cr)

In nature, chromium has several different oxidation states, namely trivalent chromium, Cr(III) and hexavalent chromium, Cr(VI). Chromium (III) is much less toxic than chromium (VI). The Cr(III) is an essential trace element for humans to remove glucose and protein metabolism from the bloodstream, whereas the Cr(VI) is considered to be one of the top priority toxic pollutants due to its mutagenicity and carcinogenicity [16]. Industrial applications of chromium compounds, in either the chromium (III) or chromium (VI) forms, which causes water pollution are mainly from leather tanning, electroplating, metal polishing, paint manufacturing, chromic salts industry, and textile dyeing. Human studies have clearly established that inhaled chromium (VI) is a human carcinogen, resulting in an increased risk of lung cancer. The World Health Organization (WHO) and the USEPA recommended the maximum allowable concentration for total chromium in drinking water to be 0.05 or 0.1 mg/L, and the regulation is becoming even tighter across the board world-wide [17].

1.3.1.2. Zinc (Zn)

Zinc is a lustrous bluish-white metal. It can be extracted mainly from zinc blende and calamine ores. Zinc is called an “essential trace element” so we get it through the foods that we eat. Next, to iron, zinc is the most common mineral in the body and is found in every cell because very small amounts of zinc are necessary for human health. Most zinc is principally used to galvanize other metals, such as iron, to prevent rusting. Galvanized steel by zinc is used for car bodies, street lamp posts, safety barriers and suspension bridges. Large quantities of zinc are used in the automobile, electrical, and hardware industries. Zn(II) is commonly found in wastewater effluents generated from industries involved in acid-mine drainage, galvanizing plants, natural

ores, and municipal wastewater treatment plants [18]. The acceptable limits of zinc in drinking water is 5 mg/L, excess of zinc metal present in the water may lead to vomiting, nausea, skin irritations, disturb the protein metabolism, cause arteriosclerosis, stomach cramps, diarrhea, and even damage to the pancreas [19].

1.3.1.3. Lead (Pb)

Lead is a dull, silvery-grey metal. It is soft and easily worked into sheets and contains two oxidation states, +2 and +4. Lead is used to make batteries, solders, and gasoline octane boosters. However, due to environmental hazards, many countries have stopped lead additive usage in gasoline. Solid and liquid sludge wastes contribute more than half of the Pb contamination into environment, mainly through the landfills, and approximately 20% of total mined lead is lost as wastage in manufacturing processes [20]. It can accumulate in human muscles, bones, kidney, brain and cause damage to some human organs such as blood cells and nerve system. Lead can enter the water system via several pathways, through mining, painting, corrosion of household plumbing, battery industrialized, petroleum industries and so on [21].

1.3.1.4. Nickel (Ni)

Nickel can be found silver and white in several oxidation states ranging from -1 to +4. The most common state is the +2 oxidation state in bio-systems. Due to its properties, nickel is mostly used in the preparation of steel and alloys, catalysts, dyes, fungicides, pigments, in the manufacture of batteries, and used in gas turbines and rocket engines due to its resists corrosion at different high temperatures [22]. Nickel is released into the environment by a large number of processes such as electroplating,

leather tanning, wood preservation, pulp processing, and steel manufacturing, and the concentration levels of nickel in the environment widely varies [23]. Nickel and certain nickel compounds have been listed by the National Toxicology Program (NTP) as being reasonably anticipated to be carcinogens. The International Agency for Research on Cancer (IARC) has listed nickel compounds within group 1 (there is sufficient evidence for carcinogenicity in humans) [7, 24].

1.3.2. Chitosan

Chitosan was first discovered by Touget when boiling chitin in hydroxide solution in 1859. However, the first report of using chitosan in heavy metal adsorption was found in 1973 [25]. Commercially, chitosan is procured by N-deacetylation of chitin using a strong alkali. Chitin is one of the most abundantly available polymers after cellulose in nature, and exists in marine media especially in the exoskeleton of crustaceans, cartilages of mollusks and cuticles of insects. Figure 1-1 represents the chemical structure of chitin and chitosan.

chitin is insoluble in water and most common solvents. It cannot readily be fabricated into useful artifacts such as adsorbents or membranes since it needs to be dissolved into a solution. Despite its abundance in nature and various advantages, the insolubility of chitin in common solvents limit its use [26]. Therefore, chitin is usually converted to its deacetylated derivative, chitosan. Chitosan is a copolymer of glucosamine and N-acetylglucosamine, and it has a high content of amine and hydroxyl functional groups which are strongly reactive with metal ions. Chitosan can be characterized as a promising material not only due to its unique physical properties (macromolecular structure, non-toxicity, high safety, good chemical reactivity, biocompatibility, biodegradability, low-cost), but also its adsorption potential.

Nonetheless, chitosan has some disadvantages (i.e. low acid stability, crystallized form, low surface area, inadequate mechanical strength, and low thermal stability) which restrict its application [27].

The hydrogel beads of pristine chitosan show poor mechanical strength which has limited their application and reuse in water and wastewater remediation. Even though a number of papers have been published in the literature on the performance of metal ion removal with chitosan hydrogel beads, little research has been done on the improvement of the mechanical strength of the chitosan hydrogel beads. In order to reduce the disadvantages of chitosan, progresses have been made to produce chitosan that has a high acid stability by chemical crosslinking and grafting of the surfaces with various agents such as acrylic acid [28], ethylene glycol diglycidyl ether (EGDE), glutaraldehyde (GA), and epichlorohydrine (ECH) [29]. Reducing the crystallinity of pristine chitosan was done by producing chitosan hydrogel beads through a gel formation process because the heavy metal ions could be adsorbed onto the amorphous surface of the crystals. Chitosan has been spread on natural substances such as sand [30], perlite [31], clay [32], and bentonite [33] to improve the mechanical strength and thermal stability of chitosan beads, and increasing the total surface area of adsorption.

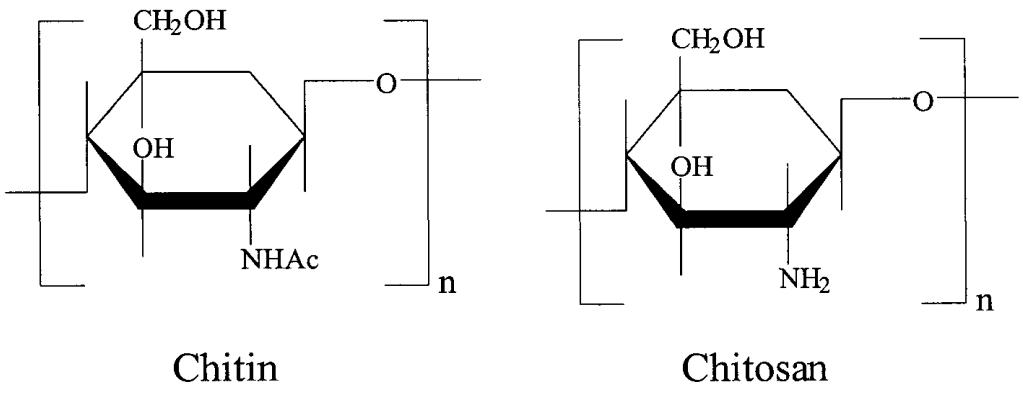

Figure 1-1. Chemical structure of chitin and chitosan

Wan et al. 2010 [34] utilized the chitosan-coated sand for adsorbing copper (II) and lead (II) ions from water, the initial metal concentration was (100, 500, 1000, and 2000 mg/g), pH solution was (2,3,4,5, and 6), the contact time was from 0.5 to 24 h. The results showed that the chitosan-coated sand bioadsorbent has a high efficiency for removing copper and lead ions from water. The amount of adsorbed metal ions was higher with increasing pH for lead ion, but was trivial for copper ion. The maximum adsorption capacity of Cu(II) and Pb(II) ions were 8.18 and 12.32 mg/g, respectively at 4 h contact time. The Langmuir isotherm model represented the best description of the metal adsorption mechanism. The kinetic studies illustrated by the pseudo second-order reaction, which means that the chemical adsorption is the rate-limiting step.

Futalan et al. 2011 [35] investigated the comparative and competitive adsorption of copper, lead, and nickel by using chitosan immobilized on bentonite from aqueous solution at different temperature from 25 to 55 °C and contact time from 0 to 720 minutes, with initial concentration metals of 50–500 mg/L and pH is 4 by using equilibrium adsorption. The total surface area of chitosan coated bentonite is 33.17 m^2/g. The results showed that the adsorption capacity is larger for Pb(II) than Cu(II) and Ni(II) for single and binary systems and the effect of increasing temperature slightly decreases removal percent and adsorption capacity for Pb(II), Cu(II), and Ni(II). Freundlich isotherm fitted the adsorption of copper and lead while the Langmuir isotherm fitted to the adsorption of nickel for single and binary systems. Kinetic studies indicated that the pseudo-second order is the best fit with $R^2 > 0.99$. The maximum adsorption capacities were 27 mg/g for lead, 23 mg/g for copper , and 12 mg/g for nickel.

Paulino et al. 2011 [36] studied the effect of magnetite chitosan-based hydrogel graft-copolymerized with methylenebisacrylamide and acrylic acid on swelling kinetics of hydrogels and adsorption kinetic of lead , copper , and cadmium ions in aqueous solution. The results showed that the best conditions to remove metals were pH between 4.5 and 5.5, initial metal concentration is 300 mg/L, and dried hydrogel mass is 100 mg. Langmuir and Freundlich models of fitted data showed that may be a variation in the physicochemical phenomena associated with metal adsorption. The isotherm models detect that the efficiency of adsorption slightly decreases in the presence of magnetite, the presence of magnetite with chitosan reduces the swelling of adsorbents. Adsorbents recovery was applied by external AC or DC magnetic fields.

Sargın and Arslan, 2015 [37] prepared Chitosan/sporopollenin microcapsules via cross-linking and characterized by employing scanning electron microscopy, Fourier transform infrared spectroscopy and thermo gravimetric analysis for removing Cu(II), Cd(II), Cr(III), Ni(II) and Zn(II) ions at different metal ion concentration(2-12 ppm), pH-solution(3-6), amount of sorbent(0.05-0.25 g), temperature(298-318 K), and sorption time(60-480 min) from aqueous solution. The results showed that the maximum sorption capacity of the chitosan/sporopollenin microcapsules was found to be Cu(II): 1.34, Cd(II): 0.77, Cr(III): 0.99, Ni(II): 0.58, and Zn(II): 0.71 mmol/g and showed higher affinity for the ions; Cu(II): 1.46, Cr(III): 1.16 and Ni(II): 0.81 mmol/g, but lower for Cd(II): 0.15 and Zn(II): 0.25 mmol/g. Adsorption isotherm analysis showed that sorption equilibrium could be well defined by Langmuir adsorption model, indicating homogeneity of the sorption sites on the surface of the microcapsules. However, the adsorption process thermodynamically was feasible and spontaneous.

Min et al. 2015 [38] prepared adsorbent of chitosan based electrospun nanofiber membrane for arsenate ions, As(V), removal from water. Batch adsorption experiments were carried out to estimate the arsenate adsorption performance with different parameters such as pH- solution, initial concentration of arsenate, contact time, presence of coexisting anions, ionic strength, and natural organic matters. The results showed that chitosan based electrospun nanofiber membrane was highly porous with a large surface area. pH- solution played a key role in arsenate adsorption onto chitosan based electrospun nanofiber membrane, and higher uptake capacity was obtained at lower pH. Kinetics study revealed the adsorption equilibrium was achieved within 0.5 h, and the kinetics process was good fitted by the pseudo-second-order model. Langmuir model correlated well with the adsorption isotherm experimental data, and the maximum adsorption capacity was found to be 30.8 mg/g of adsorbents.

Nithya et al. 2016 [39] prepared glutaraldehye cross linked silica gel/chitosan-g-poly(butyl acrylate) (Cs-g-PBA/SG) nano composite by sol–gel method for removal of toxic chromium ion, Cr(VI), from wastewater. The adsorption process was brought under batch mode to suit the optimal parameters such as contact time, pH-solution, adsorbent dose, and initial metal ion concentration. Equilibrium data agreed well with the Langmuir isotherm model (R^2= 0.9763) with maximum adsorption capacity of 55.71 mg/g. The kinetic studies showed that the adsorption follows the pseudo-second-order kinetics (R^2= 0.9999). The study demonstrated that the variation of adsorbent dose, contact time, initial metal ion concentration and pH had a marked influence on the removal of Cr(VI) ions from the aqueous solution. The experimental results showed that the optimum adsorbent dose, contact time and pH were found to be 4 g, 120 min, and pH 7, respectively.

1.3.3 Diatomaceous earth

Diatomaceous earth (DE) is composed of the fossilized shells of tiny marine organisms called diatoms, which grew and deposited in the seas or lakes. The shells are made mainly of silica which is also found in sand and glass. It is a white, light, fine powder, abundant in nature, and non-toxic material, but it is slightly abrasive and highly absorbent. Even though the diatomaceous earth is not harmful to human, breathing the dust of the mineral should be avoided. Commercially, diatomaceous earth is generally produced from natural diatomite by calcination processing at about 900 °C [40,10].

Diatomaceous earth is used as a filter medium and very suitable for water treatment and completion fluids, but also effective in other liquid filtration processes, such as beer, wine, and syrups. Moreover, It is used to remove unwanted material from drinking water. It is also used as a filler or to prevent formation of lumps in foods, medicine, paints and plastics, and pet litter. It is used to clean up spills or for insulation in industry. The typical chemical and physical properties of diatomaceous earth are given in Table 1-1 [13]. Due to its chemical makeup, diatomaceous earth is not degraded by microbes or by sunlight. Also, it does not emit vapors or dissolve well in water.

Table 1-1: Physical and chemical properties of diatomaceous earth

Parameters	Value
Color	white
Structure	porous
Wet density	0.344 g/cm³
Surface	amorphous
pH (10% slurry)	6.4 – 9.7
Porosity	86.23
Permeability	0.1–10 mD
Surface Area (m^2/g)	23.8
Solubility	Soluble in hot and strong alkali (NaOH) and hydrofluoric acid (HF)
Chemical composition	SiO_2 90%, Al_2O_3 4%, Fe_2O_3, 2 % , CaO 1.4%, others 2.6%

1.4. Overview

This dissertation consists of six chapters:

Chapter 1 outlines the motivation, objectives , and background of this study, including the effect of heavy metals on human and ecosystem. Also, presents the structure and properties of chitosan, heavy metals, and diatomaceous earth.

Chapter 2 describes the preparation and characterization of pristine chitosan adsorbent and its application in adsorption of chromium and zinc ions from aqueous solution.

Chapter 3 presents the preparation and characterization of new chitosan coated diatomaceous earth composite. Indicating adsorption behavior and performance of new prepared adsorbents for Zn(II) removal at different conditions such as solution-pH, contact time, temperature, and initial zinc concentrations in batch and continuous adsorption process and study the fixed bed breakthrough behaviors.

Chapter 4 presents the adsorption performance of prepared chitosan coated diatomaceous earth adsorbents on removal of chromium heavy metal from aqueous solution and investigating the chromium adsorption isotherms and kinetics at different temperatures and contact times.

Chapter 5 describes the adsorption behavior of nickel and lead ions onto chitosan/diatomaceous earth composite. Investigating the effect of coexisting ions on adsorption capacity of heavy metals, and study the regeneration and reusability of prepared adsorbents using various agents.

Chapter 6 presents the conclusions drawn from this research and some recommendations for future studies.

CHAPTER 2. PREPARATION AND CHARACTERIZATION OF BIOADSORBENT BEADS FOR CHROMIUM AND ZINC IONS ADSORPTION

2.1 Abstract

Low-cost chitosan beads were prepared by dropping chitosan solution into an alkaline bath and then were used for Cr(VI) and Zn(II) ions adsorption from aqueous solution. Prepared chitosan beads were characterized by Fourier transform infrared spectroscopy (FTIR), thermal gravimetric analysis (TGA), Brunauer-Emmett-Teller (BET) measurements, scanning electron microscopy (SEM), and energy dispersive X-ray spectroscopy (EDS). The effect of solution-pH, contact time, initial ion concentration, and temperature on both metal ions adsorption was investigated. The kinetics of adsorption suggested a pseudo-second-order model fits better than pseudo-first-order model for both metals. The equilibrium adsorption isotherm of both metals matches well with the Langmuir isotherm model. The maximum adsorption capacity of chitosan beads was 79.56 mg Cr(VI)/g and 109.18 mg Zn(II)/g at initial ion concentration 1000 mg/L, and temperature 10 °C. Thermodynamic parameters showed that the adsorption of Cr(VI) and Zn(II) ions onto chitosan beads was feasible, spontaneous, and exothermic under the studied conditions. While the chitosan beads enabled a good adsorption application, further lab work and field studies are necessary before using in a practical adsorption process.

2.2 Introduction

The most important and essential compound on the ground is water for all living creatures. However, rapidly growing population, climate change, and environmental deterioration affect the quality of water supplies. Water contamination caused by heavy metals has been identified as serious environmental issues worldwide, since heavy metals are highly toxic, non-biodegradable, non-metabolizable, and can cause many biological abnormalities and tend to accumulate in the food chains. Heavy metals mainly exist in the wastewaters of many industries such as metal plating, mining operations, electric device manufacturing, and battery production [41]. There are many heavy metal ions including chromium and zinc that appear in the U.S. Environmental Protection Agency's priority list of pollutants due to their high toxicity, prevalence, existence and persistence in the environment [42]. The accumulation of Cr(VI) in human body causes a stomach erosion, hemorrhaging, and death is likely. The main symptoms of Zn(II) poisoning are an electrolyte imbalance, stomachache, dehydration, nausea, dizziness, and incoordination in muscles [43]. Physical, chemical, and biological processes for heavy metals removal from wastewater have been extensively researched and used such as adsorption, reverse osmosis, ion exchange, evaporation, solvent extraction, chemical precipitation, filtration, flotation, membrane, coagulation and flocculation, and electrochemical methods [44]. Adsorption has been considered as the most cost-effective method for heavy metals removal from aqueous solution because the process is simple in design and chemical consumption or/and waste generation are not a significant issue compared with other methods. Traditional adsorbents such as activated carbon are not efficient in a low concentration of pollutants, and therefore it needs additives with a higher surface area to enhance the adsorption capacity. In recent decades,

bioadsorbent materials for biological origin have emerged as an attractive material for removing heavy metals from wastewater streams, largely because these materials are sustainable, abundant in nature, cheap, effective in low and medium metal level, and easy to regenerate for reuse [45]. Many biological materials have shown a good adsorption capacities for heavy metals from aqueous solution such as alginate [46], seaweed [47], husk [48], sugar beet pulp [49], and chitosan [50].

Chitosan is a natural organic material, commercially produced by partial deacetylation of chitin, which is the second plentiful organic component in nature next to cellulose polymer. Due to the presence of amino ($-NH_2$) and hydroxyl (-OH) groups in its structure, chitosan is capable to adsorb heavy metals from aqueous solution by creating an electronic bond between these active sites and metal ions [51, 52]. In addition, chitosan has been investigated by many studies as an excellent material for heavy metal adsorption such as cadmium and copper [28], arsenic [41], and chromium and zinc [53, 54, 55, 56].

In this study, chitosan was prepared in spherical shape instead of using its original form- powder, which has been applied in previous studies, to enhance its total surface area, reduce its agglomeration in acidic media, and to increase the metal ions spreading onto active sites, and then it was used to remove Cr(VI) and Zn(II) ions from aqueous solution. In addition, the performance of prepared chitosan beads was characterized by Fourier transform infrared spectroscopy (FTIR), thermal gravimetric analysis (TGA), Brunauer-Emmett-Teller (BET) measurements, scanning electron microscopy (SEM), and energy dispersive X-ray spectroscopy (EDS). Moreover, the adsorption process was examined as a function of solution-pH, contact time, initial metal ion concentration, and temperature. Eventually, adsorption isotherms, thermodynamic parameters, and the mechanism of adsorption were investigated.

2.3 Materials and methods

2.3.1 Materials

Medium molecular weight chitosan biopolymer (deacetylation degree is 87 %, the molecular weight is ~190,000 - 310,000 g/mol) was procured from Aldrich Chemical Corporation and used to synthesize chitosan beads. Zinc sulfate heptahydrate ($H_{14}O_{11}SZn$) and potassium dichromate ($K_2Cr_2O_7$) were used to prepare a stock solution containing 1000 mg/L of Cr(VI) or Zn(II) ions. Sodium hydroxide, oxalic acid, and deionized water were used to adjust the solution-pH and to dissolve chitosan. All chemicals that were used in this study were analytical grade and used as received without further purification.

2.3.2 Preparation of chitosan beads

Chitosan gel solution was prepared by dissolving 20 g of chitosan into 1 L of 0.2 mol/L oxalic acid solution under continuous stirring. The chitosan solution was heated to 65-70 °C to facilitate acylation. Spherical chitosan beads were prepared by using the drop-wise method - drop wise addition of the chitosan mixture gel solution into a precipitation bath containing 0.8 mol/L NaOH solution. The objective of dropping chitosan gel solution into a basic solution is to rapidly neutralize the drops and get a spherical shape of chitosan beads. The chitosan hydrogel beads remained in the NaOH solution with slowly stirred mixing (60 rpm) for 6 h for hardening. The hardened spherical chitosan beads were washed by deionized water for neutralizing and removing sodium ions that might be attached to the chitosan beads. Eventually, the chitosan beads were dried by vacuum furnace for 24 h at 70 °C. The final dry chitosan beads had an average diameter of 1 mm and they were available for adsorption experimental work as shown in Figure 2-1.

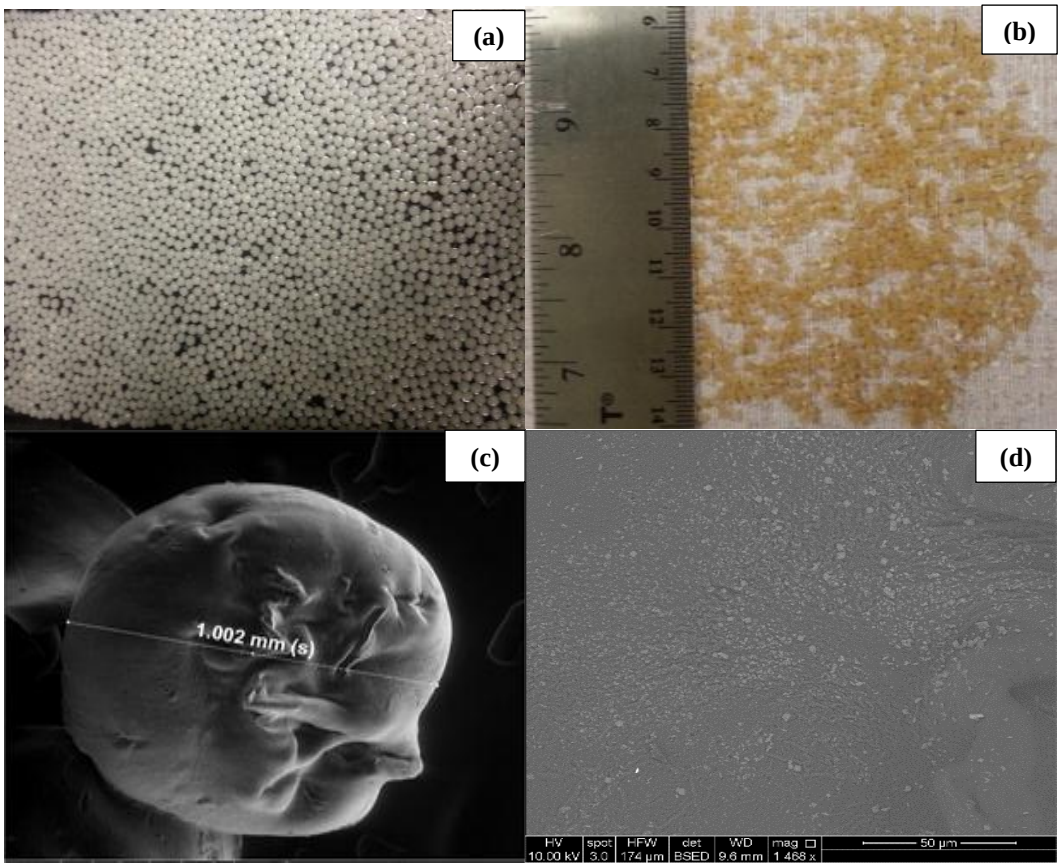

Figure 2-1 (a) wet chitosan beads, (b) dry chitosan beads, (c) single chitosan bead, (d) scanning electron microscopy (SEM) images of fresh chitosan beads (scanning electron microscopy images, 500 µm and 1000 kV image magnification).

2.3.3 Adsorption experiments

Batch adsorption experiments of Cr(VI) and Zn(II) ions adsorption onto chitosan beads from aqueous solution were studied at initial metal concentrations of 50, 100, 250, 500, and 1000 mg/L. In a series of 125 mL Erlenmeyer flasks, 50 mL of Cr(VI) or Zn(II) liquid solution at different concentrations and 0.5 g of chitosan beads were agitated in an orbital shaker at 200 rpm for 8 h. The volume of the liquid solution without chitosan beads was 42.5 mL, measured by burette after 8 h of stirring, and that volume was used to determine the chitosan beads adsorption capacity. After a certain time, samples were taken from the flasks and filtrated to determine the final

metal ion concentrations in the solution samples. Inductively Coupled Plasma-Mass Spectrometer (ICP-MS) was used to determine the metal ion concentration in the samples. When the steady state of adsorption attained, the adsorption capacity of chitosan beads was determined by using Equation (2-1) that generated from the mass balance of metal ions [57]:

$$q_e = \frac{(C_0 - C_e)V}{m} \qquad (2-1)$$

Where q_e is the equilibrium adsorption capacity (mmol/g), C_0 is the initial metal concentration in the solution (mmol/L), and C_e is the equilibrium metal concentration in the solution (mmol/L), V is the volume of solution (L), and m is the mass of chitosan beads (g). Batch adsorption runs were studied at different temperatures, different initial metal ion concentrations, different solutions-pH, and different contact times.

2.4 Results and discussion

2.4.1 Characterization of chitosan beads

Chitosan beads were characterized to estimate some of their physical and chemical properties. They provide a better interpretation of Zn(II) and Cr(VI) adsorption mechanism associated with the adsorption process. Some physical and chemical properties of dried chitosan beads are summarized in Table 2-1. We can see that the BET surface area of chitosan beads was found to be 1.9 m^2/g, which is not too large compared to other adsorbents like activated carbon and silica because chitosan material in its natural form is soft. The solution-pH of chitosan beads at the point of zero charges (pH_{ZPC}) was 6.63, that means the surface of chitosan beads has a positive charge at pH less than 6.63, which is presumably created by the protonation of amine groups in the chitosan. Therefore, the negative species are favorite to adsorb at low

pH and species that have positive charges (heavy metals) are easily adsorbed and interacted on chitosan beads at pH greater than 6.63.

Thermal gravimetric analysis (TGA) (Figure 2-2) was carried out to investigate the thermal stability of chitosan beads. About 1.842 g of chitosan beads was used during the TGA-test. The sample was heated from 22 to 900 °C at a rate of 5 °C/min. Figure 2-2 shows that there are three distinctive steps of weight loss. First, about 5% weight loss occurred at 144 °C due to the loss of water content (dehydration). Second, 24% weight loss occurred at 370 °C which may correspond to the degradation behavior of the chitosan, including dehydration of the saccharide rings and depolymerization of chitosan. Third, about 38% weight loss happened at 686 °C which may correspond to the decomposition (thermal and oxidative) of chitosan. This result is in agreement with Nieto et al. 1991[58] and Neto et al. 2005 [59].

Results of Fourier transform infrared spectroscopy (FTIR) analysis are shown in Figure 2-3. The FTIR spectroscopy technique can be used for chemical characterization of the adsorbents and to probe probable attractions between the metal ions and functional groups on the adsorbent surface. The FTIR spectra method used in this study was diffuse reflectance, considering transmission data for diffuse reflectance. Figure 2-3 presents measured of Kubelka Munk absorption coefficients for chitosan bead, for describing diffuse laser light reflectance that passes through the sample (chitosan beads). It can be seen that the chitosan beads exhibit a large band of the amine group (N-H) stretching between 3200 and 3510 cm^{-1}, and a peak between 1400 and 1655 cm^{-1} corresponds to C=N stretching bond. These observations indicate that the amine groups are present in chitosan beads and successfully bonded with heavy metals, indicating that the metal ions are adsorbed onto chitosan beads [60].

In order to determine the elemental composition of the chitosan beads, energy dispersive X-ray spectroscopy (EDS) analysis was attained. EDS X-ray microanalysis was performed on chitosan beads before and after exposure to the Cr(VI) or Zn(II) solutions. Results are shown in Figure 2-4. EDS analysis clearly shows the presence of C, N, and O. The higher percentage of O along with N enhances the interaction between chitosan beads and heavy metals. Moreover, we can see from the Figure 2-4b, that large peaks occur at 0.5 kV (Kα, Cr) and at 5.2 kV (Kβ, Cr) for Cr(VI) ions representing adsorption to chitosan beads. Similarly, in Figure 2-4c, large peaks can be seen at 1 kV (Kα, Zn) and at 8.7 kv (Kβ, Zn) which are representative for Zn(II) ion adsorption. Results from EDS X-ray show a small peak of sodium ions, which can be assigned to sodium hydroxide that was used during the preparation of the chitosan gel. The mass percentage of each element within/on chitosan beads is explained in the tables located within Figure 2-4. The total weight percentages of fresh beads, beads loaded with Cr(VI), and beads loaded with Zn(II) are 99.22, 99.00 %, and 98.40%, respectively. The remaining percentages can be explained by platinum that was used to coat chitosan beads during the EDS X-ray test to avoid burning or other damage to the chitosan beads.

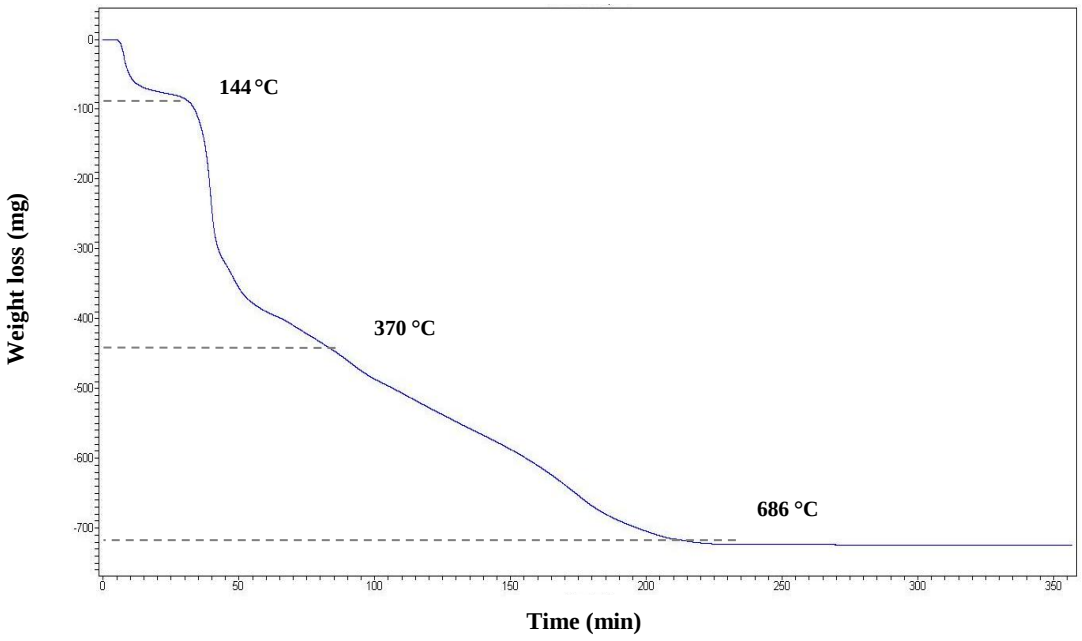

Figure 2-2 Thermal gravimetric analysis (TGA) curve of fresh chitosan beads (weight loss as a function of time).

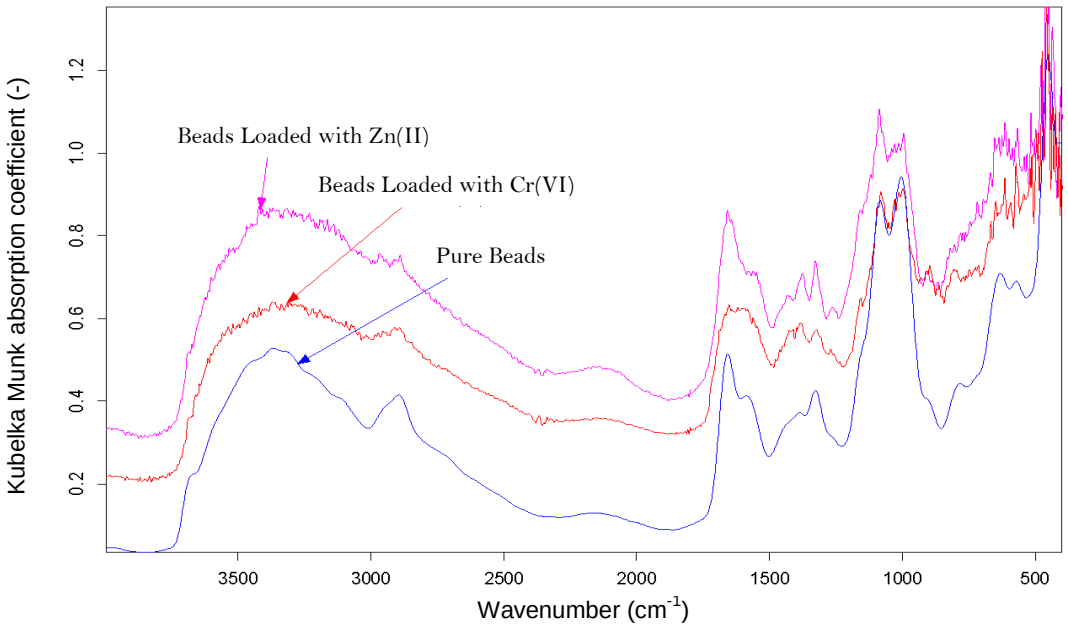

Figure 2-3 Fourier transform infrared spectroscopy (FTIR) of chitosan beads.

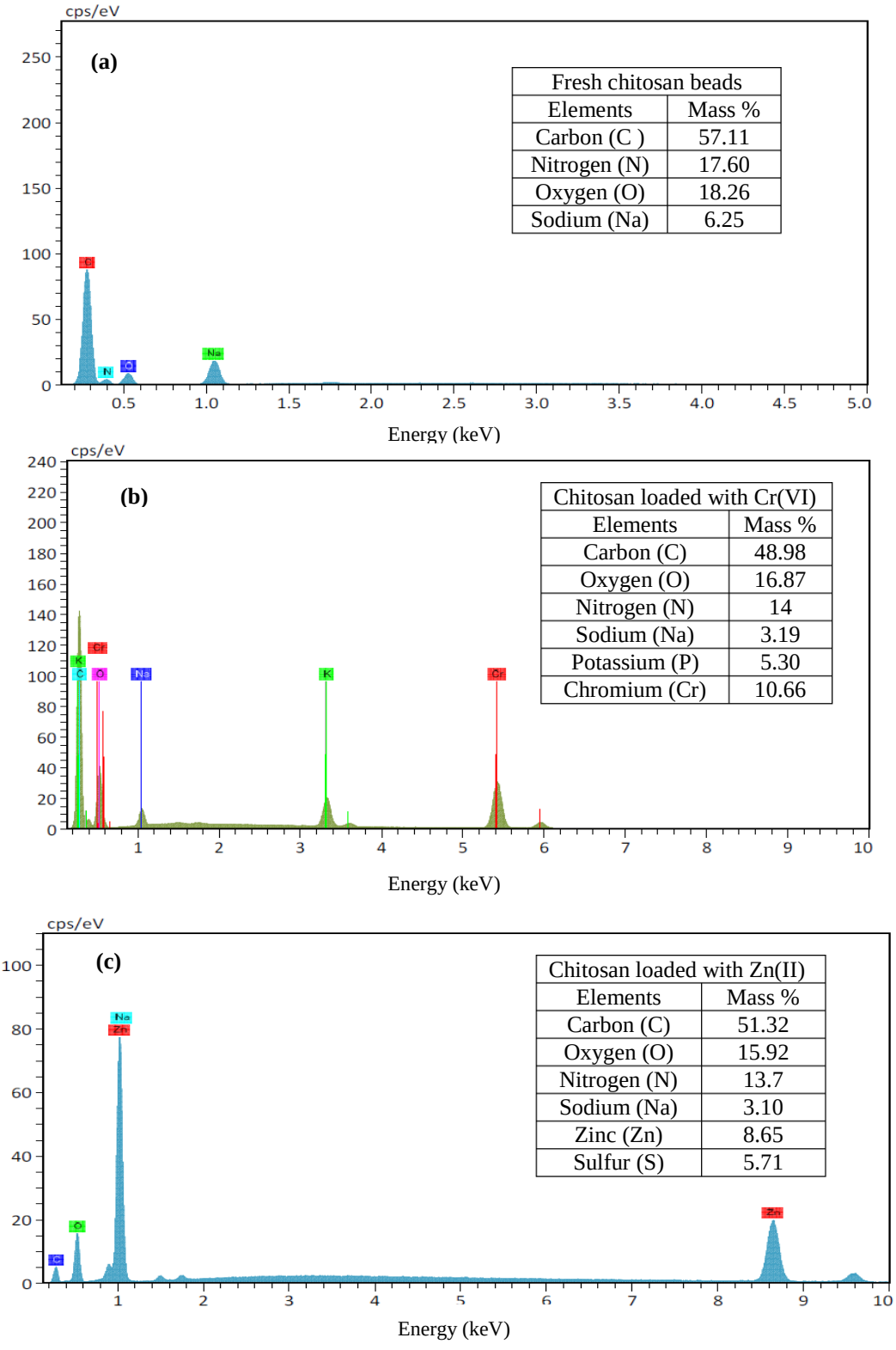

Figure 2-4 Energy Dispersive X- ray Spectroscopy (EDS) of (a) fresh chitosan beads, (b) chitosan beads loaded with Cr(VI), and (c) chitosan beads loaded with Zn(II) (cps/eV: counts per second per electron-volt).

Table 2.1 Physical and chemical properties of prepared chitosan beads.

Parameters	Value
Physical nature	porous
Average particle diameter (mm)	1
Surface area (m^2/g)*	1.9
Pore size (mm)*	3.73×10^{-6}
Pore volume (m^3/g)*	8.2×10^{-9}
pH at the point of zero charge (pH_{ZPC})	6.63
Carbon content (wt%)	57.11
Oxygen content (wt%)	18.26
Nitrogen content (wt%)	17.60
Sodium content (wt%)	6.25

*Determined by Brunauer-Emmett-Teller (BET) measurement.

2.4.2 Effect of initial pH on adsorption

Figure 2-5 shows the effect of solution-pH on the adsorption of Zn(II) and Cr(VI) ions onto chitosan beads. These results show that the Cr(VI) ion adsorption was raised up from 1.2 mmol/g at pH 2 to 1.53 mmol/g at pH 5 and then was raised down to 1.35 mmol/g at pH 8. The maximum rate of Cr(VI) removal from aqueous solution onto chitosan beads was about 1.53 mmol/g (79.56 mg/g) at pH 5. In acidic solution, the Cr(VI) ions are mostly in form of H_2CrO_4 which has a neutral charge and does not adsorb onto chitosan beads. It is assumed that the competition happened between the remaining Cr(VI) ions as CrO_4^{2-} and the positive hydrogen ions (H^+) at low pH, between 2 and 4, which presumably reduced the adsorption capacity of Cr(VI). These results are in a good agreement with Toledo et al. 2014 [49]; Arvand & Pakseresht 2013 [61]; Hu et al. 2011 [62]. In their experiments, in basic solution (pH > 7), the protonation of amine groups was reduced and the concentration of hydroxyl groups (OH^-) increased which creates a negative surface charge on chitosan beads. That leads

to produce a repulsive interaction between CrO_4^{2-} ions and chitosan beads, which decreases the adsorption capacity of Cr(VI) in basic solution [54, 63].

The increase in Zn(II) ions removal with increasing solution-pH from 2 to 6 could be explained by reducing the hydrogen proton (H^+) and positive Zn(II) ions competition at the same active sites on chitosan beads. In acidic media, chitosan beads surface is positively charged due to the protonation of amino groups, which decreases the interaction between active sites in chitosan beads and Zn(II) ions [64]. After solution-pH exceeded 6, it was observed that the zinc hydroxide was formed and precipitated in the solution. The results showed that the Zn(II) adsorption onto chitosan beads from aqueous solution was affected strongly by solution-pH and the maximum adsorption capacity for Zn(II) ion was 1.67 mmol/g (109.18 mg/g) at pH 6. In addition, it was observed that at low solution-pH (pH = 3), swelling and agglomeration of chitosan beads occurred and tended to form a gel.

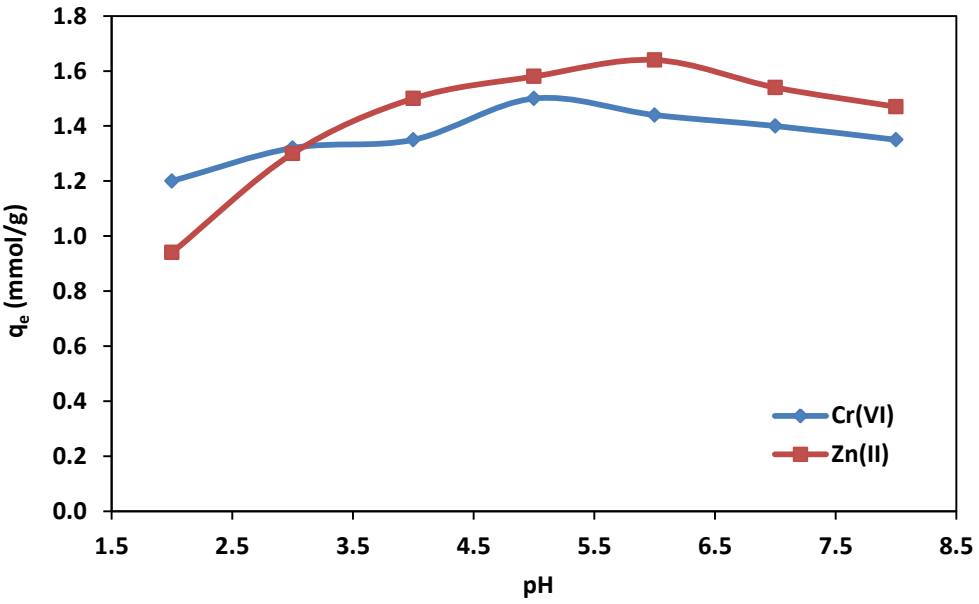

Figure 2-5 Effect of initial solution-pH on Zn(II) and Cr(VI) adsorption onto chitosan beads (initial concentration (C_0) for Zn(II) = 15.3 mmol/L; C_0 for Cr(VI) = 19.23 mmol/L; temperature = 10 °C; mass of chitosan beads = 0.5 g).

2.4.3 Effect of initial ion concentration on adsorption

The effect of initial metal concentration on adsorption capacity of Cr(VI) and Zn(II) ions onto chitosan beads was investigated by considering different ranges of initial Cr(VI) concentrations (0.96, 1.92, 4.8, 9.6, and 19.23 mmol/L) at pH 6 and temperature 10 °C. And for Zn(II) ions, initial concentrations were 0.76, 1.53, 3.8, 7.65, and 15.3 mmol/L at pH 5, temperature 10 °C, and 0.25 - 8 h contact time. Varying the initial metal concentration can affect the driving forces of adsorption and consequently affect the adsorption behavior of metal ions onto chitosan beads. The results are illustrated in Figure 2-6. Cr(VI) ions removal was significantly increased from 0.084 to 1.53 mmol/g when the initial Cr(VI) concentration increased from 0.96 to 19.23 mmol/L. However, increasing the initial Zn(II) concentration from 0.76 to 15.3 mmol/L caused an increase in Zn(II) removal from 0.1 to 1.67 mmol/g onto chitosan beads. That is because, at high initial metal concentration, the concentration gradient between bulk solution and chitosan beads surface overcomes the mass transfer resistance of Zn(II) and Cr(VI) ions. The adsorption of both metals was rapid in the first 1.5 h and then slowed down until it reached the equilibrium in around 3 h in most of the adsorption runs. It is understood that all the adsorption sites are available at the initial stage (fast adsorption), while the adsorption sites are gradually occupied with the adsorption process until all of them are not be free. These results show that the adsorption process of Cr(VI) and Zn(II) ions onto chitosan beads from aqueous solution is fast and affected significantly by initial metal ion concentration.

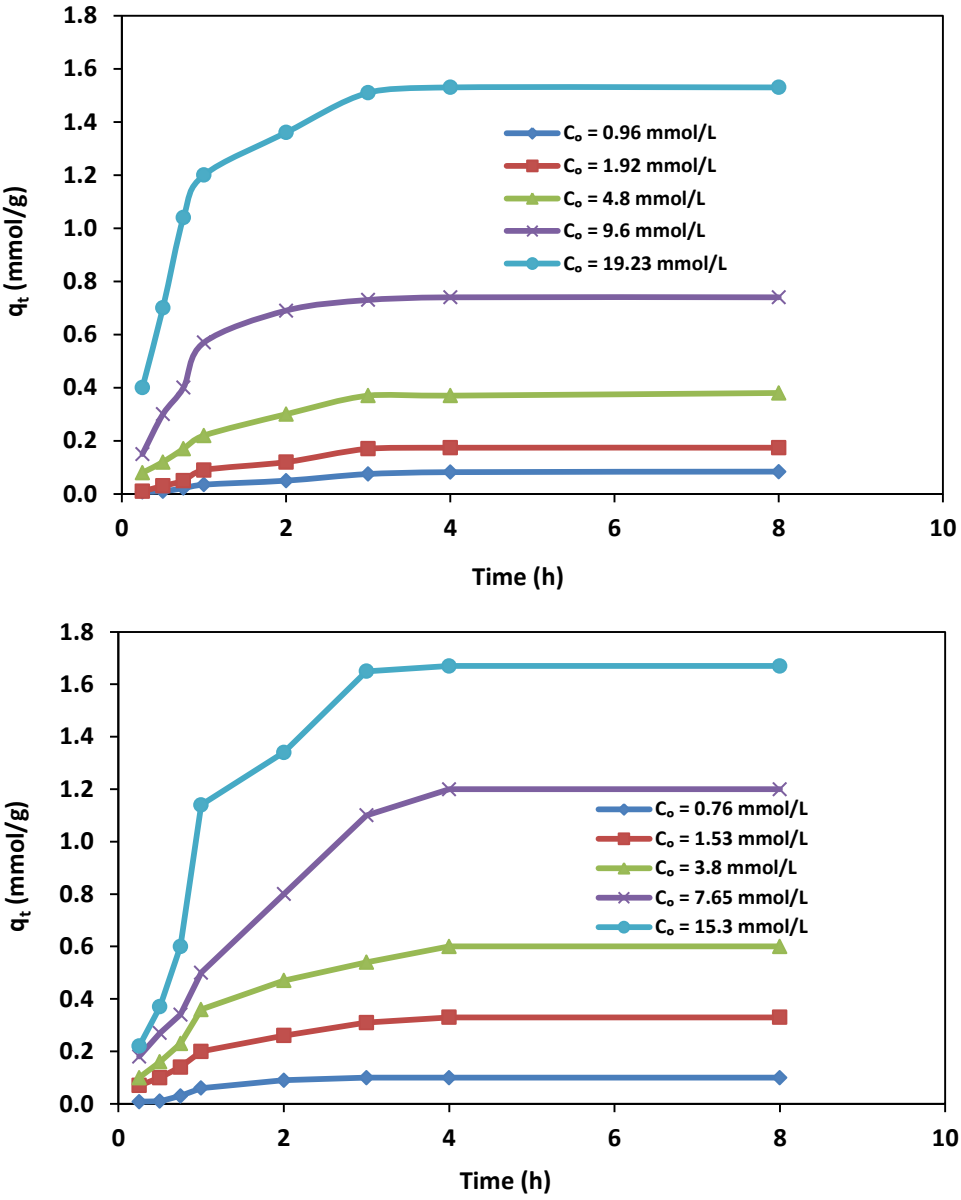

Figure 2-6 Adsorption capacity (q_t) as a function of time for different initial metal concentrations in solution (C_0) for (a) Cr(VI) ions and (b) Zn(II) ions (pH = 5; mass of chitosan beads = 0.5 g; temperature = 10 °C).

2.4.4 Effect of temperature on adsorption

The effect of temperature on the adsorption of Cr(VI) and Zn(II) ions onto chitosan beads was investigated at 10, 20, 30, and 40 °C. As shown in Figure 2-7, the results showed that the low temperatures were favorite for Cr(VI) and Zn(II) ions

adsorption onto chitosan beads. It can be seen that due to a temperature increase from 10 to 40 °C, the Zn(II) adsorption was reduced to 1.34 mmol/g from 1.67 mmol/g, whereas, the Cr(VI) adsorption was decreased from 1.53 at 10 °C to 1.12 mmol/g at 40 °C. The reason for this phenomenon is when the temperature increases, the solubility of metal ions species increases in the solution. Consequently, the Van der Waals interaction forces between the metal ions and solution are stronger than those between metal ions and adsorbent [65]. As a result, the metal ions are more difficult to adsorb at high temperature.

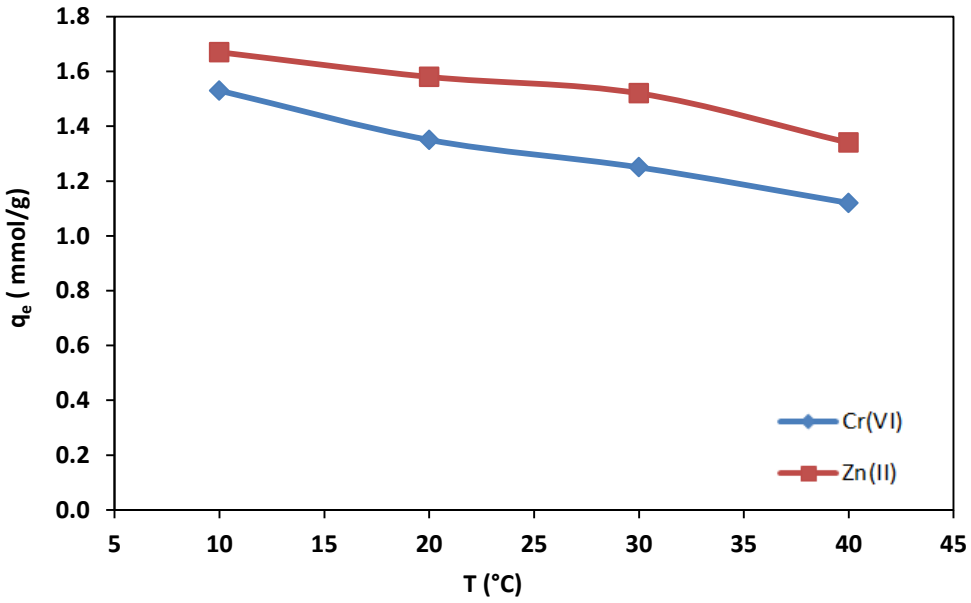

Figure 2-7 Equilibrium adsorption capacity (q_e) as a function of temperature (T) for Cr(VI) and Zn(II) (C_0 for Zn(II) = 15.3 mmol/L; C_0 for Cr(VI) = 19.23 mmol/L; pH = 5 - 6; mass of chitosan beads = 0.5 g).

Thermodynamic parameters including Gibb's free energy (ΔG°), enthalpy (ΔH°), and entropy (ΔS°) were determined for Cr(VI) and Zn(II) adsorption onto chitosan beads by using following equation [66]:

$$\Delta G^{o} = \Delta H^{o} - T\Delta S^{o} \qquad (2-2)$$

Where ΔG^o can be expressed as,

$$\Delta G^o = -RT\ln K_d \qquad (2-3)$$

Substituting Equation (2-2) into (2-3) provides the van't Hoff equation [66, 67],

$$\ln K_d = \frac{\Delta S^o}{R} - \frac{\Delta H^o}{RT} \qquad (2-4)$$

$$K_d = \frac{q_e}{C_e} \qquad (2-5)$$

Where R is the universal gas constant (8.314 J/mol.K), T is the absolute temperature (K), ΔG° is Gibb's free energy (J/mol), and K_d is the equilibrium partition coefficient between solid and liquid solution (L/g), C_e is the equilibrium concentration of metal ions in the solution (mmol/L), q_e is the equilibrium adsorption capacity onto chitosan beads (mmol/g) .

By plotting (ln K_d) against 1/T, the values of ΔH° (J/mol) and ΔS° (J/mol) can be determined (Figure 2-8). The determined ΔH° may be considered as the heat of adsorption when the adsorption capacity of chitosan beads reaches its saturated capacity of Cr(VI) or Zn(II) ions. Obtained values of lnK_d, ΔH°, ΔS°, and ΔG° are listed in Table 2-2. The results of metal ions adsorption onto chitosan beads show that the adsorption process was exothermic and the negative values of ΔG° at the low temperature specified that the adsorption was spontaneous. The thermodynamic parameter values that were obtained in this study are in a good agreement with Aydın et al. 2009 [68] and Hawari et al. 2009 [69].

Isosteric heat of adsorption (ΔH_x) is a useful pertinent thermodynamic factor for characterizing the temperature effect on the adsorption process. It is defined as the heat of adsorption occurring at constant adsorption capacities of metal ions onto adsorbent by using the well-known Clausius-Clapeyron Equation [65],

$$\frac{d(\ln C_e)}{dT} = -\frac{\Delta H_x}{RT^2} \qquad (2-6)$$

Integrating Equation (2-6), assuming that the ΔH_x does not depend on temperature, gives Equation (2-7) [65],

$$\ln C_e = -\left(\frac{\Delta H_x}{R}\right)\frac{1}{T} + K_q \qquad (2-7)$$

Where K_q is the integral constant (mmol/L), C_e is the equilibrium concentration of metal ions in the solution (mmol/L), R is the universal gas constant (8.314 J/mol.K), T is the absolute temperature (K). From the slope of plotting (ln C_e) against 1/T (Figure 2-9 and 2-10), the value of ΔH_x can be determined. Values of ΔH_x were obtained at different temperatures (10, 20, 30, and 40 °C) and at different adsorption capacities of Cr(VI) or Zn(II) ions onto chitosan beads. From Table 2-3, it could be seen that the variation of ΔH_x values with adsorption capacities of Cr(VI) or Zn(II) is indicative that the chitosan beads have energetically homogeneous surfaces. In addition, the variation of ΔH_x values with the adsorption capacities can be attributed to the possibility of the competition between the adsorbed heavy metal ions and other ions in solution such as Na, SO_4, originating from metal salts onto the same active groups (-NH_2, -OH). The results show that the ΔH_x was strongly depended on the adsorption capacities, which decreased with increasing the adsorption capacities. This can be seen as a hint on a rather homogeneous surface of chitosan beads. Otherwise, in case the surface of chitosan beads would be heterogeneous, the ΔH_x of metal ions adsorption onto chitosan beads would be constant even at varying adsorption capacities of metal ions [65, 70]. It can be assumed that the high value of ΔH_x at low adsorption capacities (q_e) refers to high initial interactions between adsorbed metal ions and chitosan beads due to the presence of highly active amine and hydroxyl groups within the chitosan [65].

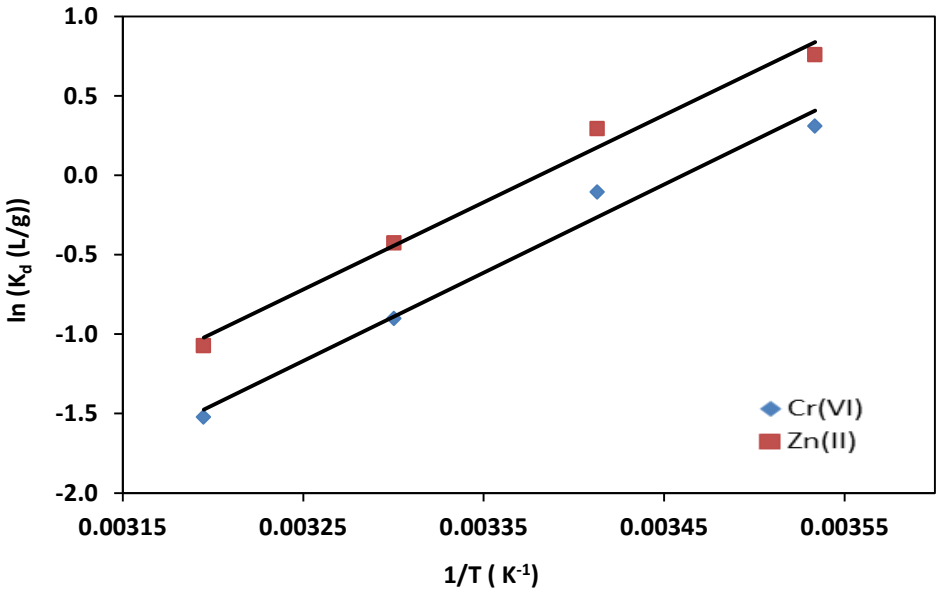

Figure 2-8 ln K_d as a function of 1/T for Cr(VI) and Zn(II). Lines indicate linear fits (C_0 = 1000 mg/L for both metals).

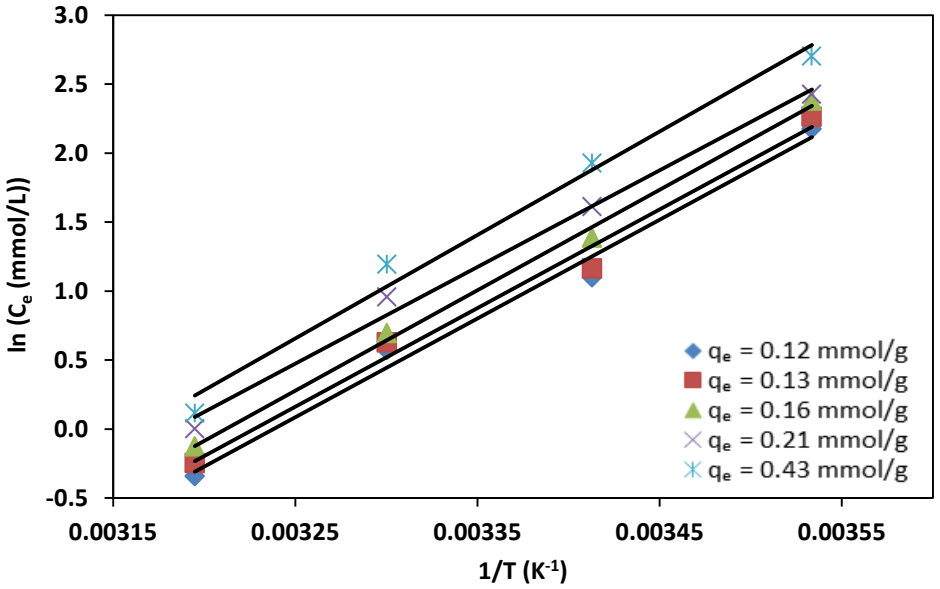

Figure 2-9 ln C_e as a function of 1/T for Cr(VI) adsorption onto chitosan beads at different adsorption capacities (q_e). Lines indicate linear fits.

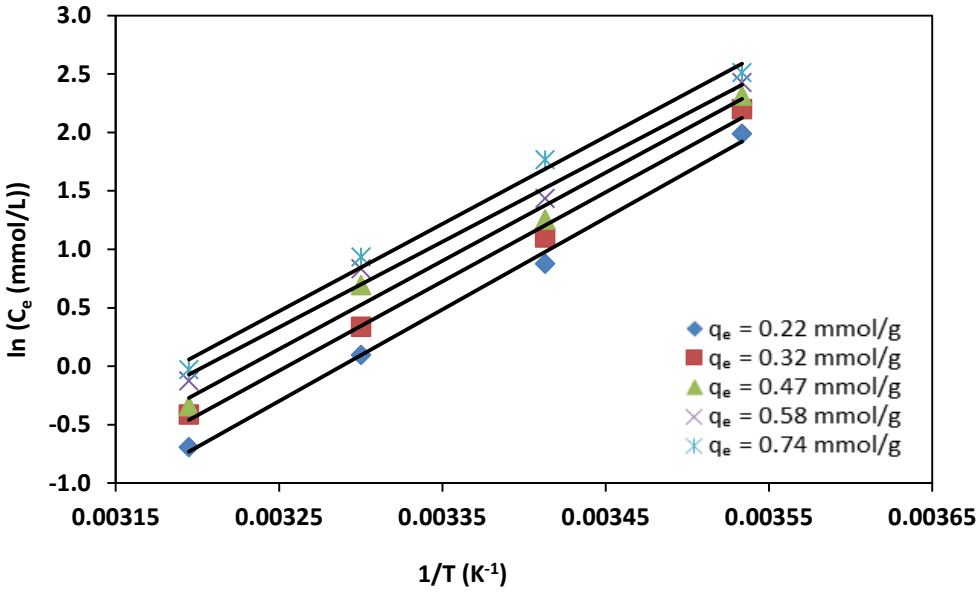

Figure 2-10 ln C_e as a function of 1/T for Zn(II) adsorption onto chitosan beads at different adsorption capacities (q_e). Lines indicate linear fits.

Table 2-2 Thermodynamic parameters and fitted ln K_d of Cr(VI) and Zn(II) adsorption onto chitosan beads.

Cr(VI)					Zn(II)			
T(K)	ln K_d (L/g)	ΔG° (kJ/mol)	ΔH° (kJ/mol)	ΔS° (kJ/mol K)	ln K_d (L/g)	ΔG° (kJ/mol)	ΔH° (kJ/mol)	ΔS° (kJ/mol K)
283	0.31	- 1.208	- 48.04	- 0.165	0.75	- 1.974	- 45.65	- 0.154
293	0.16	0.446			0.29	- 0.431		
303	- 0.9	2.101			- 0.4	1.112		
313	- 1.5	3.756			- 1.0	2.655		

Table 2-3 Isosteric heat of Cr(VI) and Zn(II) adsorption onto chitosan beads at constant adsorption capacities (q_e) with K_q-constant values, and coefficients of determination.

Heavy metals	Adsorption capacity (q_e) (mmol/g)	Isosteric heat of adsorption (ΔH_x) (kJ/mol)	K_q-constant (mmol/L)	Coefficient of determination (R^2)
Cr(VI)	0.12	- 49.786	20.307	0.9898
	0.13	- 53.117	21.551	0.9919
	0.16	- 53.623	21.969	0.9961
	0.21	- 55.782	23.038	0.9903
	0.43	- 61.477	25.532	0.9867
Zn(II)	0.22	- 57.733	23.215	0.9998
	0.32	- 58.763	23.679	0.9996
	0.47	- 59.056	24.117	0.9908
	0.58	- 59.874	24.383	0.9951
	0.74	- 64.187	26.406	0.9971

2.4.5 Adsorption kinetics

The adsorption kinetics of Cr(VI) and Zn(II) adsorption onto chitosan beads were determined by carrying out measurements after different contact times (0.25, 0.5, 0.75, 1, 2, 3, 4, and 8 h), temperature of 10 °C, a solution-pH of 6, and an initial metal concentration of 1000 mg/L. To explore adsorption behavior, both pseudo-first-order and pseudo-second-order models were used to fit adsorption data, as shown in Figure 2-11. Generally, the linear pseudo-first-order and pseudo-second-order models are respectively expressed by Equation 2-8 and 2-9 [71, 72]:

$$\ln(q_e - q_t) = \ln(q_e) - \frac{k_1}{2.303} t \qquad (2-8)$$

$$\frac{t}{q_t} = \frac{1}{k_2 q_e^2} + \frac{t}{q_e} \qquad (2-9)$$

Where q_e and q_t (mmol/g) are the adsorption capacities of metal ions onto chitosan beads at equilibrium and at time t (h), respectively, k_1 is the rate constant of the first-order adsorption process (h^{-1}), k_2 is the rate constant of the second-order adsorption process [g/(mmol.h)].

It can be clearly observed from Figure 2-11 that the adsorption data of both metals were fitted better by the pseudo-second-order model (Figure 2-11b) than the pseudo-first-order model (Figure 2-11a), suggesting that the whole adsorption process is mainly controlled by chemisorption that is involved in valence forces for sharing or exchanging electrons through coordination or chelation between amine groups in chitosan beads and heavy metal ions [2].

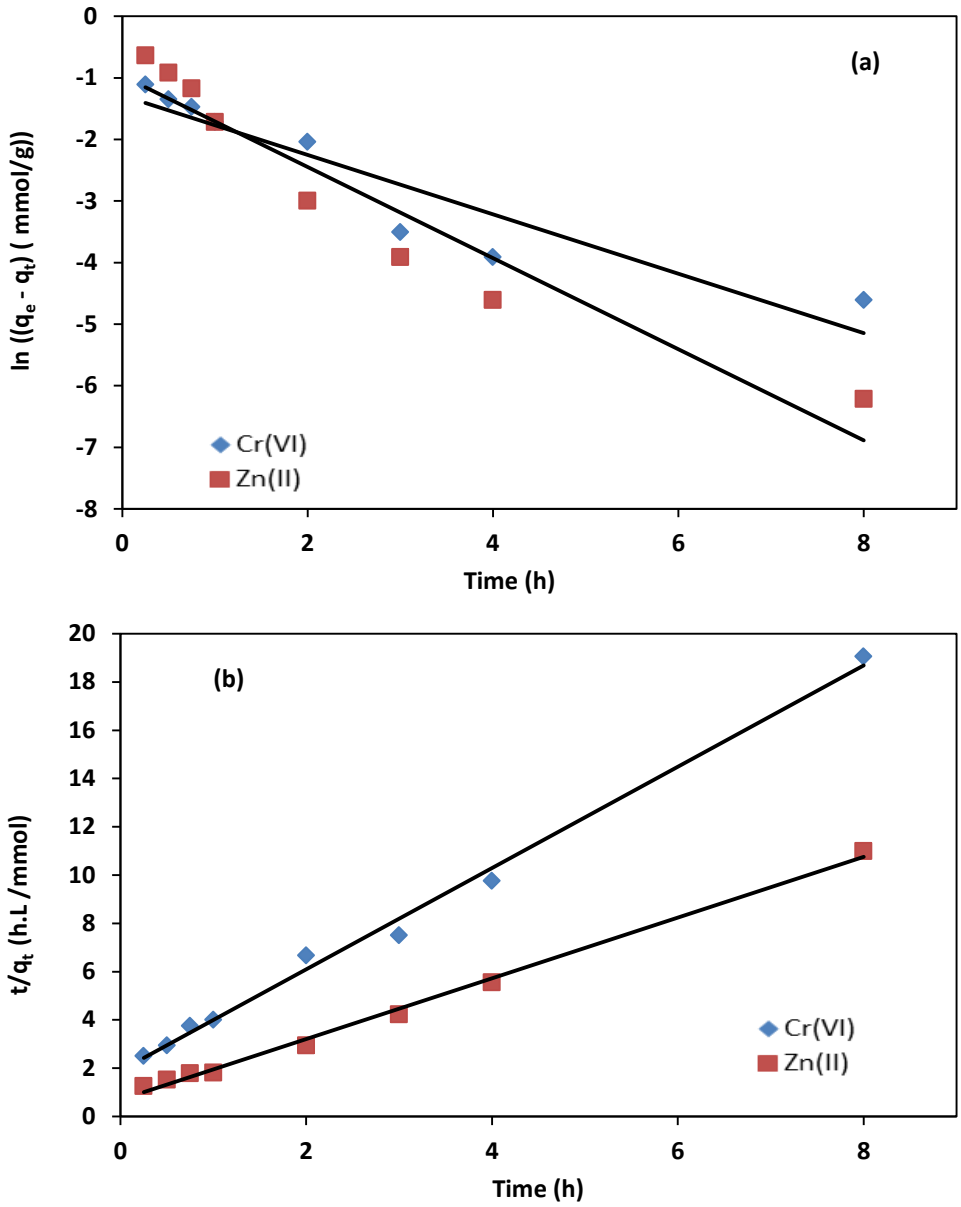

Figure 2-11 (a) Pseudo first-order kinetics (solid lines), (b) pseudo second-order kinetics (solid lines) fitted for Cr(VI) and Zn(II) adsorption experiments (pH = 5-6; mass of chitosan beads = 0.5 g; C_0 = 1000 mg/L for both metals; temperature = 10 °C).

2.4.6 Adsorption isotherms

Adsorption equilibrium was studied at different initial metal concentrations, for Cr(VI) ions at 0.96, 1.92, 4.8, 9.6, and 19.23 mmol/L, and for Zn(II) ions at 0.76, 1.53, 3.8, 7.65, and 15.3 mmol/L. The adsorption experiments were carried out at 10

°C for 8 h. The Langmuir and Freundlich models are the most commonly used isotherm models. The Langmuir isotherm model is based on monolayer adsorption onto an adsorbent surface containing a limited number of adsorptive sites with uniform energies. The Freundlich isotherm model, can be used for the adsorption onto heterogeneous surfaces and multilayer adsorption with different energies [11].

Langmuir and Freundlich isotherm models were fitted to the equilibrium adsorption data to determine the relationship between the adsorption isotherm parameters and to shed light on how the heavy metals interact with the chitosan beads surfaces. In linearized form, Langmuir isotherm is expressed as follows [73]:

$$\frac{C_e}{q_e} = \frac{1}{K_L q_m} + \frac{C_e}{q_m} \qquad (2-10)$$

Where C_e is the equilibrium concentration of metal ions in the solution (mmol/L), q_e and q_m are the equilibrium and theoretical maximum adsorption capacity (mmol/g), respectively. K_L is the Langmuir constant (L/g) related to binding energy.

The Freundlich isotherm is given as follows [73]:

$$\ln q_e = \frac{1}{n} \ln C_e + \ln K_F \qquad (2-11)$$

Where K_F is the Freundlich constant (mmol/g) and n is the Freundlich exponent (unitless). Langmuir and Freundlich isotherms for Cr(VI) and Zn(II) adsorption onto chitosan beads from aqueous solution are presented in Figure 2-12, and fitted kinetic parameters are shown in Table 2-4. Based on the contrasting results of the correlation coefficients R^2 of Langmuir isotherm (R_L^2) and Freundlich model (R_F^2), the correlation coefficients of Langmuir isotherm (R_L^2) were all above 0.91 for both metal ions, indicating that the data were fitted better by Langmuir isotherm than by Freundlich isotherm, suggesting that Langmuir isotherm model could well interpret the adsorption procedure, which indicates that the adsorption process of both metals

on the chitosan beads is driven by the formation of a heavy metal monolayer on the adsorbent surfaces. In this case, such surfaces show a homogeneous morphology of chitosan beads and a finite number of identical active sites [73, 74].

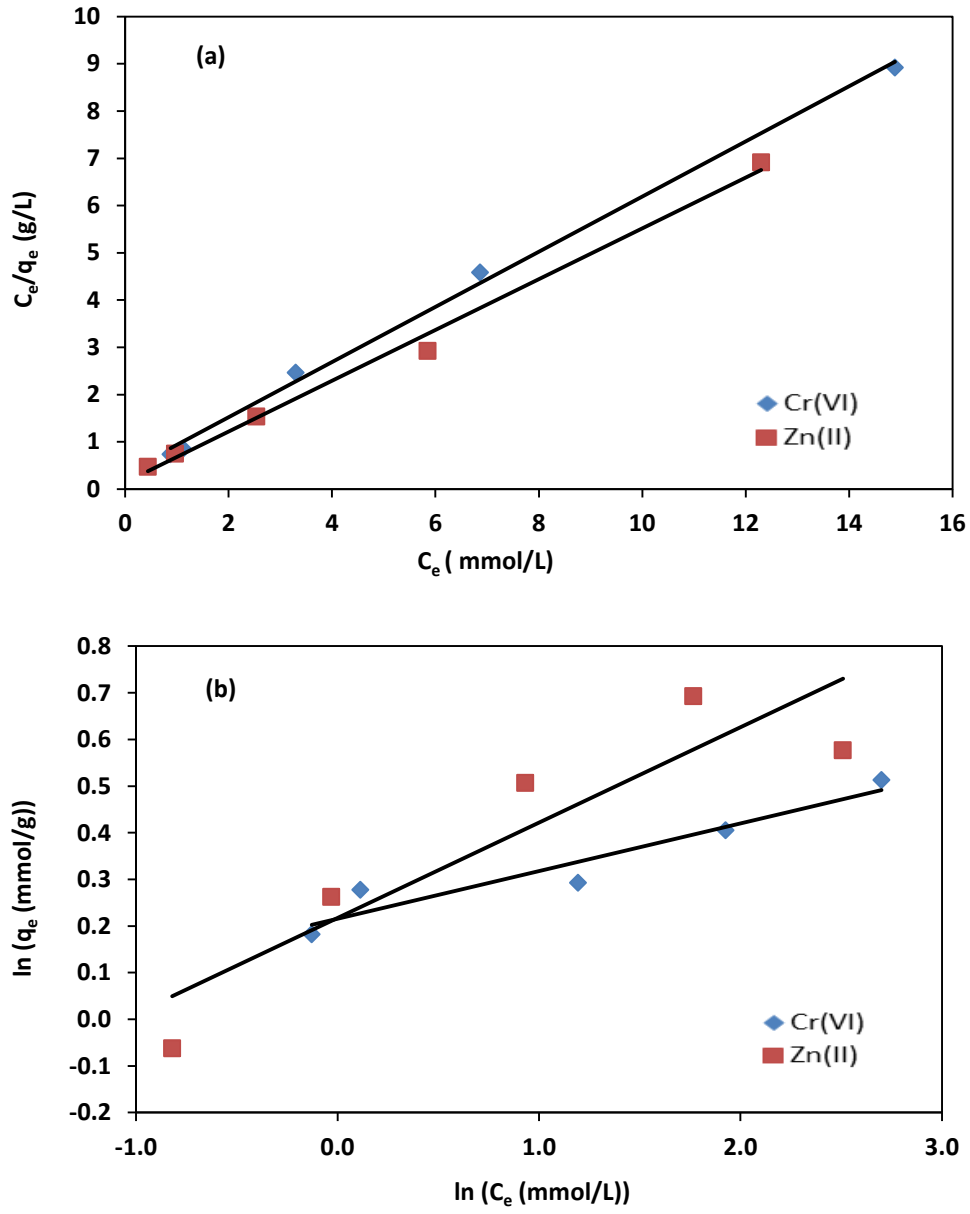

Figure 2-12 (a) Langmuir isotherms (solid lines), (b) Freundlich isotherms (solid lines) fitted for Cr(VI) and Zn(II) adsorption experiments (pH = 5-6; mass of chitosan beads = 0.5 g; temperature = 10 °C).

Table 2-4 Langmuir and Freundlich isotherm parameters for Cr(VI) and Zn(II) adsorption onto chitosan beads.

Langmuir parameters				Freundlich parameters		
Heavy metals	q_m (mmol/g)	K_L(mmol/L)	R_L^2	1/n	K_F (mmol/g)	R_F^2
Cr(VI)	1.713	1.6715	0.997	0.102	1.24	0.915
Zn(II)	1.86	3.88	0.915	0.204	1.24	0.829

2.5 Conclusions

This study indicates that the removal rate of Cr(VI) and Zn(II) ions from aqueous solution onto chitosan beads was excellent and up to 1.67 mmol/g (109.18 mg/g) for Zn(II), and 1.53 mmol/g (79.56 mg/g) for Cr(VI). The unique properties of chitosan make it an exciting and promising agent for purification of industrial wastewater purposes. The capacities of Cr(VI) and Zn(II) adsorption onto chitosan were strongly dependent on solution-pH, contact time, and temperature. The highest adsorption capacities were observed at pH 6 for Zn(II) and at pH 5 for Cr(VI), and at temperature 10 °C. Adsorption kinetic data were well-fitting with the pseudo-second-order kinetic model for both metals. Cr(VI) and Zn(II) ions adsorption onto chitosan beads could be described well by the Langmuir model with a R^2 equal to 0.997 and 0.915, respectively. Thermodynamic quantities such as Gibb's free energy (ΔG°), enthalpy (ΔH°), entropy (ΔS°), and isosteric heat of adsorption (ΔH_x) indicated that both metal ions adsorption onto chitosan beads was exothermic, spontaneous, and the surface of chitosan beads was energetically homogeneous. It was observed that at low pH, swelling of chitosan beads occurred and tended to form a gel. Therefore, it is necessary to modify chitosan physically or chemically before applicable use in adsorption.

CHAPTER 3. ADSORPTION OF Zn(II) IONS BY CHITOSAN COATED DIATOMACEOUS EARTH

3.1 Abstract

In this work, chitosan coated diatomaceous earth (CCDE) beads were synthesized by a drop-wise method and characterized by FTIR, BET, SEM, EDS, and zeta potential for Zn(II) ion removal from aqueous solution in batch and continuous processes. Several parameters have been studied such as solution-pH, initial Zn(II) ion concentration, temperature, flow rate, and contact time to investigate the Zn(II) ion uptake. The maximum adsorption capacity of Zn(II) ion onto CCDE beads was 127.4 mg/g in batch studies. The adsorption followed Pseudo second order and was well fitted to Langmuir model, indicating monolayer adsorption behavior. The continuous adsorption studies showed decreasing breakthrough and exhausted time with increasing flow rate of solution. The breakthrough points were 220 and 115 min at flow rate 3 and 6 mL/min, respectively. Loaded CCDE beads with Zn(II) ions were successfully regenerated by 0.2M NaOH without damaging the adsorbents and up to 87 % recovery in the fourth cycle. Anions in the solution had an insignificant effect on Zn(II) ion uptake by CCDE beads. Overall results suggested that the prepared adsorbents could be employed as a low-cost, sustainable, and excellent alternative material for Zn(II) ion removal from wastewater.

3.2 Introduction

Wastewater from various industries contains a high concentration of many heavy metals like chromium, copper, cadmium, zinc, or nickel. Among these metals, zinc is an essential heavy metal for biological functions, but at high concentrations, it can be harmful to ecosystem and animals and cause many human diseases like nausea, anemia, and pancreas damage [7]. The main source of zinc is from galvanic industries, batteries production, electroplating, mining effluents, and acid mine drainage [75]. Zinc concentrations recorded over 620 mg/L in drainage from abandoned copper mines in Montana, USA [4]. Zinc is classified as a toxic element and serious environmental contaminant according to Environmental Protection Agency (EPA), USA. Removing and separation zinc ions from aqueous solutions and industrial wastewater plays an important function for the environmental treatment. Traditional methods such as chemical precipitation [76], filtration [14], electrodialysis [14], ion exchange [77], reverse osmosis [78], adsorption [79] and ultrafiltration [80] have been used to remove heavy metals from wastewater streams. Among the above-mentioned techniques, adsorption is a more promising and attractive technique because it is economical, simple in design and efficient. Also, chemical consumption or/and waste generation are not significant issue compared with other methods. The adsorption process often involves using activated carbon as adsorbent. However, activated carbon has some disadvantages of being very expensive and less effective for removing some metals [81]. In recent years, bioadsorbents gain a wide attention and extensively studied in heavy metals removal from aqueous solution because they are inexpensive, available in large quantities, easy to regenerate for reuse, and eco-friendly such as marine algae [41], seaweed [42], chitin [82], bark [83] and chitosan [45]. Chitosan is a natural polyaminosaccharide, commercially produced by partial

deacetylation of chitin, which is the second plentiful organic material in nature next to cellulose, and can be extracted from crustaceans such as shrimp, lobsters, crayfish, and crabs. Chitosan has excellent characteristics such as biocompatible, biodegradable, abundant in nature, non-toxic, hydrophilic, and antibacterial [84]. However, it has great physicochemical properties like chemical stability, excellent chelation behavior, high reactivity, and metal ion binding groups like amino ($-NH_2$) and hydroxyl ($-OH$). Chitosan possesses some disadvantage properties such as swelling in acidic media, tendency to agglomerate, low specific surface area, and poor mechanical properties, which limited its application in adsorption [90]. In recent years, chitosan has been modified chemically and physically in order to enhance its properties and reduce its disadvantages by fabricating chitosan with chitosan/thiocarbamoyl [86], chitosan/polyaniline [87], chitosan/cellulose [88], chitosan/ montmorillonite magnetic microspheres [89], Chitosan/sporopollenin microcapsules [90], and chitosan/glutaraldehyde [91].

In this study, chitosan was successfully modified by inert natural material - diatomaceous earth. Diatomaceous earth is a non-hazardous amorphous natural material formed from the remains of diatoms, it has unique physical characteristics such as high permeability, high porosity up to 65%, small particle size, adsorption capabilities, low thermal conductivity and density, and high surface area (10 – 30 m^2/g) [10]. The modified chitosan was achieved by spreading the chitosan onto diatomaceous earth and formed into spherical beads by using drop-wise method, and then it was used to remove Zn(II) ions from aqueous solution. The prepared adsorbents were characterized before and after Zn(II) ion adsorption by Fourier transform infrared spectroscopy (FTIR), Scanning Electron Microscope (SEM), Brunauer, Emmett,Teller (BET), and Energy Dispersive X- Ray Spectroscopy (EDS).

In addition, we investigated the major adsorption factors effect such as of solution-pH, contact time, temperature, and initial Zn(II) ion concentration on batch adsorption process. Moreover, the regeneration of the exhausted bed column was investigated by using diluted sodium hydroxide. The experimental data were fitted with adsorption isotherm models and kinetic models in batch adsorption.

3.3 Materials and methods

3.3.1 Materials

Medium molecular weight biopolymer chitosan (deacetylation 87%, viscosity = 1000 mPa.s, molecular weight ~190,000 – 310,000 g/mol, and ash content 1%) and diatomaceous earth powder (92% SiO_2, 4% Al_2O_3, 2% Fe_2O_3) were procured from Aldrich Chemical Corporation (St. Louis, MO, USA). Zinc sulphate heptahydrate ($H_{14}O_{11}SZn$) was used to prepare stock solution containing 1000 mg/L of Zn(II) ions by dissolving 4.398 g of $H_{14}O_{11}SZn$ in 1L of deionized water. Sodium hydroxide and oxalic acid were used to dissolve chitosan and adjusted solutions-pH using calibrated pH-meter.

3.3.2 Preparation of chitosan coated diatomaceous earth (CCDE) beads

About 20 g of chitosan was slowly added into 1L of 0.2 M oxalic acid solution under continuous stirring, 200 rpm. The solution was heated to 60 ^oC for 6 h to dissolve chitosan and facilitate acylation to form a viscous chitosan gel. About 20 g of diatomaceous earth powder was added to the formed chitosan gel, keeping temperature and mixing at 60 ^oC and 200 rpm for another 6 h. The spherical beads of

chitosan coated diatomaceous earth were formed by dropping the final gel mixture into a 0.8 M concentrated NaOH precipitation beaker.

The objective of dropping chitosan- diatomaceous earth gel into the basic solution was to rapidly neutralize the drops and get spherical beads of CCDE. The hydrogel beads remained in the NaOH solution with low mixing to become harden. Eventually the hardened spherical beads were washed with deionized water to neutralize and remove sodium ions that were attached to the beads. The beads were dried by vacuum furnace for 24 h at 70 ^{o}C. The final dry chitosan coated diatomaceous earth beads had an average diameter about 2 mm.

3.3.3 Adsorption experiments

Batch adsorption experiments of Zn(II) ion uptake from aqueous solution were carried out to determine the prepared CCDE beads adsorption capacities at different Zn(II) ion concentrations of 50 mg/L, 100 mg/L, 250 mg/L, and 500 mg/L at 0.25 g dosage beads. About 100 mL of various initial concentrations of Zn(II) ions solutions were put into Erlenmeyer flasks with adsorbent (0.25 g) and agitated in an orbital shaker (200 rpm) at different solution-pH ranging from 2 to 8, and 15- 420 min contact times. After a certain mention actual time, samples were taken from the flasks and filtrated to determine the final Zn(II) ion concentrations in the filtrate. Inductively Coupled Plasma-Mass Spectrometer (ICP-MS) was used to determine the Zn(II) ion concentrations. When the steady state of adsorption was attained, the Zn(II) ion removal capacity onto CCDE beads was determined by doing a mass balance on Zn(II) ions, Equation 3-1 [92].

$$q_e = \frac{(C_o - C_e)V}{m} \qquad (3-1)$$

Where q_e : the equilibrium adsorbed Zn(II) ion amount (mg/g), C_o and C_e : the initial and equilibrium Zn(II) ion concentrations (mg/L), V : volume of the filtrate (L), and m is the mass of adsorbents (g). Batch adsorption runs were studied at different temperatures, different initial Zn(II) ion concentrations, different initial solutions-pH, and different contact times. Dynamic experiments of Zn(II) ions adsorption were investigated in a porous bed system that consists of an acrylic lab-scale column of 2 cm internal diameter and 16 cm length. About 21 g of CCDE beads were packed into the column. The feed solution containing zinc (100 mg/L) was pumped by peristaltic pump at different flow rates (3, 4, 5, and 6 mL/min) downward through the column. At specific interval time, effluent samples were collected and filtrated to determine the Zn(II) ion concentration as shown in Figure 3-1. Eventually, the exhausted fixed bed was regenerated by using NaOH solution at low concentration to examine the potentiality of the CCDE beads for repeated use.

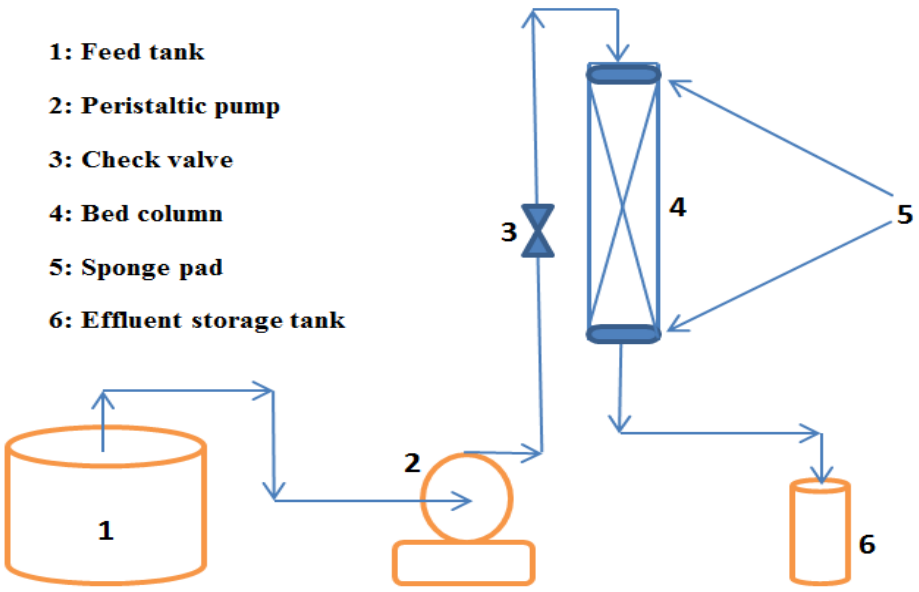

Figure 3-1 Experimental setup of lab-scale column for Zn(II) ion adsorption onto CCDE beads.

3.4 Results and discussion

3.4.1 Characterization of CCDE beads

The chitosan coated diatomaceous earth beads were characterized to assess various physical and chemical properties to provide a better interpretation of Zn(II) ions removal mechanism associated with adsorption process. The physicochemical properties of CCDE beads are summarized in the Table 3-1.

Table 3-1 The main physicochemical properties of the prepared CCDE beads.

Parameters	Value
Physical nature	porous
Average particle diameter, (mm)	2
Surface area (m^2/ g) (based on BET)	6.4
Bulk density (g /cm^3)	0.338
Particle density, (kg/m^3)	481
Porosity	0.298
pore size (mm) (based on BET)	3.23×10^{-6}
pore volume (m^3/g) (based on BET)	7.4×10^{-9}
pH - point of zero charge (pH_{PZC})	5.8

3.4.2 Fourier transform infrared spectroscopy (FTIR)

To identify the mechanism of Zn(II) ion removal onto CCDE beads, FTIR-spectra were determined before and after Zn(II) ion adsorption. As shown in Figure 3-2, FTIR results of fresh adsorbents showed a peak at 3308 cm^{-1}, which means a band of stretching vibration of N-H, and at 960 cm^{-1} that is related to C-C bond. Extra bond was observed at 1625 cm^{-1} which corresponded to C=N stretching bond, and 2870 cm^{-1} is for C-H stretching vibration. The FTIR-spectra for CCDE beads loaded by Zn(II) ions have showen that the peaks at 1625 cm^{-1} (C=N) and 2870 cm^{-1} (C-H) were

sharper and separately shifted to 1635 and 2860 cm^{-1}. However, after Zn(II) ion adsorption, there was a peak change in the FTIR- spectra at 1440 cm^{-1} which specified to the -N-H deformation vibration and 1320 cm^{-1} which was assigned to -C-N- stretching vibration in chitosan structure. The FTIR-spectra results were in agreement with the previous published work by Qi et al. [60]. The changing in the peaks might suggest that the oxygen atoms in the hydroxyl groups in chitosan molecules contribute to Zn(II) ion uptake onto CCDE as well [27].

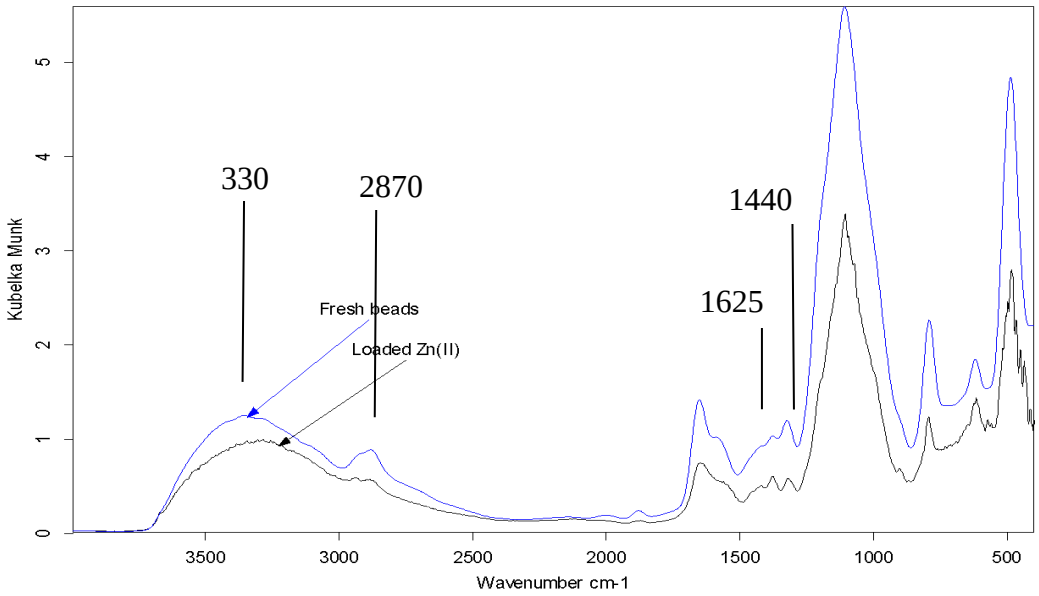

Figure 3-2 Fourier transform infrared spectroscopy (FTIR) of CCDE beads.

3.4.3 Scanning electron microscope (SEM)

Scanning electron microscopy (Figure 3-3 (a) and (b)) shows amorphous surface of the outer surface of fresh chitosan coated diatomaceous earth beads and loaded beads by Zn(II) ion at 50 μm, and 1000 kV image magnification. From Figure 3-3(a), it can be observed that fresh beads were significantly porous, which enhanced the Zn(II) ion spreading and binding with active sites. Figure 3-3(b) shows the exposed adsorbents by Zn(II) ions, it seems that Zn(II) ions were adsorbed onto CCED beads and that looks obvious from the bright spots on the surface. However, the morphology

of loaded adsorbents is less than fresh beads due to adsorbed Zn(II) ions onto adsorbent surface.

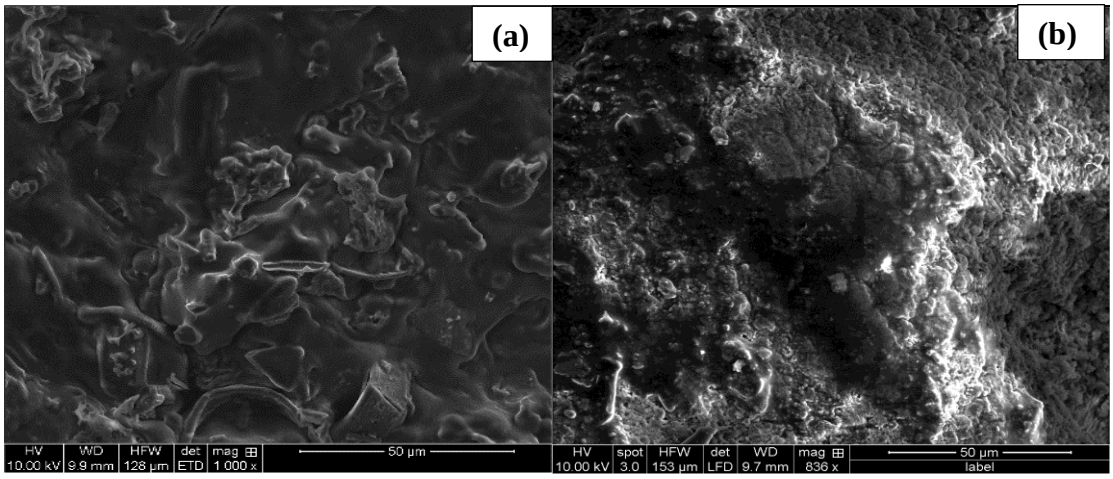

Figure 3-3 Scanning Electron Microscope of (a) Fresh CCDE beads and (b) Loaded CCDE beads by Zn(II) ions.

3.4.4. Energy dispersive X- ray spectroscopy (EDS)

The EDS X-ray microanalysis was performed on CCDE beads before and after their exposure to Zn(II) ion solutions, the EDS X-ray for fresh beads is showed in Figure 3-4(a). While Figure 3-4(b) shows the beads after being loaded by Zn(II) ions, Figure 3-4(b) also shows a large peak at about 1.0 kv for Zn(II) ions. The quantitative elemental composition of each component of CCDE beads were explained in tables Figure 3-4(a) and (b). The adsorbed Zn(II) ions reached as high as 7.73 % in loaded adsorbents. The total weight percentages of fresh and loaded beads were 98.71 and 96.99 %, respectively, the difference in percentages were some impurities like Fe, Al, and Na. To avoid damage or burn the CCDE beads, platinum was used to coat the adsorbents during the EDS X-ray test. The results indicate that the CCDE beads have high adsorption capacity for Zn(II) ion removal.

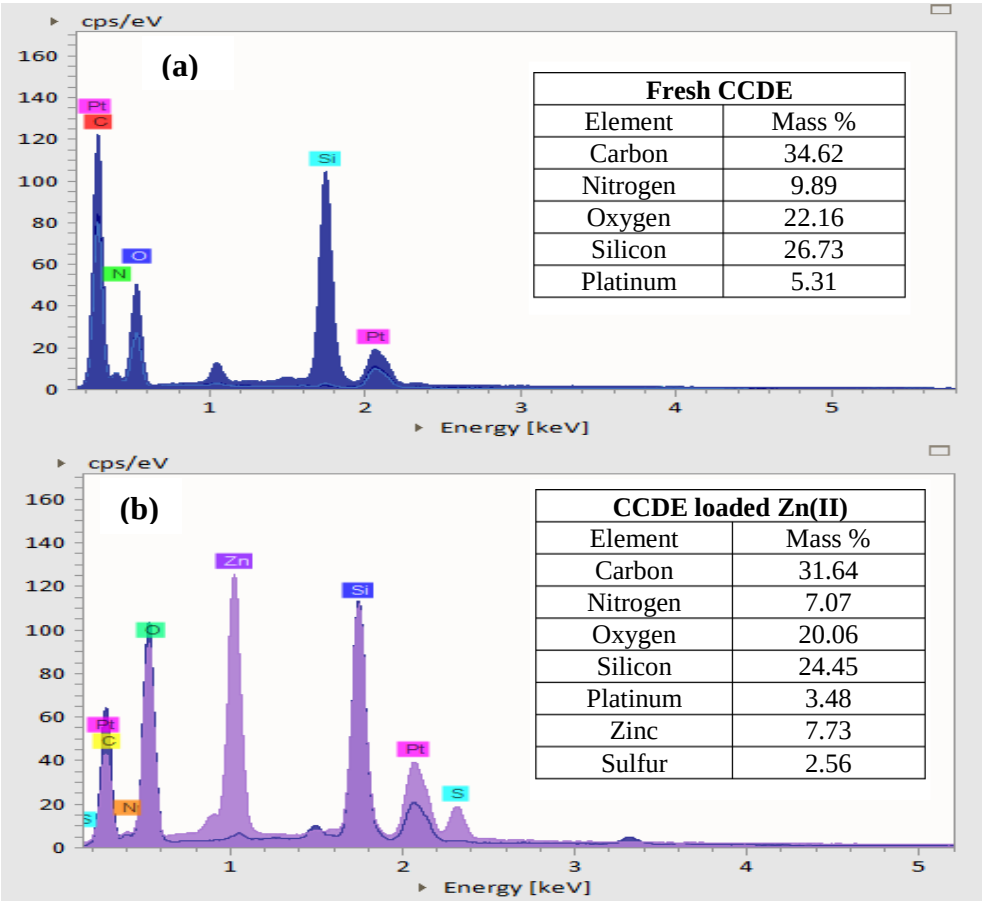

Fresh CCDE	
Element	Mass %
Carbon	34.62
Nitrogen	9.89
Oxygen	22.16
Silicon	26.73
Platinum	5.31

CCDE loaded Zn(II)	
Element	Mass %
Carbon	31.64
Nitrogen	7.07
Oxygen	20.06
Silicon	24.45
Platinum	3.48
Zinc	7.73
Sulfur	2.56

Figure 3-4 Energy Dispersive X- ray Spectroscopy (EDS) of (a) Fresh CCDE beads and (b) CCDE beads loaded Zn(II) ions.

3.4.5 Zeta potentials

The zeta potential values over a range of pH values that were covered using dilute $C_2H_2O_4$ or NaOH were measured by using photon correlation spectroscopy and electrophoretic light scattering. A 10 mg of CCDE powder were suspended in 10 mL deionized water and irradiated. In Figure 3-5, the results showed that the CCDE beads have positive charges in acidic media and negative charges in basic media. However, pH - point of zero charge (pH_{PZC}) was at pH 5.8. The positive zeta potential at low pH was created by the protonation of amine groups in chitosan. Therefore, the negative species were adsorbed preferentially at low pH and species that have positive charges were easily adsorbed and interacted on CCDE beads in basic medium.

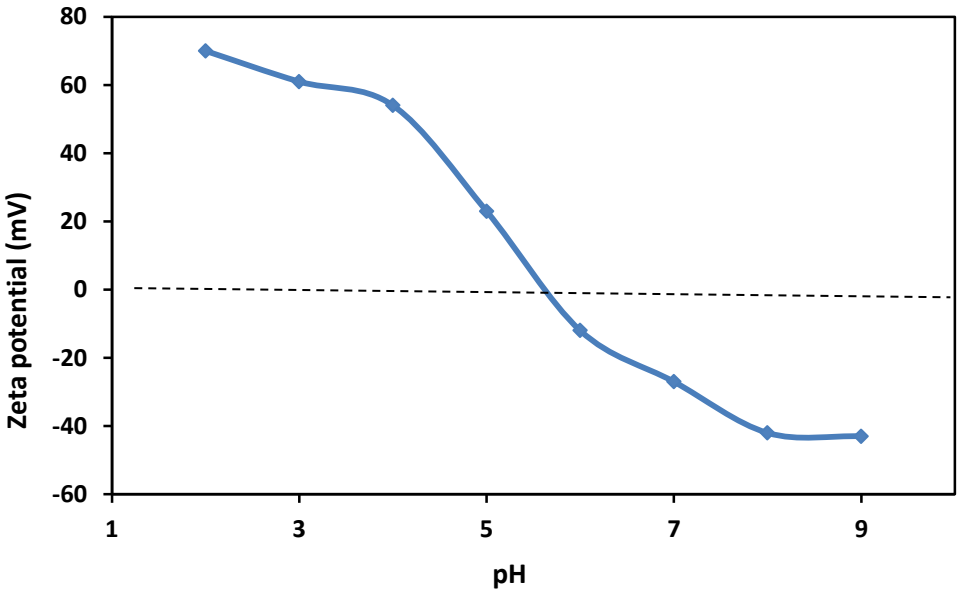

Figure 3-5 Zeta potentials of CCDE beads at different solution-pH values.

3.4.6 Effect of pH on Zn(II) ion uptake

The effect of initial solution-pH on Zn(II) ion adsorption onto CCDE beads was studied at different pH values between 2 and 8. Zn(II) ion was uptake mostly done by NH_2 groups due to the presence of electron pairs on nitrogen atom in chitosan. In acidic media-low pH, amine groups were protonated to NH_3^+ that reduced the adsorption capacity of metals that existed in the form of cations [62]. As reported, the zeta potential results (Figure 3-5) showed that the CCDE beads have a zero charge at pH 5.8 (pH_{PZC}), therefore, the prepared adsorbents have a negative charge above 5.8. Figure 3-6 represents the effect of initial pH on Zn(II) ion removal at initial concentration 500 mg/L and 283 K. The results indicated that the Zn(II) ion removal increased sharply when the initial solution-pH was increased from 2 to 5, and then it increased slightly at pH between 5 and 6 until it reached the maximum uptake. The increase in Zn(II) ion removal with increasing solution-pH from 2 to 5 could be explained by reducing the proton (H^+) and positive Zn(II) ions rivalry at the same

active sites on adsorbents. In acidic media, CCDE beads surface was positively charged due to increasing protonation of amino groups that decreased the interaction between active sites (NH_3^+) and Zn(II) ions on adsorbents. The results showed that the Zn(II) ion uptake was affected strongly by solution- pH and the maximum adsorption capacities were at pH 6 with 127.4 mg/g and 60.2 mg/g onto CCDE beads and pure chitosan beads, respectively. It was noticed that at pH higher than 6, the zinc hydroxide starts to form and precipitates in the solution which caused reduction in the adsorption capacity of Zn(II) ion at pH greater than 6. These results were in good agreement with Kyzas et al. [93] and Ahmed et al. [94]. Table 3-2 shows the comparative Zn(II) ion adsorption capacities at different adsorbents.

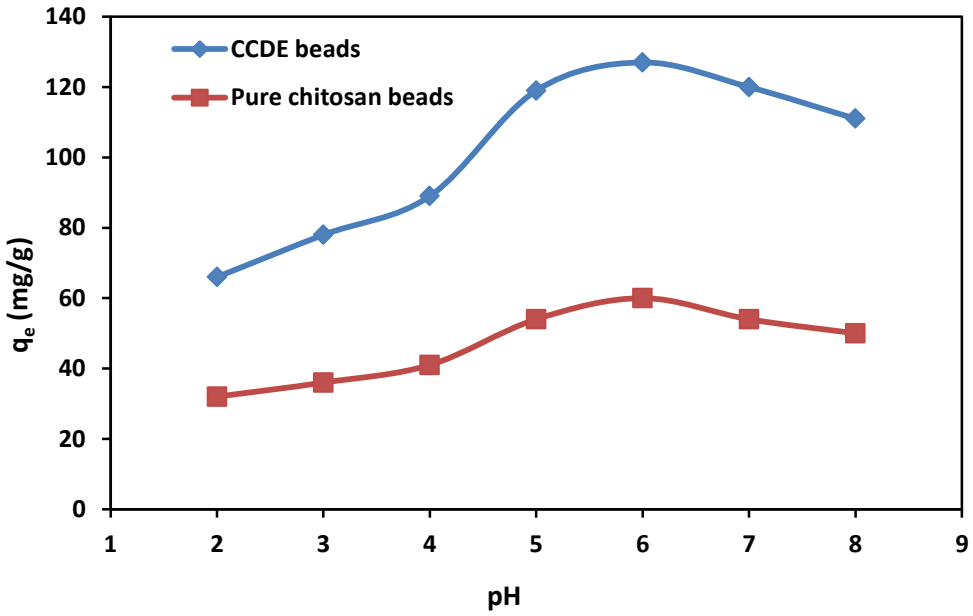

Figure 3-6 Effect of initial solution-pH on Zn(II) ion uptake onto CCDE beads [C_o = 500 mg/L; temperature = 283K; adsorbent dosage = 0.25 g].

Table 3-2 Maximum adsorption capacity of Zn(II) ion onto different adsorbents.

Adsorbents	pH	Initial concentration (mg/L)	Adsorption capacity (mg/g)	Reference
crab carapace	4.3	460	67.6 (batch) 76.9 (fixed bed)	[4]
Chitosan/cellulose	--	--	19.81	[89]
succinyl-grafted chitosan	5	200	168	[93]
Candida utilis	5.17	300	181.7	[94]
fly ash coated chitosan	--	196	55.52	[95]
Pure chitosan	7	10	5.49	[64]
CCDE beads	6	500	127.4	Present study

3.4.7 Effect of initial zinc ion concentrations on Zn(II) ion uptake

The effect of initial Zn(II) ion concentration on the adsorption capacity of prepared CCDE beads was studied in the range 50 – 500 mg/L at pH 6, temperature 283 K, and 15 – 420 min contact times. The results illustrated in Figure 3-7. It was observed that the amount of Zn(II) ion uptake onto CCDE beads increased from 19 to 127.4 mg/g, with increasing the initial Zn(II) ion concentration from 50 to 500 mg/L. It could be because the concentration gradient between bulk solution and adsorbents surface overcomes the mass transfer resistance of Zn(II) ion at high initial concentration [96]. Zinc adsorption was rapid in the first 90 min due to the availability of adsorption active sites, and slowed down until it reached the equilibrium around 130 min in the most of the batches run. At contact time 200 min, it

was observed that the highest Zn(II) ion removal (127.4 mg/g) happened at initial zinc concentration 500 mg/L.

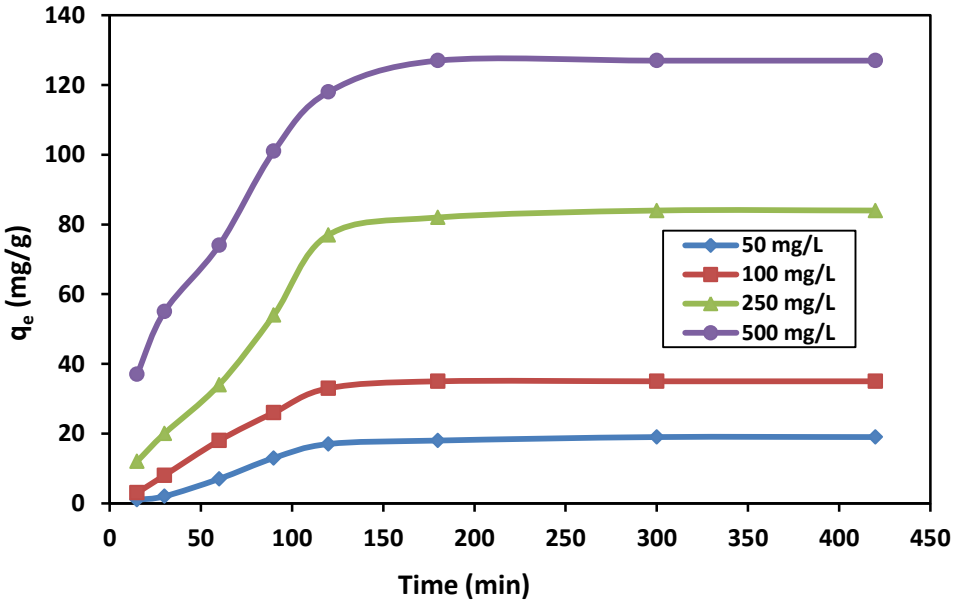

Figure 3-7 The effect of contact time and initial zinc concentrations on Zn(II) ion uptake onto CCDE beads [pH = 6; adsorbent dosage = 0.25 g; temperature = 283K].

3.4.8 Effect of temperature and thermodynamic parameters on Zn(II) ion uptake

The effect of adsorption temperature on Zn(II) ion uptake was examined at 283, 293, 303, and 313 K. The results showed that the temperature had a negative impact on the adsorption capacity of Zn(II) ion onto CCDE beads. It showed that with increasing the temperature from 283 to 313 K the Zn(II) ion removal was reduced from 127.4 to 106.8 mg/g as shown in Figure 3-8, the reason for decreasing Zn(II) ion removal at high temperature was the Zn(II) ion solubility in the solution increased with temperature, which reduced the interaction forces between Zn(II) ion and active sites in adsorbents and makes this forces weaker than those between Zn(II) ion and solution. The low temperatures were favorite for Zn(II) removal onto CCDE beads.

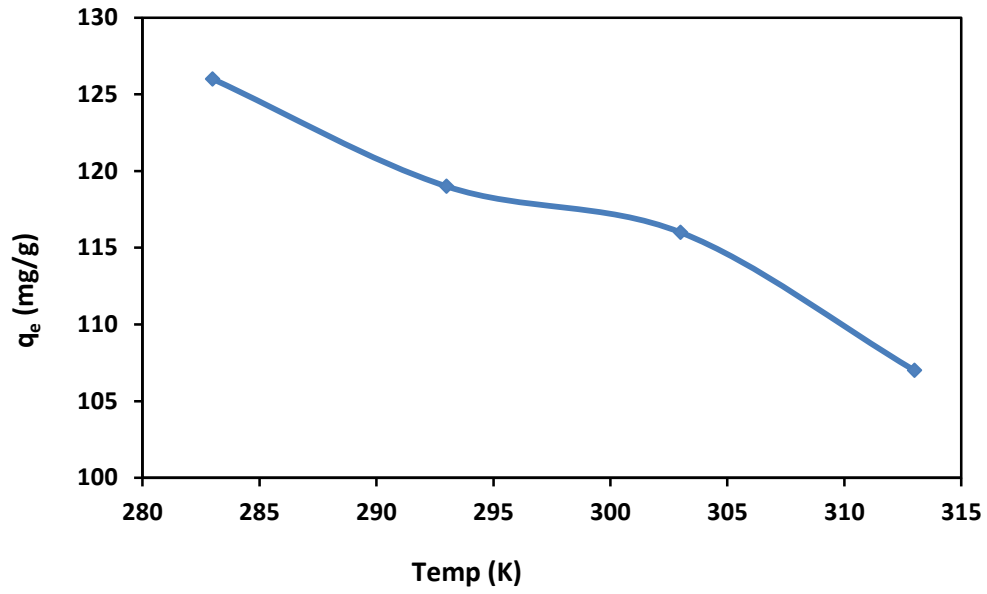

Figure 3-8. Effect of temperature on Zn(II) ion uptake onto CCDE beads [C_o = 500 mg/L; pH = 6; adsorbent dosage = 0.25 g].

Thermodynamic parameters such as Gibb's free energy (ΔG^o), enthalpy (ΔH^o), and entropy (ΔS^o) were calculated for Zn(II) ion adsorption onto CCDE beads by using following equations:

$$\Delta G^o = \Delta H^o - T\Delta S^o \qquad (3-2)$$

Where ΔG^o is expressed as:

$$\Delta G^o = -RT\ln K_d \qquad (3-3)$$

Substituting Equation (3-3) into Equation (3-2), provides van't Hoff equation [66]:

$$\ln K_d = \frac{\Delta S^o}{R} - \frac{\Delta H^o}{RT} \qquad (3-4)$$

Where R is the universal gas constant (8.314 J/mol.K) and T is the absolute temperature (in Kelvin), K_d is the distribution constant ($K_d = q_e/C_e$). The slope of plotting $\ln K_d$ versus 1/T provides the value of ΔH^o and the intercept is the value of ΔS^o. The calculated ΔH^o may be considered as the heat of adsorption when the adsorption capacity of adsorbents reached its saturated capacity of Zn(II) ions. The

values of ΔH^o, ΔS^o, and ΔG^o are listed in Table 3-3. The ΔH^o value of Zn(II) ion uptake onto CCDE beads indicated that the adsorption process was exothermic and the negative value of ΔG^o indicated the feasibility and spontaneity of the adsorption process in all used temperatures. These results were in agreement with Hu et al. [62] and Adamczuk and Kołodyńska [95].

Isosteric heat of adsorption (ΔH_x) is useful pertinent thermodynamic factors to characterize the temperature effect throughout the adsorption process. It is defined as the heat of adsorption determined at constant amount of adsorbate [62]. The isosteric heat of adsorption at constant Zn(II) ion adsorbed amount was calculated by using the well-known Clausius-Clapeyron equation, assuming it is temperature independent:

$$\ln C_e = -\left(\frac{\Delta H_x}{R}\right)\frac{1}{T} + K_c \qquad (3-5)$$

Where, C_e is the equilibrium adsorbate concentration in the solution (mg/L), ΔH_x is the isosteric heat of adsorption (kJ/ mol), R is the ideal gas constant (8.314 J/mol.K), K_c is a constant, and T is temperature (K). The slope of plotting ($\ln C_e$) versus 1/T is the isosteric heat of adsorption that was calculated at different amounts of Zn(II) ion adsorbed onto CCDE beads (Table 3-4). It can be seen that the variation in ΔH_x with surface that loaded Zn(II) ions was indicative of the fact that the CCDE beads had energetically homogeneous surfaces. However, the variation in ΔH_x with Zn(II) ion uptake amount can be attributed to the possibility of having interaction between the adsorbed Zn(II) ions and other ions. The results showed that the ΔH_x was strongly depended on the adsorbed amount which decreases with increasing in Zn(II) ions adsorbed amount due to the interaction between adsorbents and adsorbed Zn(II) ions in the solution. The high value of ΔH_x at low adsorbed Zn(II) ions (q_e) refers to a high initial interaction between adsorbed ions and adsorbents due to the presence of

high active amine and hydroxyl groups on chitosan. If it were a heterogeneous CCDE beads surface, the ΔH_x of Zn(II) ions adsorption could have been unchanged [62].

Table 3-3 Thermodynamic parameters of Zn(II) ion adsorption onto CCDE beads.

T(K)	ln K_d	ΔG^o (KJ/ mol)	ΔH^o (KJ/mol)	ΔS^o (KJ/ mol.K)
283	2.028	- 4.772	- 54.855	- 0.177
293	1.029	- 2.527		
303	0.741	- 1.864		
313	-0.362	0.942		

Table 3-4 The isosteric heat of Zn(II) ion adsorption onto CCDE beads at constant adsorbed amount.

Adsorbed amount (mg/g)	ΔH_x (KJ/mol)	K- constant	R^2
106.8	- 97.0	- 37.8	0.9972
116.0	- 68.0	- 24.8	0.9659
119.0	- 66.0	- 23.4	0.9681
127.4	- 17.7	- 2.64	0.9951

3.4.9 Adsorption kinetics

The kinetics of Zn(II) ion adsorption process have been carried out at a time ranging from 15 to 120 min and distinct runs of adsorption experiments keeping temperature, solution-pH, and initial Zn(II) ion concentration constant to follow the adsorption with time. The adsorption rate was determined by the pseudo first-order and pseudo second-order models. The pseudo-first order adsorption kinetic equation is expressed as follows [65]:

$$\ln(q_e - q_t) = \ln q_e - \frac{k_1}{2.303} t \qquad (3-6)$$

Where q_e and q_t (mg/g) are the adsorption capacities at equilibrium and at time t (min), respectively, k_1 is the rate constant of pseudo-first-order model (min^{-1}).

The pseudo second-order adsorption kinetic equation is given as follows [71]:

$$\frac{t}{q_t} = \frac{1}{k_2 q_e^2} + \frac{t}{q_e} \qquad (3-7)$$

Where k_2 [g / (mg.min)] is the rate constant of pseudo second- order model.

The experimental results of Zn(II) ion adsorption onto CCDE beads were found to be fitted to the pseudo first order and pseudo second order models (Figure 3-9 a and b). But, the reported R^2 values showed a better fitting to pseudo-second order model (R^2 = 0.9895). However, the calculated (q_e) value of the pseudo-second order kinetic model (130.7 mg/g) was close to the experimental value (127.4 mg/g) rather than that of pseudo-first order kinetic model value (118 mg/g). Therefore, the pseudo second-order kinetic model was more appropriate for Zn(II) ion adsorption process onto CCDE beads.

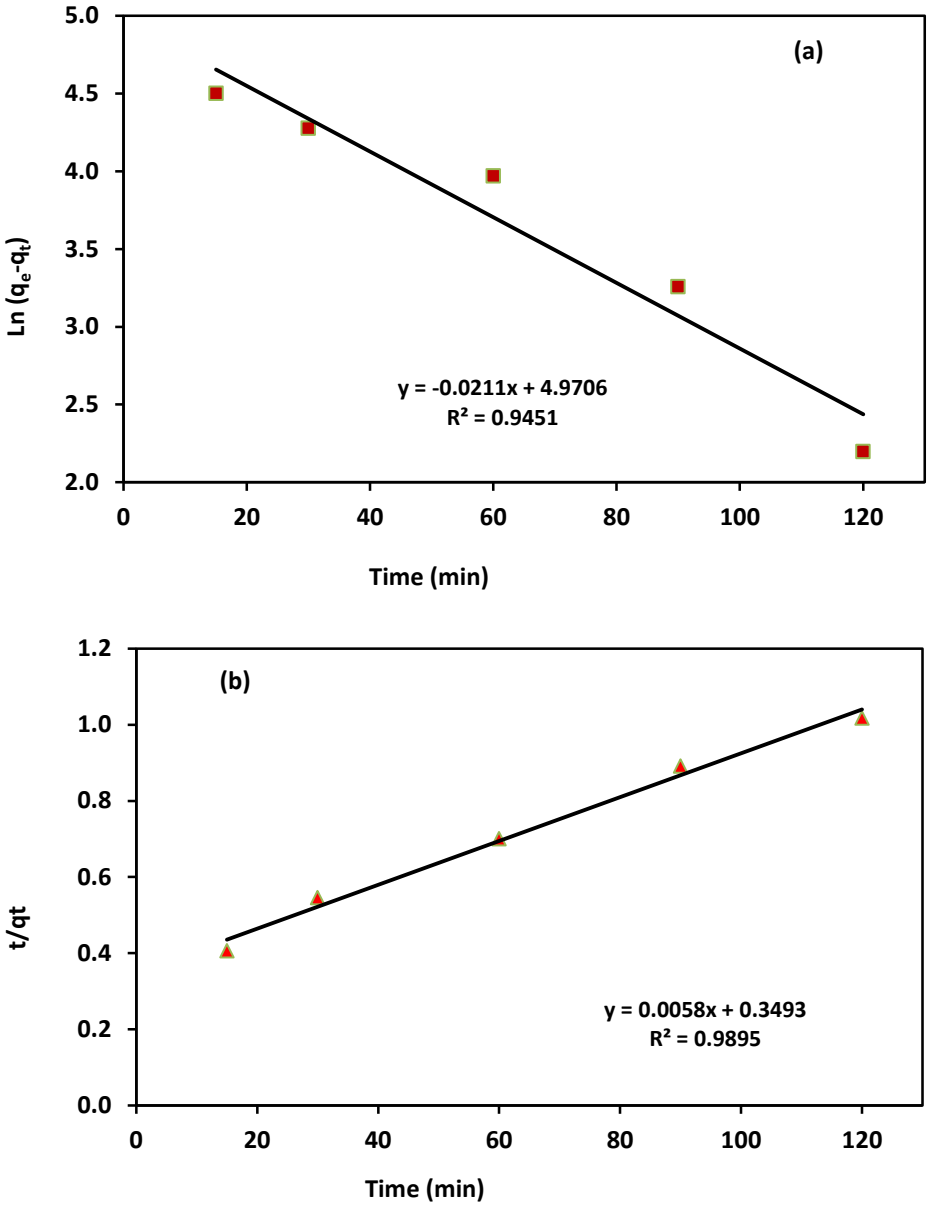

Figure 3-9 (a). Pseudo first order model; (b). Pseudo second order model of Zn(II) ion uptake onto CCDE beads [pH = 6; adsorbent dosage = 0.25 g; temperature = 283 K].

3.4.10 Adsorption isotherm

Equilibrium isotherm of Zn(II) ion adsorption onto CCDE beads was studied at concentrations ranging from 50 to 500 mg/L, temperatures 283 K, and 120 min contact time. The equilibrium results were analyzed using Langmuir and Freundlich

adsorption isotherm models. The Langmuir isotherm equation is expressed as follows [72]:

$$\frac{C_e}{q_e} = \frac{1}{K_L q_m} + \frac{C_e}{q_m} \qquad (3-8)$$

Where C_e is the equilibrium concentration of metal ions (mg/L), q_e is the adsorption capacity at equilibrium (mg/g), q_m is the theoretical maximum adsorption capacity (mg/g), and K_L is the Langmuir adsorption constant (L/mg).

The Freundlich isotherm equation is given as follows [72]:

$$\ln q_e = (1/n)\ln C_e + \ln K_f \qquad (3-9)$$

Where K_f is the maximum adsorption capacity and 1/n is heterogeneity factor.

Langmuir and Freundlich adsorption isotherms of Zn(II) ion removal onto CCDE beads are represented in Figure 3-10 (a) and (b). They showed that the adsorption isotherms were largely linear and well-fitting with Langmuir isotherm with correlation coefficient 0.9969, which indicated that the Zn(II) ion adsorption onto the surface of CCDE beads was a monolayer adsorption and a heterogeneous surface adsorbents with a limited number of same binding sites, this means all active sites were energetically identical.

It has been reported that separation factor (based on Langmuir model) is defined as:

$$f_s = \frac{1}{1 + K_L C_o} \qquad (3-10)$$

When (f_s) is between 0 and 1, the adsorption isotherm is favorable on adsorbents however when (f_s) is greater than 1, the adsorption isotherm is unfavorable [73]. For Zn(II) ion adsorption onto CCDE beads, the separation factor was 0.112 at initial concentration 500 mg/L, which indicated that the removal of Zn(II) ion onto prepared CCDE beads is favorable.

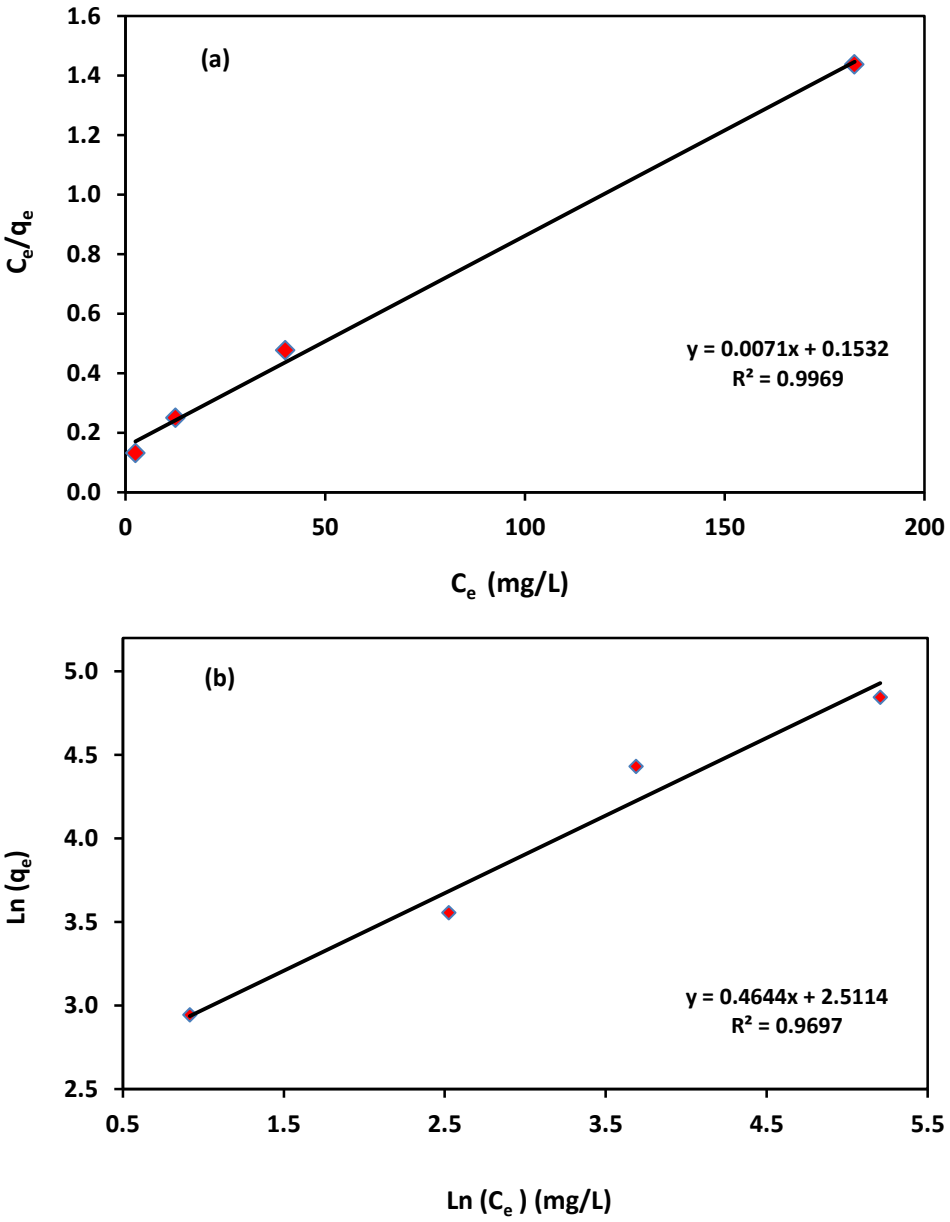

Figure 3-10 (a) Langmuir adsorption isotherm; (b) Freundlich adsorption isotherm of Zn(II) ion uptake onto CCDE beads [pH = 6; adsorbent dosage = 0.25 g; temperature = 283 K].

3.4.11 Effects of anions on Zn(II) ion uptake

The sulphate, chloride, and nitrate anions are usually present in the industrial wastewater streams and could interfere with Zn(II) ion removal. Therefore, the effect of these anions were studied at pH 6, initial zinc concentration 500 mg/L, and temperature 283 K. The experimental studies were carried out at different

concentrations of these anions ranging from 0.05 to 0.2 mol/L. As shown in Figure 3-11. The sulphate, chloride, and nitrate anions did not show a significant effect on Zn(II) ion adsorption onto CCDE beads, the Zn(II) removal capacity was reduced by 5.2 % (reduced from 127.4 to 120.77 mg/g) with existence of sulphate ions, and by 7% in presence of nitrate ions, whereas the Zn(II) ion adsorption was decreased only by 4.4% in the presence of chloride ions in solution. As reported (Figure 3-5), the amine groups are deprotonated at pH greater than 5.8. Therefore, the anions are expected to compete with Zn(II) ions on the same active sites of amine groups and that led to reduction in total Zn(II) ion adsorption capacity onto CCDE beads.

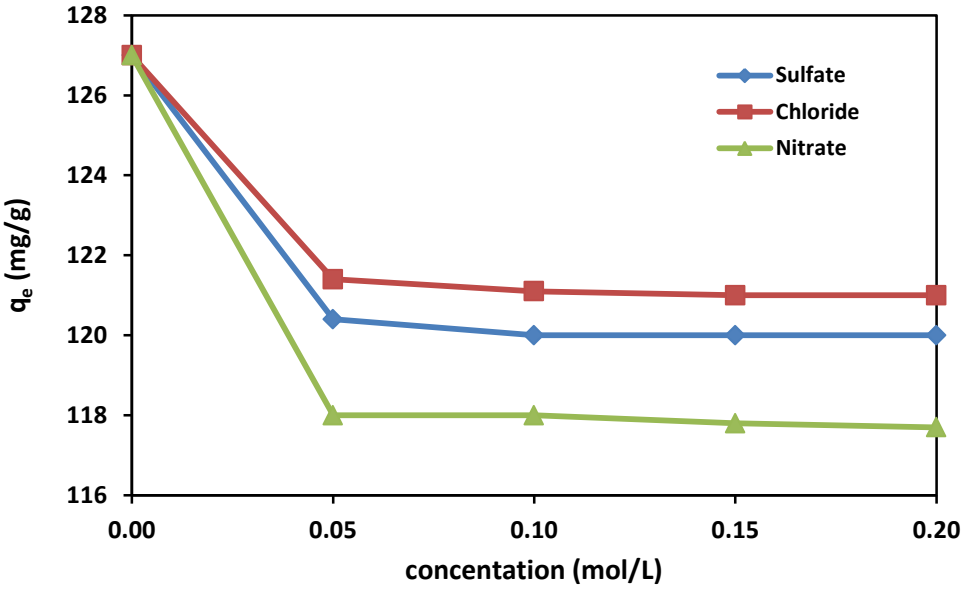

Figure 3-11. Effect of various anions on Zn(II) ion adsorption onto CCDE beads [pH = 6; adsorbent dosage = 0.25 g; temperature = 283K; C_o= 500 mg/L].

3.4.12 Dynamic studies

Dynamic experiments were investigated in a porous bed system, consisting of an acrylic column, with 16 cm height and 2 cm internal diameter. Figure 3-12 represents the results of column experiments in form of breakthrough curves for Zn(II) ion

removal from aqueous solution onto CCDE beads. The breakthrough curves were determined by plotting the C_t/C_o against the time (where C_t: effluent zinc concentration, C_o: initial zinc concentration). In high flow rate, a large amount of zinc solution passes through the column producing more Zn(II) ions binding with active sites in adsorbents, which makes it saturated in short time at a high Zn(II) ions uptake. In contrast, long breakthrough time, the time when the effluent concentration (C_e) reached 50% of the feed concentration (C_o), and low Zn(II) ion adsorption capacity occurred at low flow rate due to the high residence time of Zn(II) ions inside the column. However, the results showed that the breakthrough time (t_b) was 220 min and the exhausted time (t_s), the time when the effluent concentration (C_e) reached 95% of the feed concentration (C_o), was 335 min at flow rate 3 mL/min, while at flow rate 6 mL/min, the breakthrough time (t_b) and exhausted time (t_s) were just 115 min, 195 min, respectively.

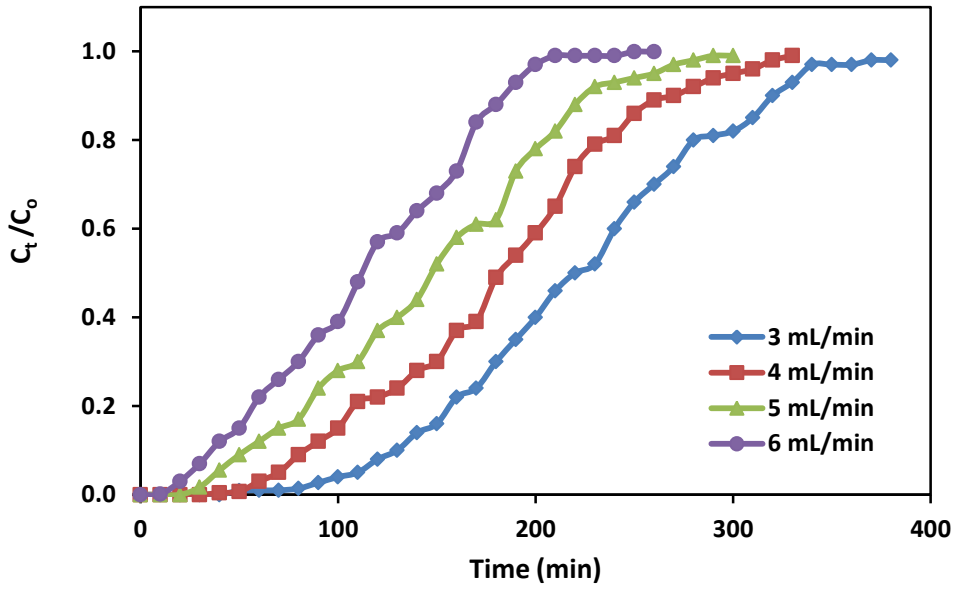

Figure 3-12. Effect of flow rate on the breakthrough curve of Zn(II) ions adsorption onto CCDE beads [pH = 6; beads size = 2 mm; C_o = 100 mg/L].

3.4.13 Desorption and reusability

The performance of any adsorbents should not only depend on the adsorption capacity, but also on their regeneration and sustainable reuse. From batch adsorption studies (Figure 3-6), the amount of Zn(II) ion uptake decreased with increasing the solution-pH. Consequently, the regeneration of CCDE beads was allowed to pass through a basic solution (0.2 mol/L NaOH) through the backed-bed column at flow rate 2 ml/min for about 3 h (360 ml of NaOH - solution), and then allowed to pass deionized water at the same flow rate. Figure 3-13 shows the Zn(II) ion desorption behavior from the CCDE beads in first and fourth cycles of adsorption- desorption processes. It was observed that the desorbed percentages of Zn(II) ion from adsorbents were 94.6% and 87% in the first and fourth cycle, respectively. Therefore, the reuse study of adsorbent indicated that CCDE beads were efficient and proficient stable adsorbent for Zn(II) ion uptake from aqueous solution.

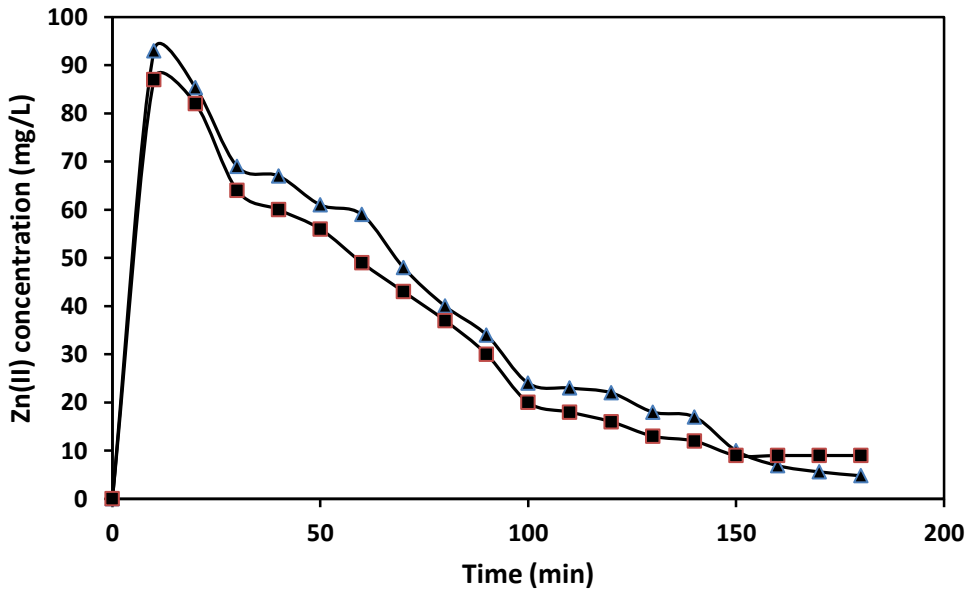

Figure 3-13. Regeneration bed column by 0.2 M NaOH after loaded by 100 mg/L Zn(II) ion solution [▲(first cycle), ■ (fourth cycle)].

3.5 Conclusions

The study indicated that the removal rate of Zn(II) ions from aqueous solution onto CCDE beads was excellent and up to 127.4 mg/g. The adsorption capacity of Zn(II) ion was found to be depended on the solution-pH, flow rate, contact time, and temperature. The highest Zn(II) ion uptake capacity onto prepared CCDE beads was at pH 6, initial concentration 500 mg/L, and temperature 283 K. Adsorption kinetic data were well-fitted with the pseudo second order model. Langmuir model was revealed to be the best fitting model for Zn(II) ions removal with R^2 value 0.9969. The values of thermodynamic quantities such as Gibb's free energy change, enthalpy, entropy, and isosteric heat of adsorption indicated that the adsorption process of Zn(II) ions onto CCDE beads was exothermic, spontaneous, and the CCDE beads had energetically heterogeneous surface adsorbents. The studies on column operations showed that the flow rate had a big impact on adsorption rate and exhausted time of adsorbents. However, adsorbed Zn(II) ions on CCDE beads were chemically regenerated by 0.2M NaOH and reused for adsorption process.

CHAPTER 4. PREPARATION AND CHARACTERIZATION OF CHITOSAN-COATED DIATOMACEOUS EARTH FOR HEXAVALENT CHROMIUM REMOVAL

4.1 Abstract

A novel chitosan coated diatomaceous earth (CDE) beads were prepared by the drop-wise method and characterized by Fourier transform infrared spectroscopy (FTIR), Brunauer-Emmett-Teller (BET), scanning electron microscopy (SEM), energy dispersive X-ray spectroscopy (EDS), and zeta potential. Prepared CDE beads were used for Cr(VI) adsorption from aqueous systems. The effect of several factors including solution-pH, initial Cr(VI) concentration, temperature, and contact time on adsorption process was examined. The adsorption results revealed that the Cr(VI) adsorption was fitting well the Langmuir model indicating a homogeneous adsorption surface for Cr(VI) on the CDE beads. The kinetics of adsorption suggested a pseudo-second-order model fittings better than the pseudo-first-order model. The maximum Cr(VI) adsorption capacity onto prepared CDE beads was 84.23 mg/g. In competition adsorption, the affinity of CDE beads toward mixed metal ions was high for Cr(VI) followed by Pb(II) and it was low for Zn(II) and Ni(II). Loaded CDE beads with Cr(VI) were successfully regenerated by NaOH and reused up to five cycles. The overall results emphasize that the CDE beads could be used as an economically applicable and sustainable adsorbent for Cr(VI) removal from aqueous solutions.

4.2 Introduction

Heavy metals contamination is one of the biggest concern because of their harmful effect on natural resources and the environment, even at very low concentrations. Hexavalent chromium is in the priority pollutants list/group A of the US Environmental Protection Agency (EPA). It is not biodegradable in nature and has a significant effect on human health such as skin ulceration, liver damage, and pulmonary congestion [17]. The main source of chromium is from various industrial wastewaters such as leather tanning, electroplating, metal polishing, paint manufacturing, and textile coloring [87]. However, industrial wastewater typically contains high concentrations of chromium ranging from 0.5 to 270 mg/L [3]. Removing chromium from water and wastewater is extremely necessary and mandatory to reduce its influence on the ecosystem. Physical, chemical, and biological processes for Cr(VI) removal from wastewater have been extensively researched and used such as precipitation, adsorption, ion exchange, reverse osmosis, and electrodialysis [97]. Adsorption has been considered as one of the favorable processes of heavy metal removal from aqueous solutions, because it is a simple process, an inexpensive method, and flexible in design, chemical consumption or/and waste generation are not a significant issue compared to other methods, and it is suitable for removing very low metal ion concentrations [98]. In recent years, bioadsorbents have been considered as an effective material to remove heavy metal ions from aqueous solutions because they are inexpensive, abundant in nature, sustainable, friendly to the environment, effective in low and medium metal levels, and easy to regenerate for reuse [45]. Many bioadsorbents have been studied for removing toxic heavy metal contaminants from aqueous solution such as microalgal [99], alginate [46], seaweed [47], chitin [83], and chitosan [50,100]. Among these

biosorbents, chitosan has been repeatedly characterized as the excellent adsorbent for heavy metal ion adsorption.

Chitosan (poly-β-(1→4)-2-amino-2-deoxy-D-glucose) is commercially produced by the partial deacetylation of chitin, the second most abundant natural polymer in the world after cellulose [101, 102]. In addition, Chitosan is biocompatible, biodegradable, non-toxic to human, and it shows antimicrobial and antioxidant activities [103]. It has unique physicochemical properties such as chemical stability, high reactivity, metal ion binding groups ($–NH_2$, –OH), excellent chelation behavior, and high selectivity towards pollutants. Recently, chitosan has received much attention because it can be produced from renewable sources like seafood waste. Even though chitosan is biodegradable and biocompatible, it has a low specific surface area, swelling properties, a tendency to agglomerate, poor mechanical properties and dissolution in highly acidic solution, which limit its application in adsorption[88, 104]. Therefore, it is necessary to supply physical or chemical support on chitosan to enhance its properties. Various chemical and physical modifications of chitosan material have been investigated and are summarized in Table 4-1 along with their maximum Cr(VI) adsorption capacity.

To overcome some limitations associated with pure chitosan adsorbent, in this study, a new composite chitosan was prepared by coating chitosan onto an inert substance, diatomaceous earth, and then forming it into spherical beads by using a drop-wise method. Diatomaceous earth is a non-hazardous amorphous natural material formed from the remains of diatoms, which has grown and deposited in sea or lake beds and has unique physical and chemical properties such as high permeability, high porosity (35 – 65%), small particle size, adsorption capabilities, low thermal conductivity and density, and high surface area (10-30 m^2/g) [67]. The

chitosan-coated diatomaceous earth beads were characterized by Fourier transform infrared spectroscopy (FTIR), Brunauer, Emmett, Teller (BET), scanning electron microscopy (SEM), energy dispersive X-ray spectroscopy (EDS), and zeta potential. In addition, The effect of solution-pH, temperature, initial Cr(VI) concentration, and contact time on the adsorption process for Cr(VI) removal were systematically investigated. Moreover, the regeneration of the CDE beads was investigated by using diluted sodium hydroxide. The experimental data were fitted with adsorption isotherm and kinetic models.

Table 4-1 Maximum adsorption capacities of Cr(VI) onto different chitosan modifications

Adsorbents	**pH**	**C_0 (mg/L)**	**q_{max} (mg/g)**	**Reference**
Chitosan/zeolite	4	260	17.28	88
Chitosan/cellulose	4	260	13.05	88
Chitosan/bentonite	3	200	66.6	105
Chitosan/ceramic alumina	4	5000	153.8	106
Chitosan/thiocarbamoyl	4	1000	434.8	86
Chitosan/graphite oxide	2	2000	219.5	87
Chitosan/polymethylmethacrylate	3	1000	67	17
Chitosan/montmorillonite magnetic microspheres	2	80	73	107
Chitosan/zirconium	5	50	175	50
Chitosan/fly ash	-	156	36.22	95
Chitosan/perlite	4	5000	153.8	108
Chitosan/zwitterionic	2	25	99.3	109
Chitosan/sporopollenin microcapsules	4	12	51.47	90
Hydrolyzed crosslinked chitosan	6	350	11.3	91
Chitosan/diatomaceous earth	3	1000	84.23	Present study

4.3 Experimental Section

4.3.1 Materials

Medium molecular weight chitosan (deacetylation 87%, viscosity = 1000 mPa.s, molecular weight ~190,000 – 310,000 g/mol) and diatomaceous earth powder (90% SiO_2, 4% Al_2O_3, 2% Fe_2O_3, 4% others) were procured from Aldrich Chemical Corporation (St. Louis, MO, USA). 2.829 g of potassium dichromate ($K_2Cr_2O_7$) was dissolved in 1 L of deionized water to prepare a stock solution containing 1000 mg/L of Cr(VI). Adequate concentrations (50, 100, 250, 500, 1000 mg/L) were prepared from standard stock solutions by consecutive dilution. Sodium hydroxide and oxalic acid were used to dissolve chitosan and adjust the solution-pH. Deionized water was used during the experimental studies. All chemicals used in this study were of analytical grade. The pH-meter was calibrated with buffer solutions (pH 4, 7 and 9) and the initial solution-pH was adjusted to the required values.

4.3.2 Preparation of CDE Beads

Since chitosan is dissolvable in highly acidic solution, we used oxalic acid to dissolve chitosan. About 20 g of chitosan was gradually added into 1 L of 0.2 mol/L oxalic acid solution under stirring at 200 rpm. The solution was heated to 65 – 70 °C for 6 h to get a homogenous solution gel of chitosan. About 20 g of acid- treated diatomaceous earth was added into the chitosan gel under heating at 60 °C and mixing at 300 rpm for another 6 h. The spherical beads of chitosan-coated diatomaceous earth were formed by dropping the final gel mixture into a 0.8 mol/L of NaOH precipitation container. The objective of adding acidic chitosan-diatomaceous earth mixture into NaOH-solution was to rapidly neutralize the gel mixture drops and obtain the spherical shape. The hydrogel beads remained in the NaOH-solution under 30 rpm

mixing for 6 h for hardening. Eventually, the prepared beads were washed with deionized water to a neutral pH. The beads were dried by vacuum furnace for 24 h at 70 °C. The final dry chitosan coated diatomaceous earth (CDE) beads have an average diameter of about 2 mm as shown in Figure 4-1.

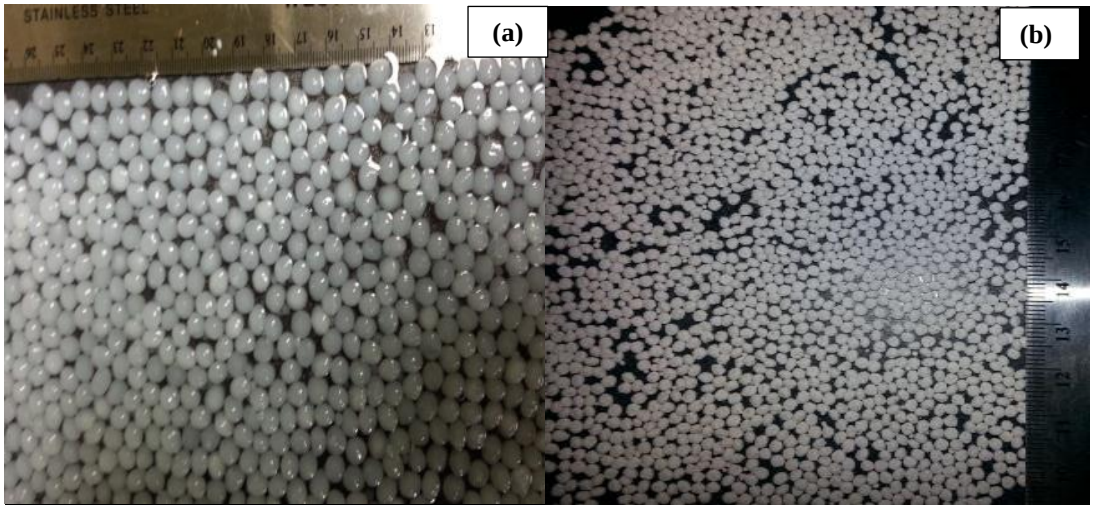

Figure 4-1 (a) Wet chitosan-coated diatomaceous earth beads; (b) Dry chitosan-coated diatomaceous earth beads.

4.3.3 Adsorption Experiments

Batch experiments of Cr(VI) adsorption from aqueous systems onto CDE beads were investigated to determine the CDE adsorption capacity at different initial Cr(VI) concentrations ranging from 0.96 to 19.23 mmol/L (50 – 1000 mg/L). In a series of 50 mL Erlenmeyer flasks, 0.5 g of CDE beads was immersed in 50 mL of Cr(VI) solution and agitated for 12 h in an orbital shaker at different temperatures ranging from 10 to 40 °C and speed 200 rpm. After a certain time, samples were taken from the flasks and filtrated to determine the final Cr(VI) concentration in the filtrate. Coupled plasma-mass spectrometer (ICP-MS) was used to determine Cr(VI) concentrations. When steady state adsorption was attained, the Cr(VI) removal capacity in samples was determined by mass balance on the Cr(VI) ion, according to Equation 4-1 [91]:

$$q_e = \frac{(C_0 - C_e)V}{m} \qquad (4-1)$$

Where q_e is the Cr(VI) adsorbed at equilibrium (mg/g), C_0 and C_e (mg/L) are the initial and equilibrium concentrations of Cr(VI) ions, respectively, V (L) is the volume of solution, and m (g) is the dry weight of CDE beads. Batch adsorption runs were performed at different initial solution-pH, temperatures, initial Cr(VI) concentrations, and contact times.

4.4 Results and Discussion

4.4.1 Characterization of CDE Beads

The CDE beads were characterized to evaluate their physical and chemical properties (Table 4-2), in order to provide a better interpretation of the adsorption process mechanism. Surface area, pore volume, and pore diameter were evaluated by nitrogen adsorption/desorption at 77 K using a Micrometrics ASAP 2010 surface analyzer. The BET (Brunauer-Emmett-Teller) surface area of chitosan, diatomaceous earth, and prepared CDE beads were found to be 1.9, 23.8, and 6.4 m^2/g, respectively. It appears that chitosan blocked a number of pores in diatomaceous earth, and the chitosan film was not porous enough to retain the original porosity of diatomaceous earth. The decrease of surface area was significant in the case of CDE beads since chitosan was coated on diatomaceous earth. The average diameter of the pores in CDE beads was found to be 0.00323 μm, whereas the average pore diameter of pure chitosan beads were 0.0022 μm. The average pore volume of pure chitosan bead and CDE bead were found to be 2.61×10^{-9} and 7.4×10^{-9} m^3/g, respectively.

Table 4-2 The main physicochemical properties of CDE beads.

Parameters	Value
Physical nature	porous
Average particle diameter (mm)	2
Surface area (m^2/g) (based on BET*)	6.4
Bulk density (g/cm^3)	0.338
Particle density (kg/m^3)	481
Porosity	0.298
Pore diameter (mm) (based on BET)	3.23×10^{-6}
Pore volume (m^3/g) (based on BET)	7.4×10^{-9}
pH - point of zero charge (pH_{PZC})	5.8
Compositions (based on EDS**) (excluding Pt) : Carbon content (Wt%)	35.47
Oxygen content (Wt%)	23.11
Nitrogen content (Wt%)	10.3
Silica content (Wt%)	28.37
Others (Fe, Al) (Wt%)	2.42

*BET : Brunauer, Emmett,Teller measurement.

**EDS : energy dispersive X- ray spectroscopy.

4.4.2 Fourier Transform Infrared Spectroscopy (FTIR)

To identify the mechanism of Cr(VI) bonding with the CDE beads, FTIR-spectra were determined for the CDE beads before and after Cr(VI) adsorption. As shown in Figure 4-2, FTIR results of fresh CDE beads showed peaks at 3300 cm^{-1} which is a band of stretching vibration of O-H, and at 1100 cm^{-1} which is related to C-C bond. Extra bond was observed between 1430 and 1650 cm^{-1} which corresponds to C=N stretching bond, and at 2800 up to 2900 cm^{-1} which is for C-H stretching vibration. The stretching bonds of the Si-O and Si-O-Si groups and the deformation bonds for these groups correspond to 630 cm^{-1} in CDE beads, whereas they do not exist in CS

beads. The FTIR-spectra for loaded CDE beads with Cr(VI) showed that the peaks at 1650 cm^{-1} (C=N) and at 2800 cm^{-1} (C-H) were sharper and separately shifted to 1625 and 2870 cm^{-1}, respectively. However, after Cr(VI) adsorption, a peak change in the FTIR-spectra at the 1450 cm^{-1} occurred which corresponds to the -N-H deformation vibration and at the 1320 cm^{-1} which is assigned to -C-N- stretching vibration in chitosan structure. Depending to these changes and shifts in peaks, we conclude that the amine groups are the main adsorption sites for Cr(VI) adsorption onto the CDE beads. Moreover, FTIR-spectra were changed at 3430 cm^{-1} which indicates -O-H stretching vibration in the alcohol group, and at 860 cm^{-1} which indicates -C-O stretching vibrations. The changes suggest that the hydroxyl groups in chitosan molecules contribute to Cr(VI) adsorption as well [27].

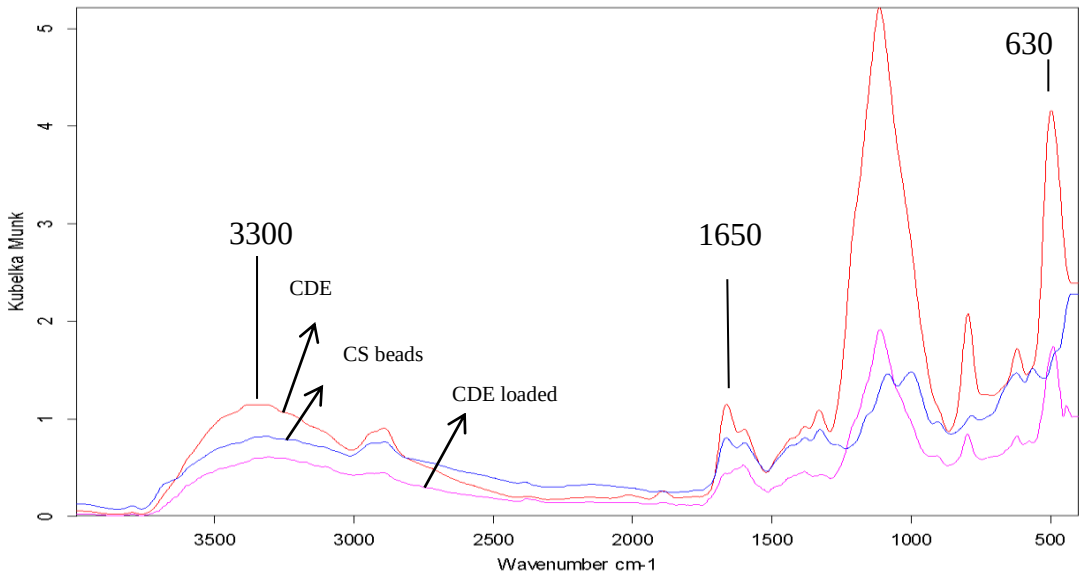

Figure 4-2 Fourier-transform infrared (FTIR) spectra of CDE beads and chitosan (CS) beads.

4.4.3 Scanning Electron Microscopy (SEM)

The CDE beads were analyzed by using high-resolution Hitachi S - 4700 Field Emission Scanning Electron Microscopy (SEM) in terms of morphology. Figure 4-3 displays the SEM images of fresh and loaded CDE beads surface morphology at 50

μm, and 1000 kV image magnification. The SEM image of fresh beads showed that the outer surface of CDE beads was significantly porous and had wrinkles structure, which enhances the Cr(VI) ions spreading over the CDE beads and binding with active sites, whereas the beads loaded with Cr(VI) ions had less rough surface due to the Cr(VI) adsorption. One can see that the Cr(VI) ions are adsorbed onto CDE beads which is obvious from the bright layer on the surface of CDE beads (Figure 4-3b).

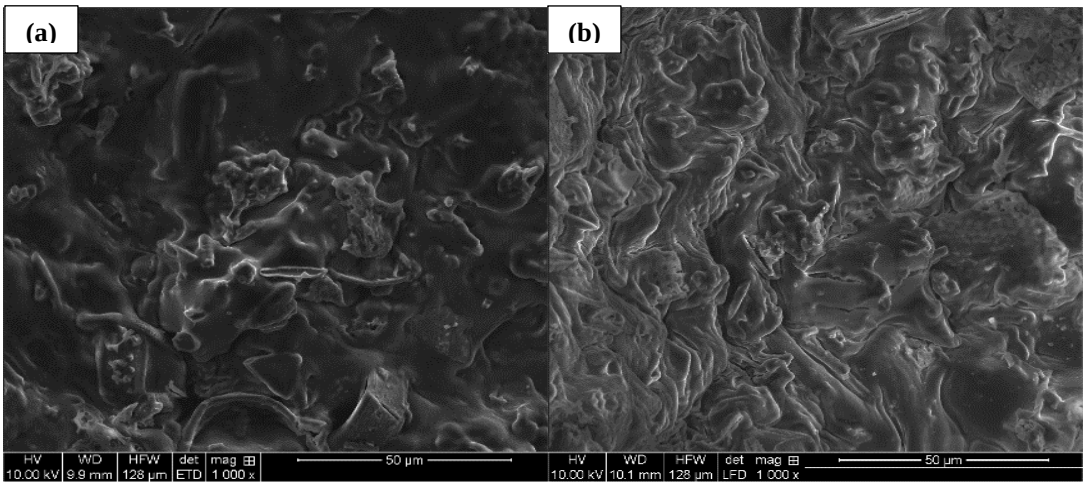

Figure 4-3 Scanning Electron Microscopy of: (a) fresh CDE beads, (b) CDE beads loaded with Cr(VI).

4.4.4 Energy Dispersive X-ray Spectroscopy (EDS)

The use of EDS X-ray can confirm the adsorption of Cr(VI) ions onto CDE beads and determine the weight percentage of Cr(VI) ions that is adsorbed. The EDS X-ray microanalysis was carried out on CDE beads before and after their exposure to the Cr(VI) solution, as shown in Figure 4-4. Figure 4-4b shows large peaks at 0.5 kV (kα, Cr) and at 5.2 kV (kβ, Cr) for Cr(VI) ions. The quantitative elemental compositions of each component in the CDE beads are indicated in the insert tables in Figures 4-4a and b. The content of adsorbed Cr(VI) onto CDE beads reached as high as 7.53 %wt. The total weight percentages of fresh and loaded beads were 98.64 and 97.28 %,

respectively, while the difference from 100 % indicates impurities like Fe, Na, and Al. To avoid damaging or burning the CDE beads by the electronic beam, platinum was used to coat the CDE beads during the EDS X-ray test. The results indicates that the prepared CDE beads have a high adsorption capacity of Cr(VI) from the aqueous solution.

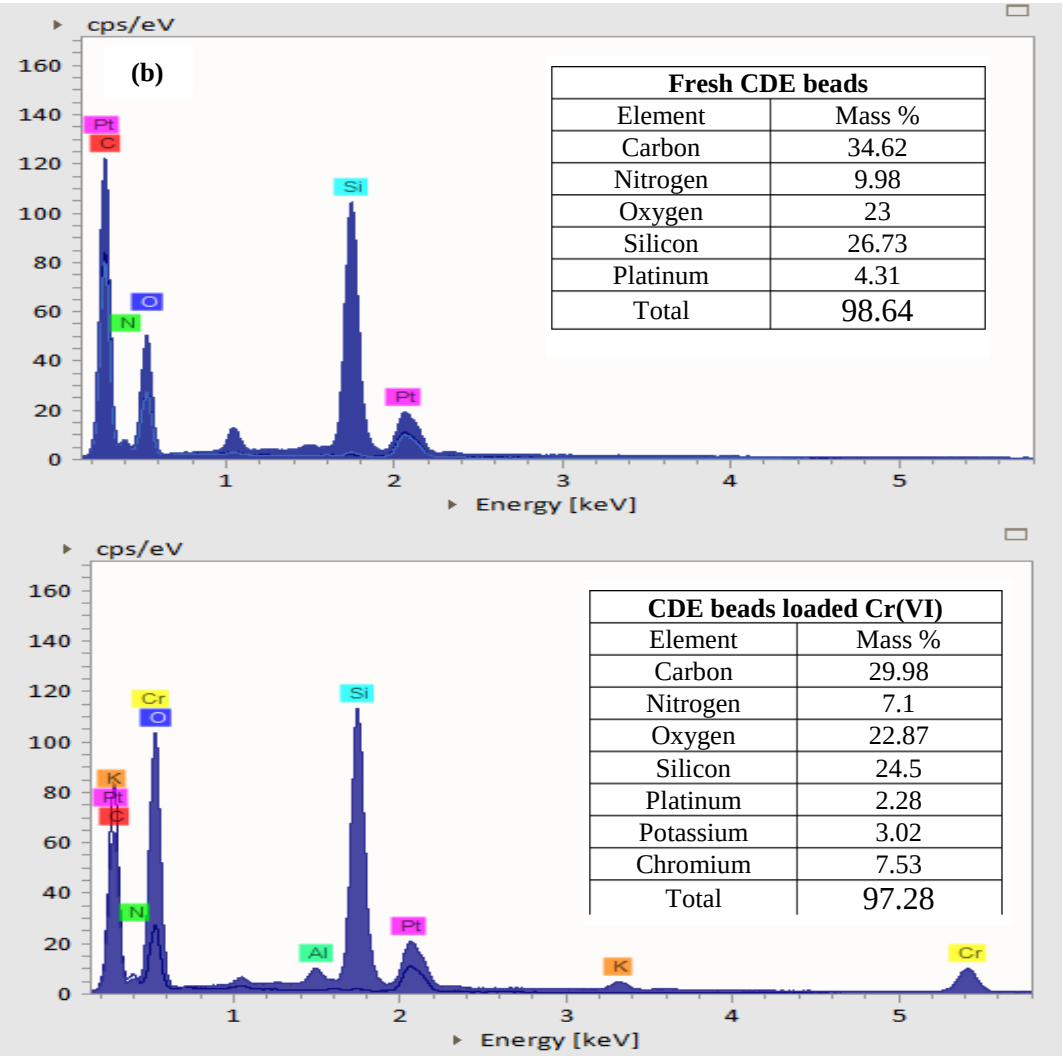

Fresh CDE beads	
Element	Mass %
Carbon	34.62
Nitrogen	9.98
Oxygen	23
Silicon	26.73
Platinum	4.31
Total	98.64

CDE beads loaded Cr(VI)	
Element	Mass %
Carbon	29.98
Nitrogen	7.1
Oxygen	22.87
Silicon	24.5
Platinum	2.28
Potassium	3.02
Chromium	7.53
Total	97.28

Figure 4-4 Energy Dispersive X- ray Spectroscopy (EDS) of: (a) Fresh CDE beads; (b) CDE beads loaded with Cr(VI).

4.4.5 Zeta Potentials

The zeta potential values over a range of solution-pH values adjusted using diluted $C_2H_2O_4$ or NaOH were measured by using photon correlation spectroscopy and electrophoretic light scattering. A 10 mg of chitosan-coated diatomaceous earth powder was suspended in 10 mL of deionized water and irradiated. As shown in Figure 4-5, the results showed that the prepared CDE adsorbents have positive charges in acidic media and negative charges in basic media. However, the pH - point of zero charge (pH_{PZC}) of CS and CDE beads were 6.63 and 5.8, respectively. The positive zeta potential at low pH was presumably created by protonation of amine groups in chitosan. Therefore, the negative species are favorite to adsorb onto the CDE beads at low pH and species that have positive charges were easily interacted with CDE beads in basic condition.

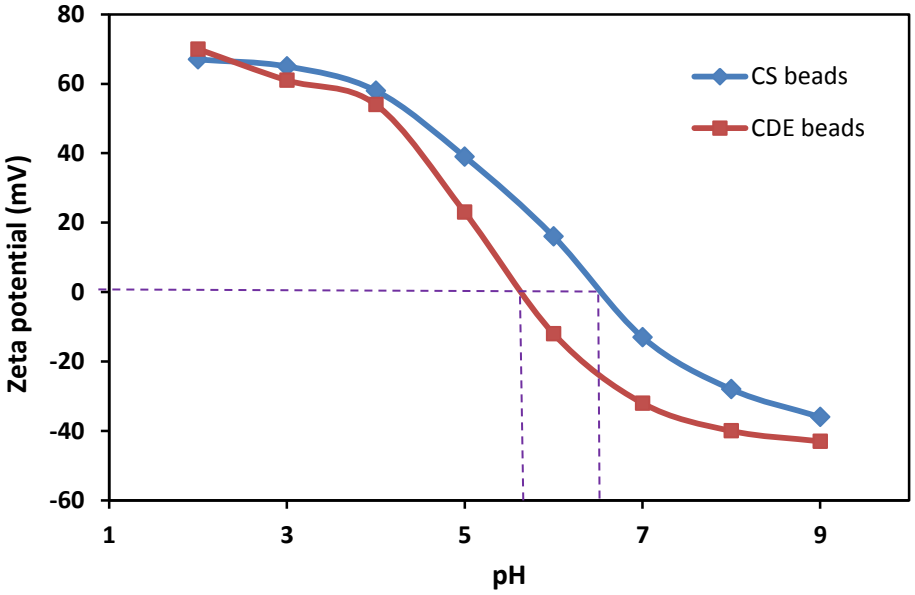

Figure 4-5 Zeta potentials of CDE beads and pure chitosan beads (CS beads) at different solution-pH.

4.4.6 Effect of Initial Solution-pH

In aqueous solution, Cr(VI) ions exist in different anion forms depending on solution-pH. Dichromate ($Cr_2O_7^{2-}$) and hydrogen chromate ($HCrO^{4-}$) are present at pH range 2 - 6, whereas chromate (CrO_4^{2-}) is present at pH > 6 [88]. The amine groups ($-NH_2$) in chitosan are mainly responsible for metal ion adsorption, and can be protonated to NH^{3+} in acidic medium. As reported, the zeta potential results (Figure 4-5) show that the CDE beads had zero charge (pH_{PZC}) at pH 5.8, therefore, the prepared CDE beads have negative charge above pH 5.8. Consequently, the surface charge of the CDE beads determines the bond type created between the Cr(VI) ions and the CDE beads surface. Figure 4-6 shows that the highest removal of Cr(VI) onto CDE beads was 1.62 mmol/g (84.23 mg/g) at pH 3 due to the predominance of $Cr_2O_7^{2-}$ and $HCrO^{4-}$ ions in the solution, whereas it was 1.06 mmol/g (55.10 mg/g) onto pure chitosan beads. The reduced removal capacity at low pH, less than 3, was due to the rivalry between protons (H^+) in the aqueous solution and the Cr(VI) ions onto the same active adsorption site of chitosan. In this case, H_2CrO_4 was formed and because it does not have a charge, does not favor adsorption onto adsorbents [54]. The extent of amine groups protonation would be reduced with rising solution-pH above 3. Therefore, the surface charge of CDE beads might have been partially deprotonated, which inhibited the adsorption capacity of Cr(VI) species resulting in decreased Cr(VI) adsorption at pH greater than 3 [62]. These results are in a good agreement with Hasan et al. 2003 [108].

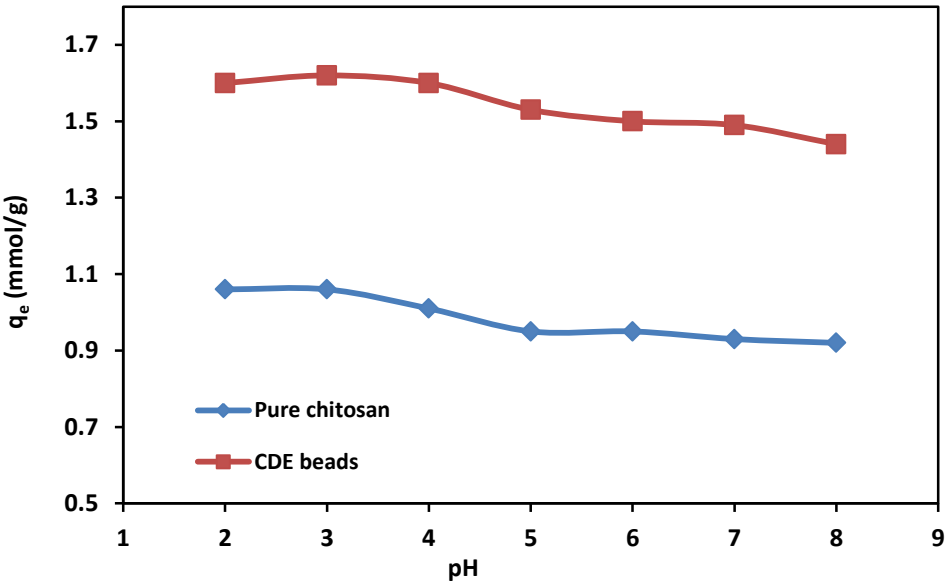

Figure 4-6 Effect of solution-pH on Cr(VI) adsorption onto CDE beads (C_0= 19.23 mmol/L; temperature = 10 °C; adsorbent dosage = 0.5 g).

4.4.7 Effect of Initial Chromium Concentration

The effect of initial Cr(VI) concentration on the adsorption capacity of CDE beads was investigated in the range 0.96 - 19.23 mmol/L or 50 - 1000 mg/L, pH 3, temperature 10 °C, and 0.25 - 12 h contact time. The results are illustrated in Figure 4-7. It was observed that the amount of Cr(VI) removal onto CDE beads increased from 0.12 to 1.62 mmol/g with increasing initial Cr(VI) concentration from 0.96 to 19.23 mmol/L; this occurs because at high initial Cr(VI) concentration, the concentration gradient between bulk solution and CDE beads surface overcomes the mass transfer resistance of Cr(VI) ions. Adsorption of Cr(VI) ions onto CDE beads was rapid in the first 1.5 h due to the availability of active adsorption sites, and slowed down until it reached the equilibrium at around 3.5 h in all adsorption batch runs.

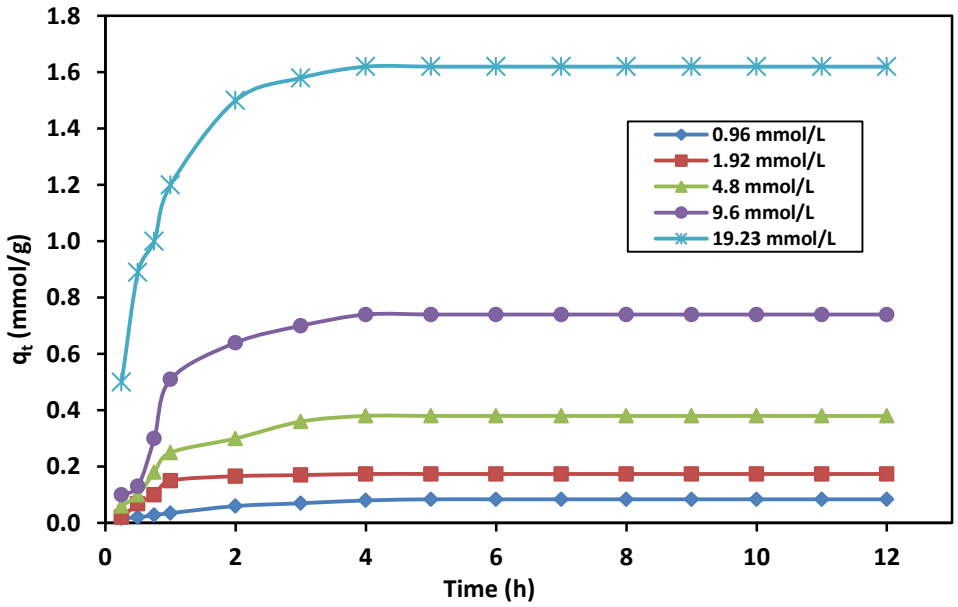

Figure 4-7 Effect of initial Cr(VI) concentrations and contact time on Cr(VI) removal onto CDE beads (pH = 3; temperature = 10 °C; adsorbent dosage = 0.5 g).

4.4.8 Effect of Temperature

The effect of temperature on Cr(VI) removal onto CDE beads was investigated at 10, 20, 30, and 40 °C (283, 293, 303, and 313 K). As shown in Figure 4-8, the results showed that the temperature had a negative influence on Cr(VI) adsorption capacity. Similar to our previous studies [99], the adsorption of Cr(VI) onto pure chitosan beads was found to be strongly affected by increasing temperature. With increasing temperature from 10 to 40 °C, the Cr(VI) removal decreased from 1.62 to 1.44 mmol/g. The reason of decreasing Cr(VI) removal at high temperature is the increasing Cr(VI) ions solubility in the solution with increasing temperature, which reduces the interaction forces between Cr(VI) ions and the active sites in the CDE beads, and makes these forces weaker than those between Cr(VI) ions and solution. As a result, the Cr(VI) ions are more difficult to adsorb at high temperature. Therefore, low temperatures are favorable for Cr(VI) ion removal onto prepared CDE beads.

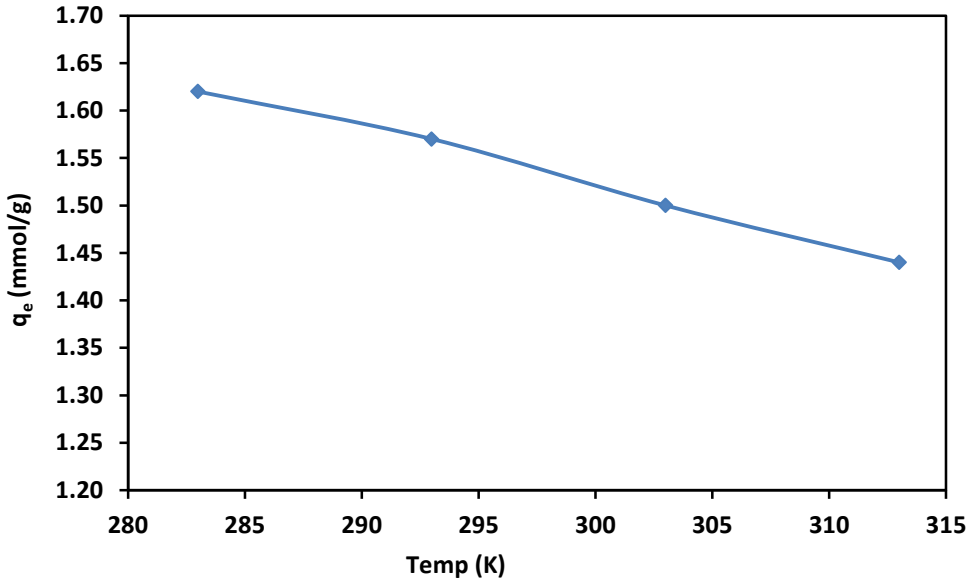

Figure 4-8 Effect of temperature on Cr(VI) removal onto CDE beads (pH = 3; C_0 = 19.23 mmol/L; adsorbent dosage = 0.5 g).

The thermodynamic parameters (ΔH^o, ΔS^o, and ΔG^o) for Cr(VI) ions adsorption on prepared CDE beads can be calculated by using following equations:

$$\Delta G^o = \Delta H^o - T\Delta S^o \qquad (4-2)$$

Where ΔG^o can be expressed as,

$$\Delta G^o = -RT\ln K_d \qquad (4-3)$$

Substituting Equation (4-2) into Equation (4-3) provides van't Hoff equation [108]:

$$\ln K_d = \frac{\Delta S^o}{R} - \frac{\Delta H^o}{RT} \qquad (4-4)$$

Where R is gas constant (8.314 J/mol.K) and T is the absolute temperature (K), K_d is the distribution constant (K_d (L/g) = q_e/C_e), ΔG^o is Gibbs free energy, ΔH^o is enthalpy change, and ΔS^o is entropy change. The slope of plotting $\ln K_d$ versus 1/T provides the value of ΔH^o and the intercept is the value of ΔS^o (Figure 4-9). ΔH^o may be considered as the heat of adsorption when the adsorption capacity of CDE beads

reaches its saturation capacity of Cr(VI) ions. The values of ΔH^o, ΔS^o, and ΔG^o are presented in Table 4-3. The results of Cr(VI) uptake onto CDE beads show that the adsorption process was exothermic due to the negative value of ΔH^o, and the negative values of ΔG^o indicated that the adsorption process are spontaneous. The results are in good agreement with Tellinghuisen 2006 [66] and Hu et al. 2011 [62].

Table 4-3. Thermodynamic parameters of Cr(VI) adsorption onto CDE beads.

T(K)	ln K_d (L/g)	ΔG^o (kJ/mol)	ΔH^o (kJ/mol)	ΔS^o (kJ/mol.K)
283	1.676	- 3.944	- 14.565	- 0.0374
293	1.492	- 3.635		
303	1.267	- 3.191		
313	1.092	- 2.841		

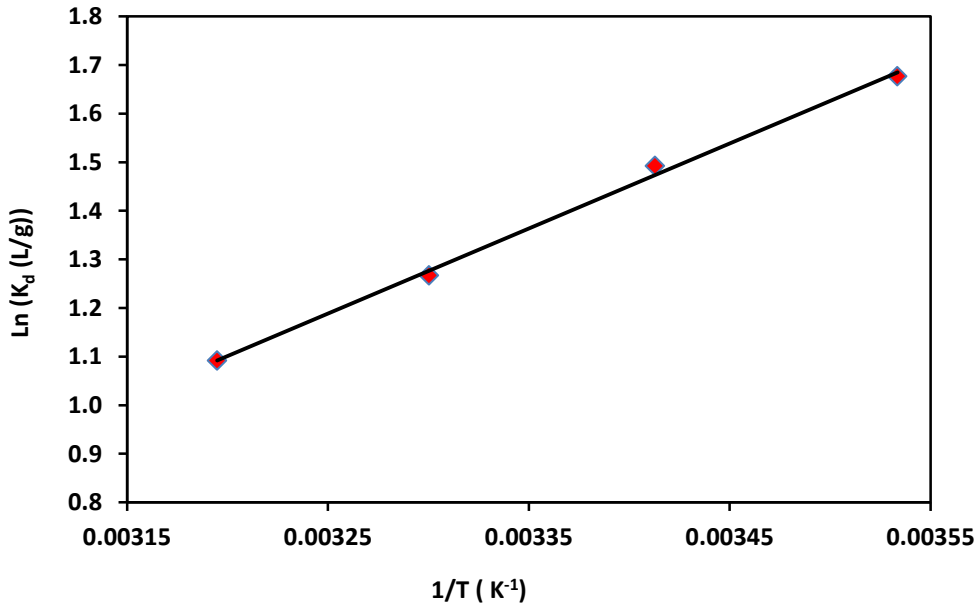

Figure 4-9 The van't Hoff's plot of (lnK_d) against (1/T) for Cr(VI) adsorption onto CDE beads.

4.4.9 Adsorption Isotherm

The equilibrium of Cr(VI) uptake on CDE beads was studied at initial Cr(VI) concentrations ranging from 0.96 to 19.23 mmol/L. The adsorption experiments were carried out at temperature 10 °C and 12 h contact time. The adsorption isotherms of CDE beads for Cr(VI) were determined by Langmuir and Freundlich adsorption isotherm models. The Langmuir isotherm equation was expressed as follows [73]:

$$\frac{C_e}{q_e} = \frac{1}{K_L q_m} + \frac{C_e}{q_m} \qquad (4-5)$$

Where q_e and q_m are the adsorption capacity at equilibrium and the theoretical maximum adsorption capacity (mmol/g), respectively, K_L is the Langmuir adsorption constant (L/mmol), and C_e is the equilibrium concentration of Cr(VI) ions (mmol/L).

The Freundlich isotherm equation is given as follows [73]:

$$\ln q_e = \frac{1}{n} \ln C_e + \ln K_f \qquad (4-6)$$

Where K_f (mg/g $(L/mg)^{1/n}$) and 1/n are the removal capacity of the CDE beads and adsorption intensity, respectively.

The Langmuir and Freundlich adsorption isotherms of Cr(VI) removal from aqueous solution onto CDE beads are presented in Figure 4-10. The results show that the adsorption isotherm was largely linear and well-fitting with Langmuir isotherm with R^2 corresponding to 0.99 rather than the Freundlich isotherm (0.94), which indicated that the Cr(VI) adsorption onto CDE beads occurs in a monolayer adsorption with a finite number of identical sites.

It has been reported that the separation factor (based on Langmuir model) is defined as:

$$\alpha = \frac{1}{1 + K_L C_0} \qquad (4-7)$$

If α is between 0 and 1, the adsorption isotherm is favorable onto adsorbents, and if α is greater than 1, the adsorption isotherm is unfavorable onto adsorbent [110]. For Cr(VI) adsorption onto CDE beads, the separation factor was 0.018 at initial concentration 19.23 mmol/L, which suggests that the Cr(VI) ions are favorable to adsorb onto the prepared CDE beads.

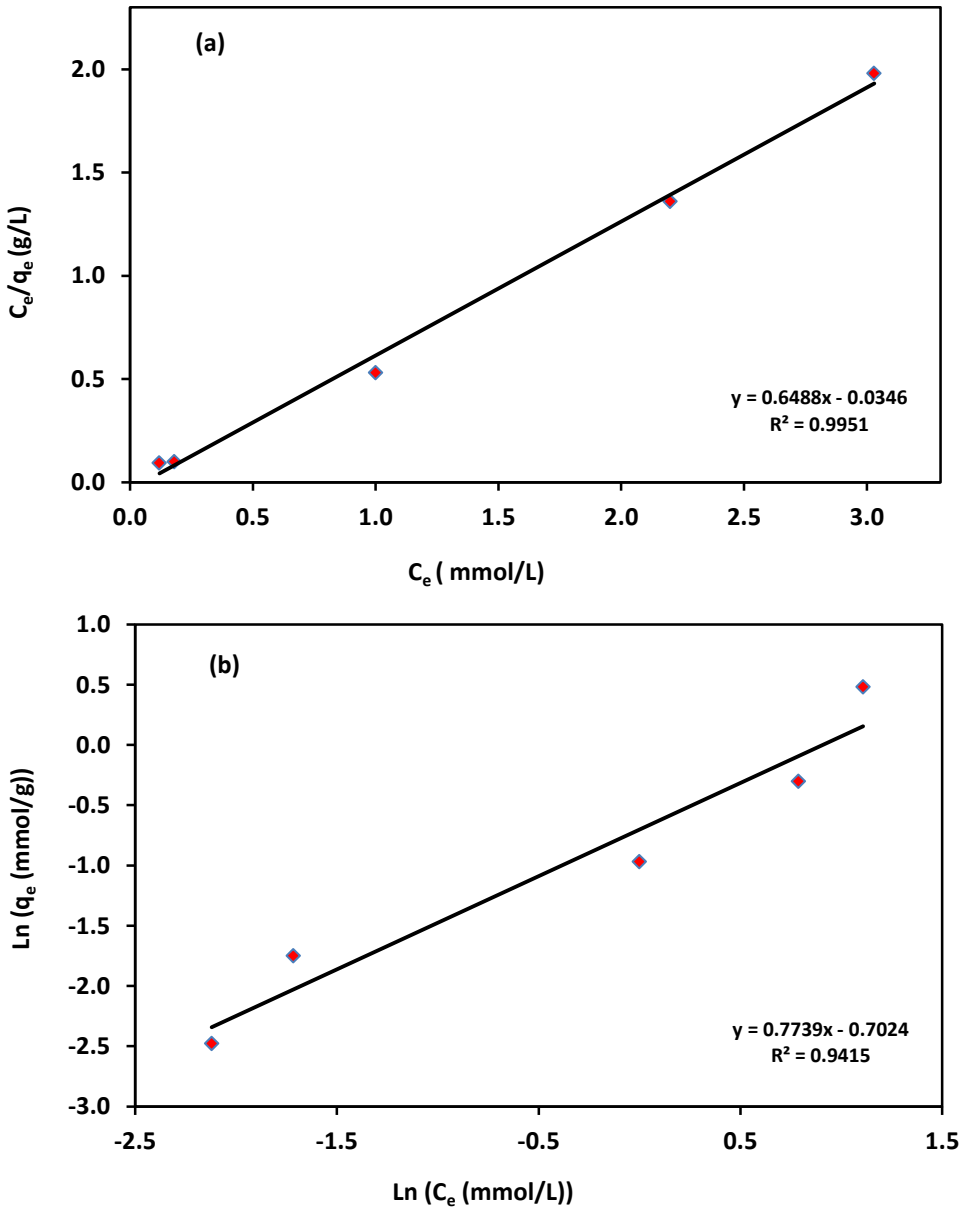

Figure 4-10 (a) Langmuir adsorption isotherm of Cr(VI) adsorption onto CDE beads; (b) Freundlich adsorption isotherm of Cr(VI) adsorption onto CDE beads.

4.4.10 Adsorption Kinetics

The adsorption kinetics of Cr(VI) removal onto CDE beads were investigated at times ranging from 0.25 to 12 h and distinct runs of adsorption experiments keeping temperature, solution-pH, and initial Cr(VI) concentration constant. Pseudo-first-order kinetic model and pseudo-second-order kinetic model were applied to the experimental results to clarify the adsorption kinetics of Cr(VI). The pseudo-first-order kinetic equation is expressed as follows [71]:

$$\ln(q_e - q_t) = \ln q_e - \frac{k_1}{2.303} t \qquad (4-8)$$

Where q_e (mmol/g) is the adsorption capacities at equilibrium, q_t (mmol/g) is the adsorption capacities at time t (h), k_1 is the pseudo-first-order rate constant (h^{-1}).

The pseudo-second-order kinetic equation is given as follows [72]:

$$\frac{t}{q_t} = \frac{1}{k_2 q_e^2} + \frac{t}{q_e} \qquad (4-9)$$

Where k_2 is the rate constant of pseudo-second- order model (g/(mmol.h)).

The experimental results of Cr(VI) adsorption onto CDE beads confirmed the validity of the pseudo-first-order and pseudo-second-order models to describe the adsorptive removal of Cr(VI) from aqueous solution (Figure 4-11). The R^2 values show that the fit to pseudo-second-order model was better (R^2 = 0.999). However, the determined adsorption capacity (q_e) value of the pseudo-second-order kinetic model (1.614 mmol/g) was close to the experimental value (1.62 mmol/g) more than that of pseudo-first-order kinetic model value (1.585 mmol/g). Therefore, the Cr(VI) adsorption process onto prepared CDE beads was described well by the pseudo-second- order-kinetic model.

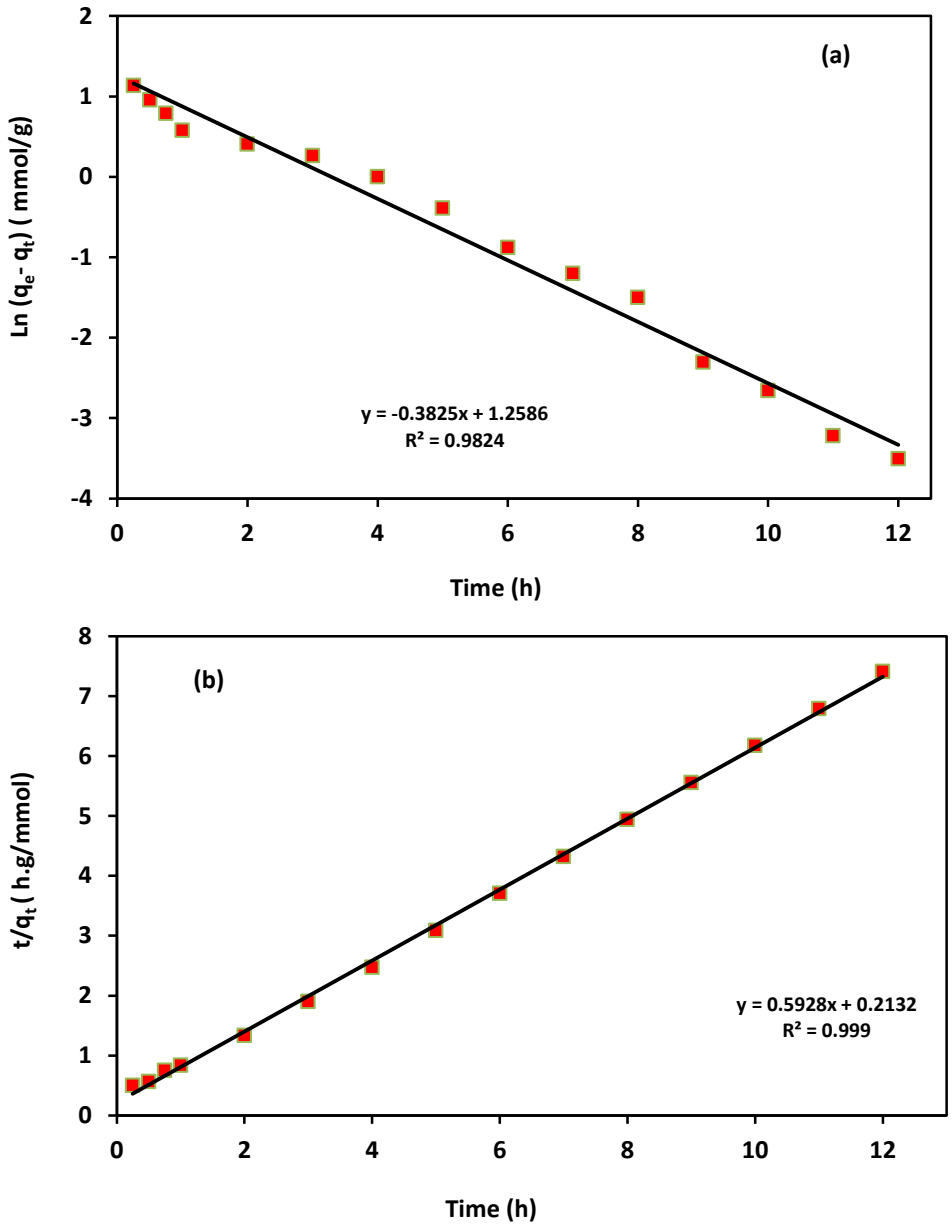

Figure 4-11 (a) Pseudo-first-order plot of Cr(VI) adsorption onto CDE beads; (b) Pseudo-second-order plot of Cr(VI) adsorption onto CDE beads.

4.4.11 Effect of Coexisting Ions on Adsorption Capacity

The adsorption of metals is usually studied in single component systems, even though they coexist in some wastewaters [111]. In this particular study, the influences of coexisting heavy-metal ions (Zn(II), Ni(II), and Pb(II)) on Cr(VI) adsorption capacity was tested at pH 3 and mixture of each metal ion at 1000 mg/L initial

concentration. The results are shown in Figure 4-12. The selectivity of Cr(VI) was determined by using Equation (4-10) [112]. The results of selectivity factors of prepared CDE beads for Cr(VI) adsorption showed that the CDE beads had high selectivity values (S (Cr/Pb) = 0.80, S (Cr/Zn) = 1.32, and S (Cr/Ni) = 1.35). At pH 3, the CDE beads had a strong selective ability for Cr(VI) when it existed with Pb(II), Zn(II), and Ni(II) in the system, indicating that the three other metals do not present strong competition for the active surface sites of CDE beads. In acidic media, the protonation of amine groups contributed to the high adsorption of Cr(VI) as an anion species, whereas other metal ions existing in cationic forms which reduce its adsorption capacity. The adsorption amount of Cr(VI) onto CDE beads was reduced only by about 19.27 % compared to the noncompetitive adsorption. Interestingly, this result showed that the CDE bead had a high affinity for Cr(VI) followed by Pb(II) and less affinity for Zn(II) and Ni(II) when they are simultaneously present in aqueous systems. Therefore, the results verify that the CDE beads have a good selective adsorption for Cr(VI) from coexisting ions in acidic media. The metal adsorption selectivity factor S is defines as:

$$S_{(Cr/M)} = \log \frac{(q_e/C_e)_{Cr}}{(q_e/C_e)_M} \qquad (4-10)$$

Where C_e (mg/L) and q_e (mg/g) are the equilibrium concentration and adsorption capacity, respectively, measured after Cr(VI) adsorption on the CDE beads, and M represents metal, i.e., Pb(II), Zn(II), or Ni(II), when these metal ions are present in the aqueous solution. Larger S-values imply a stronger selective ability for Cr(VI).

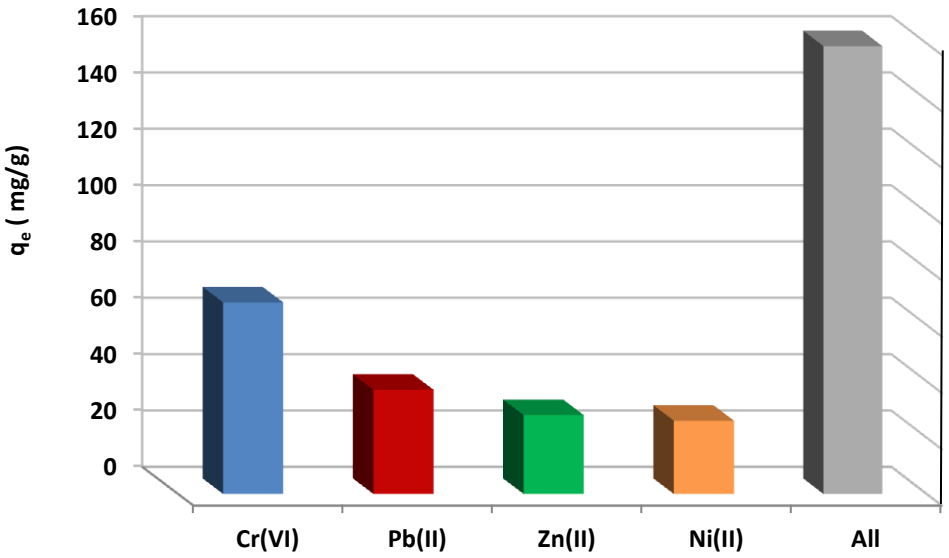

Figure 4-12 Competitive adsorption data for Cr(VI), Pb(II), Zn(II), and Ni(II) onto CDE beads (pH = 3, C_0 = 1000 mg/L for each metal ion, adsorbent dosage = 0.5 g).

4.4.12 Effects of Anions on Cr(VI) Ion Adsorption

Industrial wastewater commonly contains anions such as NO^{3-}, PO_4^{3-} and SO_4^{2-}, which change the ionic strength of the wastewater and affect heavy metal removal. Consequently, the equilibrium adsorption capacity of Cr(VI) onto CDE beads was investigated in the presence of these ions. Figure 4-13 shows the effect of different anions on Cr(VI) adsorption performance at 0.05 mol/L ionic concentrations for each anion separately, pH 3, initial Cr(VI) concentration 1000 mg/L, and temperature 10 °C. The results showed that the three anions had a significant influence on the Cr(VI) adsorption behavior, the Cr(VI) adsorption was decreased noticeably by 35.38, 27.93, and 26.93 mg/g in the presence of PO_4^{3-}, NO^{3-}, and SO_4^{2-}, respectively. The different effect between the three anions is related to their difference in radii (PO_4^{3-} < SO_4^{2-}, NO^{3-}) [113].

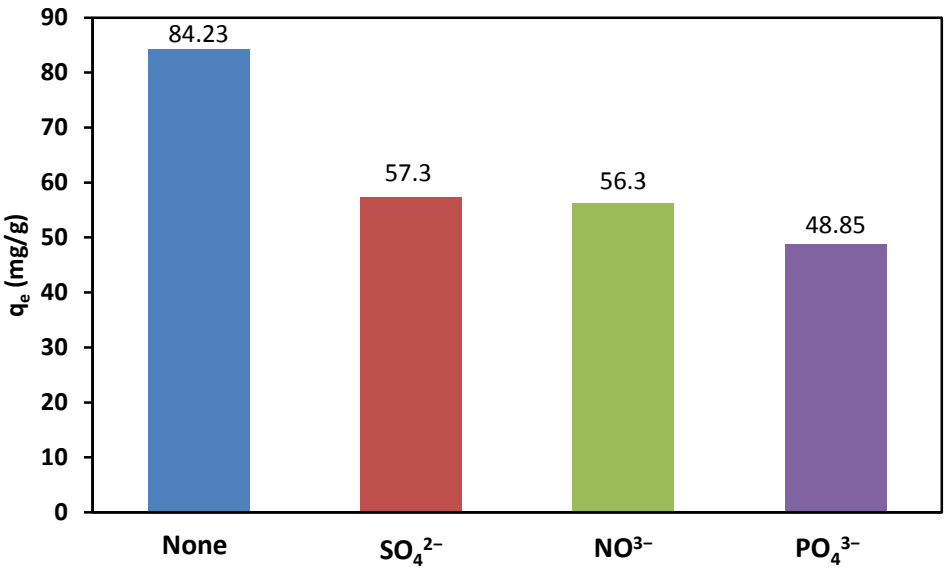

Figure 4-13 Effect of anions on Cr(VI) adsorption onto CDE beads (C_0 = 1000 mg/L, pH = 3, anionic concentration = 0.05 mol/L, adsorbent dosage = 0.5 g).

4.4.13 Desorption and Reusability

Desorption performance and reusability are important parameters to evaluate the properties of an adsorbent. From batch adsorption studies (Figure 4-6), the amount of Cr(VI) removal onto CDE beads decreased with increasing solution-pH. Consequently, the regeneration of CDE beads was subjected by using basic solution (0.2 mol/L NaOH). The five adsorption-desorption successive cycles of Cr(VI) adsorption onto CDE beads are shown in Figure 4-14. The adsorption capacity of Cr(VI) onto CDE beads did not show any significant decrease after five cycles. Therefore, the reuse study of CDE beads indicates that the prepared CDE beads are efficiently and proficiently stable adsorbent for Cr(VI) uptake from aqueous systems. One can see that the Cr(VI) adsorption capacity onto CDE beads was about 84 mg/g in the first cycle and 72 mg/g in the fifth cycle.

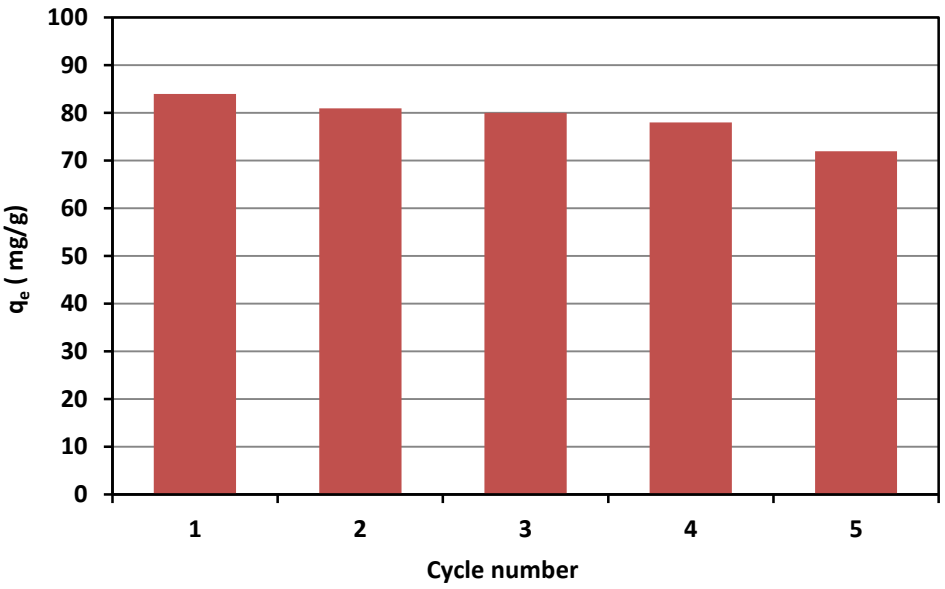

Figure 4-14 Adsorption-desorption cycles of Cr(VI) adsorption onto CDE beads.

4.5 Conclusions

This study indicates that the Cr(VI) adsorption onto CDE beads was excellent and up to 1.62 mmol/g (84.23 mg/g). The unique properties of chitosan make it an exciting and promising agent for purification of industrial wastewater. The adsorption capacity of Cr(VI) was found to be dependent on the solution-pH, contact time, and temperature. The highest Cr(VI) uptake capacity was at pH 3 and temperature 10 °C. The adsorption followed pseudo-second-order kinetics. The Langmuir model was revealed to be the best fitting model for Cr(VI) removal with R^2 value 0.9951. The values of the thermodynamic quantities indicated that the Cr(VI) adsorption process onto CDE beads was exothermic, spontaneous, and the beads surface was energetically homogeneous. In addition, the separation of Cr(VI) on CDE beads from an aqueous systems that contains heavy metals was successfully obtained at low solution-pH. Loaded beads with Cr(VI) ions can be chemically regenerated by 0.2 mol/L NaOH without damaging of adsorbents and up to five cycles. It is important to

mention here that the prepared CDE beads are sustainable material, and its cost is very low in comparison with other adsorbents.

CHAPTER 5. HIGHLY EFFICIENT REMOVAL OF Pb(II) AND Ni(II) BY CHITOSAN/DIATOMACEOUS EARTH COMPOSITE

5.1 Abstract

A novel adsorbent for an effective removing of Pb(II) and Ni(II) from aqueous systems in both noncompetitive and competitive modes was prepared by dispersion chitosan onto the diatomaceous earth (CSDE), and then was synthesized into a spherical shape by using a drop-wise method. Its chemical composition, microstructure morphology, and metal-binding mechanism were characterized by dispersive X-ray spectroscopy (EDS), scanning electron microscopy (SEM), Fourier transform infrared spectroscopy (FTIR), and Brunauer-Emmett-Teller (BET) techniques. Batch adsorption studies were utilized to evaluate the potential suitability of the prepared CSDE beads and to examine the impact of major adsorption parameters such as solution-pH, initial metal concentration, and contact time on the Pb(II) and Ni(II) adsorption. Under optimal conditions, the maximal adsorption capacities of the CSDE beads based on the Langmuir isotherm model were 175.22 mg/g for Pb(II) and 149.64 mg/g for Ni(II) for noncompetitive adsorption and 234.8 mg/g for both metals in competitive adsorption. The common foreign ions such as Na^{+}, Mg^{2+}, and Ca^{2+} had insignificant effect on the Pb(II) adsorption while Mg^{2+} and Ca^{2+} affected the Ni(II) adsorption. Adsorption kinetics of both metals followed a pseudo-second-order model better than pseudo-first-order model. The prepared CSDE beads could be reused at least ten consecutive adsorption-desorption cycles with marginal decrease in the total adsorption capacity of both metals.

5.2 Introduction

Heavy metal contaminations have been progressively received a considerable attention for removing from wastewater streams in the whole world. This is due to their non-bioaccumulation in nature, high toxicity, carcinogenicity, prevalence, existence and persistence in the environment [114]. Exposure to heavy metals, even at very low concentration, is highly dangerous to the human beings and the ecosystem. For example, in 2013 UNICEF announced that ca. 2000 children below five years old die every day of diarrheal illness due to contaminated drinking water. In addition, the first 10 major chemical contaminations in health community were recognized by the World Health Organization (WHO), four of them are heavy metals, including lead [115].

Lead is not essential element for human body functioning, but it could be accumulated in the kidney and the nervous system, leading to cancer or deformity after intake from water even at very low levels [2]. The main source of lead is from different industries such as mining, acid battery manufacturing, metal plating, printing, textile, photographic materials [116]. Therefore, it usually exists in the wastewater streams or the discharges of these industries. The lead concentrations in different industrial wastewaters are up to 100 - 150 mg/L with low solution-pH [5]. According to U.S. Environmental Protection Agency (EPA), the maximum contaminant level (MCL) of the lead ions in the drinking water, has been set at a low level of 0.015 mg/L [5].

Nickel is an essential and important metal for plants and micro-organisms [117]. The major sources of nickel pollutions in the water streams come from various industrial processes such as electroplating, battery and accumulator manufacturing, paint formulation, mining production, metal finishing, paper industries, mineral

processing, porcelain enameling and forging [118]. The concentration of Ni(II) in the wastewater from mining drainage and metal finishing has been reported up to 130 mg/L [6]. Exposure and accumulation of Ni(II) and its compounds in the human body over the permissible levels (0.1 mg/L in the drinking water according to World Health Organization) can cause a serious damage to the human health such as pulmonary fibrosis, renal edema, skin dermatitis, gastrointestinal distress, lung and kidney problems, and dermatitis [119].

Development of an efficient technology to remove Pb(II) and Ni(II) from the aqueous solutions is very necessary and mandatory. Physical, chemical, and biological processes for heavy metals removal from aqueous solutions have been extensively researched and used such as adsorption, reverse osmosis, ion exchange, evaporation, solvent extraction, chemical precipitation, filtration, flotation, membrane, coagulation and flocculation, and electrochemical methods [100]. Adsorption has been currently considered as one of the most cost-effective and technically flexible process for heavy metals removal. In addition, it is easy handling and the chemical consumption or/and waste generation is not a significant issue compared with other methods like precipitation, membrane, and filtration [120]. Adsorption studies with sustainable, efficient, low-cost, and renewable resources material such as marine algae, seaweed, surfactant-modified alumina (SMA), activated metal oxide, surfactant modified laterite (SML), large α-alumina beads chitin, bark, rice husk and chitosan have played a vital role due to its outstanding results in heavy metals and other contaminants removal [121,122,123,124,125]. Among these available sustainable natural biopolymer materials, chitosan has been repeatedly characterized as the excellent material for chemically or physically adsorbing various heavy metal ions from aqueous solution.

Chitosan (poly-β-(1→4)-2-amino-2-deoxy-D-glucose) is commercially produced in large quantities by partial deacetylation of chitin in hot alkali, which is the second plentiful organic material in the nature next to cellulose, and can be extracted from crustaceans such as shrimp, lobsters, crayfish, and shells of crabs. It is biocompatible, biodegradable, hydrophilic, and nontoxic to human and environment. Moreover, chitosan has unique properties such as chemical stability, high reactivity, metal ion binding groups ($-NH_2$, -OH), excellent chelation behavior, and high selectivity towards pollutants. Despite these advantages, chitosan has low specific surface area, swelling properties, tendency to agglomerate, poor mechanical properties and poor stability in highly acidic solution, which limited its widespread applications in heavy metal ions adsorption [116,126]. Therefore, many studies that summarized in Table 5-1 with maximum adsorption capacities have been modified chitosan physically and chemically in order to overcome some of its shortcomings. Notably, when chitosan modified chemically by cross-linking or grafting, its adsorption capacity reduced due to consuming and covering part of active site groups like amino and hydroxyl.

In this particular study, chitosan has been modified physically by coating/ dispersion onto an inert substance, diatomaceous earth, and formed into spherical adsorbents by using drop-wise method for increasing its total surface area, improving its mechanical strength, and preserving the active amine groups. Diatomaceous earth is non-hazardous amorphous natural material formed from the remains of diatoms, which grew and deposited in the seas or lakes. It has unique physical characteristics, such as high permeability (0.1–10 mD), porosity (35 – 65%), small particle size, adsorption capabilities, low thermal conductivity and density, and high surface area (up to 30 m^2/g) [10]. The novel prepared chitosan-diatomaceous earth (CSDE) beads have been characterized before and after adsorption by Pb(II) and Ni(II) from aqueous

solutions via Fourier-transform infrared spectroscopy (FTIR), Brunauer-Emmett-Teller (BET) measurements, scanning electron microscopy (SEM), and energy dispersive X- ray spectroscopy (EDS). Also, the effect of experimental factors such as solution-pH, contact time, and initial metal ions concentration on adsorption process of Pb(II) and/or Ni(II) in single and binary metal ion solutions have been investigated. Furthermore, adsorption kinetics, adsorption isotherms, mechanism of adsorption, and adsorption-desorption behavior were employed.

Table 5-1 Maximal adsorption capacities of Pb(II) and Ni(II) onto different chitosan modifications.

Adsorbents	Metal ion	pH	Initial conc. (mg/L)	Adsorption capacity (q_e) (mg/g)	Reference
Nanospheres chitosan, Pseudomonas biomass and gelatin (CPG)	Pb(II)	6	350	91.1	[124]
Xanthate-modified magnetic chitosan	Pb(II)	--	250	76.9	[125]
Xanthate-Modified Chitosan Sponge	Pb(II)	5	500	216.45	[126]
Xanthate-Modified Chitosan Sponge	Ni(II)	5	500	41.88	[126]
Chitosan–polyacrylonitrile blend	Pb(II)	5	50	20.08	[10]
Magnetic chitosan/graphene oxide	Pb(II)	5	100	79	[127]
Ion-imprinted tetraethylenepentamine modified chitosan	Pb(II)	6	4000	259.68	[128]
Chitosan-tripolyphosphate	Pb(II)	4.5	300	57.33	[129]
Chitosan / diatomaceous earth	Pb(II)	6	400	175.22	Present study
Magnetic chitosan chelating resin	Ni(II)	6	100	40.15	[130]
Thiourea-modified magnetic chitosan microspheres	Ni(II)	6	100	15.3	[131]
Glutaraldehyde-crosslinked chitosan	Ni(II)	4	50	21.2	[132]
Chitosan coated polyvinyl chloride (PVC) beads	Ni(II)	5	500	120.5	[133]
Epichlorohydrin crosslinked chitosan–clay	Ni(II)	6	100	32.36	[134]
Histidine modified chitosan beads	Ni(II)	5	1000	55.6	[135]
Chitosan coated calcium alginate	Ni(II)	5	500	222.2	[136]
Chitosan / diatomaceous earth	Ni(II)	6	400	149.64	Present study
Chitosan / diatomaceous earth	Ni(II) + Pb(II)	6	400	234.8	Present study

5.3 Materials and methods

5.3.1 Chemicals and materials

Chitosan (deacetylation 87%, viscosity 1000 mPa.s, molecular weight ~190,000-310,000 g/mol) and diatomaceous earth powder which is mainly composed of silicon dioxide (90% SiO_2, 4% Al_2O_3, 2% Fe_2O_3, others 4%) were obtained from Aldrich Chemical Corporation (St. Louis, MO, USA). Sodium hydroxide and oxalic acid were used to dissolve chitosan and adjust the solution-pH. Deionized water was used during the experimental studies. Two heavy metals, Pb(II) and Ni(II), were chosen for this study, which are not biodegradable under any natural environmental conditions. Nickel(II) chloride and lead(II) nitrate were procured from Aldrich Chemical Corporation (St. Louis, MO, USA). Appropriate amounts of nickel chloride (2.208 g) or lead nitrate (1.598 g) as the salts for the corresponding metal source were dissolved in 1 L of deionized water to prepare stock solutions containing 1000 mg/L of Pb(II) or Ni(II) ions. Adequate concentrations (50, 100, 200, 300, 400 mg/L) were prepared from standard stock solutions by consecutive dilution for working solutions in batch experimental runs. All used chemicals in this study were analytically graded.

5.3.2. Preparation of CSDE beads

Chitosan/diatomaceous earth composite beads were prepared by dispersion chitosan onto the diatomaceous earth (CSDE) and were synthesized into a spherical shape by using drop-wise method, dropping of an acidic solution of chitosan and diatomaceous earth into precipitation beaker [137]. A 25 g of chitosan was dissolved in 1 L of 0.15 mol/L oxalic acid solution under continuous stirring, 200 rpm, and 60 ^{o}C temperature until viscous chitosan gel was formed. Next step, 50 g of diatomaceous earth powder was slowly added into the chitosan gel with keeping

temperature at 60 ^{o}C and stirred for three hours to obtain a homogeneous mixture of diatomaceous earth and chitosan. The spherical beads of chitosan - diatomaceous earth were formed by wisely dropping the final gel mixture into 1 mol/L of NaOH-solution precipitation beaker. Finally, the spherical adsorbents were separated from the NaOH-solution and washed by deionized water until neutralization, and then were dried by vacuum furnace at 70 ^{o}C for 24 hours. The final prepared dried adsorbents have an average diameter about 2 mm and sealed as CSDE beads as shown in Figure 5-1.

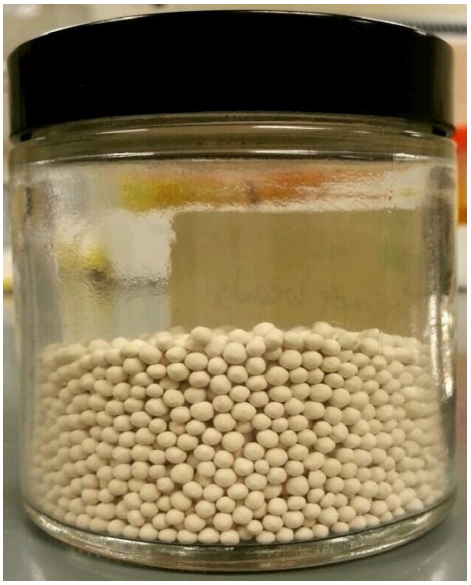

Figure 5-1. Chitosan - diatomaceous earth beads (CSDE beads).

5.3.3 Material characterizations

The prepared CSDE beads were characterized by Brunauer-Emmett-Teller (BET) measurements to determine the total surface area, pore volume, and pore size distribution. Hitachi S-4700 Field emission scanning electron microscopy, SEM (Model 1530VP, LEO, Germany), was used to investigate the morphology and the structure of the adsorbents before and after heavy metals adsorption operating at 20 kV. The mechanism of Pb(II) and Ni(II) bonding to the CSDE beads and the nature of

the functional groups were carried out before and after adsorption using Fourier-transform infrared spectroscopy (FTIR) (Bruker model FTIR spectrometer) operating in a wavenumber range of 400 - 4000 cm^{-1} with resolution of 4 cm^{-1}. Using the energy dispersive X- ray Spectroscopy (EDS) was to confirm the adsorption of Pb(II) and/or Ni(II) onto CSDE beads and to determine the weight percentages of these metal ions and the elemental composition of CSDE beads. Finally, the surface charge of the CSDE beads at different solutions-pH was measured using zeta-sizer (Malvern, Ltd., U.K.). The concentrations of heavy metals in solution were determined by inductively coupled plasma-mass emission spectrometry (ICP-MS) (PerkinElmer, USA).

5.3.4 Batch adsorption experiments

The batch experiments in single and binary systems were carried out in six parallel 125 mL Erlenmeyer flasks, containing 0.1 g of prepared adsorbent and 100 ml of various desired initial Pb(II) and/or Ni(II) concentrations (50, 100, 200, 300, 400 mg/L) at 200 rpm and 25 ^{o}C temperature, to determine the adsorption capacities, adsorption kinetics, and adsorption isotherms of the prepared CSDE beads. The pH-values were adjusted from 2 to 8 by 0.1 mol/L NaOH or 0.1 mol/L oxalic acid. For each metal, the pH-value with the highest adsorption capacity was used for adsorption isotherm and kinetic studies. The final Pb(II) and Ni(II) concentrations in the solutions were measured by Inductively Coupled Plasma-Mass Spectrometer (ICP-MS) after being separated and filtrated solutions from adsorbents. All experimental runs were repeated three times. Eventually, the amount of Pb(II) and Ni(II) adsorbed onto CSDE beads was measured by conducting a mass balance on the heavy metals, Equation (5-1).

$$q_e = \frac{(C_0 - C_e)V}{m} \qquad (5-1)$$

Where q_e is the metal ions adsorbed at equilibrium (mg/g) onto CSDE beads, C_0 is the initial metal ion concentration (mg /L), C_e is the equilibrium metal ion concentration (mg/ L), V is the volume of the solution (L), and m is the mass of CSDE beads (g).

5.3.5 Desorption and regeneration

The regeneration of the loaded CSDE beads by Pb(II) and/or Ni(II) was assessed by separating adsorbents from the solutions and collected them in flasks, and then they were washed by deionized water to remove the attached (unabsorbed) metal ions on the adsorbents surface with 200 rpm stirring. Next step, the adsorbents were agitated with 50 mL of three different solutions, 0.1 mol/L ethylene diamine tetra acetic acid (EDTA), 0.1 mol/L sodium hydroxide (NaOH), and 0.1 mol/L hydrochloric acid (HCl). After 120 min, the adsorbents were separated from the eluents and repeatedly washed with deionized water. The final concentration of Pb(II) and Ni(II) in the solution was determined. The performance of the CSDE beads was tested by repeating the regeneration process ten times (ten consecutive adsorption-desorption cycles), using the same adsorbents and the same conditions.

5.4 Results and discussion

5.4.1 Characterization of CSDE beads

The CSDE beads were characterized to estimate various physical and chemical properties, it could be provided a better interpretation of Pb(II) and Ni(II) removal mechanism associated with adsorption process. The physicochemical properties of prepared CSDE beads are summarized in Table 5-2.

Table 5-2 The main physicochemical properties of the CSDE beads.

Parameters	Value
Physical nature	porous
Average particle diameter, (mm)	2
Surface area (m^2/ g) (based on BET)	14.4
Bulk density (g /cm^3)	0.338
Particle density, (kg/m^3)	481
Porosity	0.298
pore size (mm) (based on BET)	3.23×10^{-6}
pore volume (m^3/g) (based on BET)	7.4×10^{-9}
pH - point of zero charge (pH_{PZC})	5.8

Figure 5-2 represents the SEM images of pure chitosan (CS) and CSDE beads at different level of magnifications. SEM observation revealed that the surface morphology of CS beads have a layered structure with a relatively homogeneous and smooth surface without any visible protuberances (Figure 5-2a), whereas, CSDE beads surface had an integral, rough structure, and a good porous surface (Figure 5-2b), which is suitable for allowing the metal ions diffuse during the adsorption process. Moreover, Figure 5-2c displays the surface of CSDE beads after loaded by Pb(II) and Ni(II) ions. It can be seen that the surface of loaded adsorbent is changed to less porous and adsorbed metal ions created a bright thin layer on the surface which confirms that the metal ions were adsorbed onto CSDE beads.

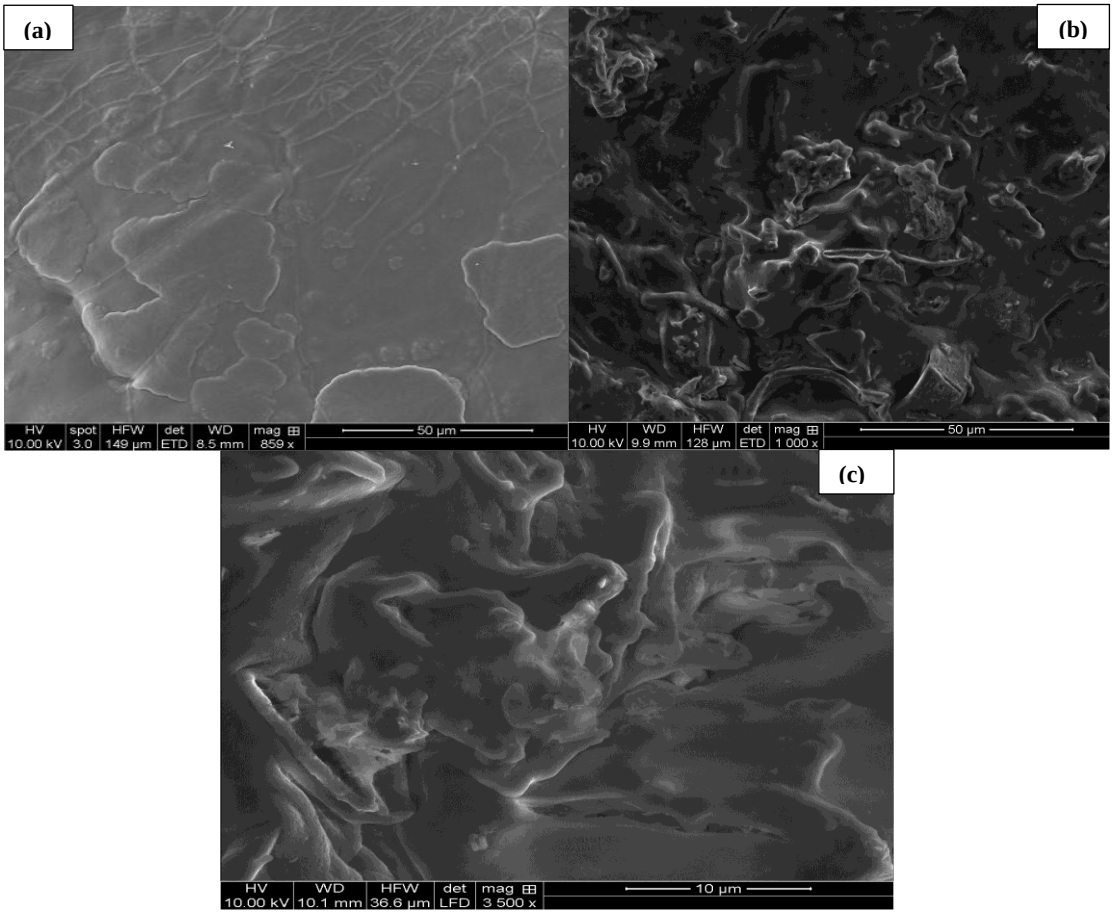

Figure 5-2 SEM images of (a) Pure CS, (b) Fresh CSDE beads, (c) Loaded CSDE beads by Pb(II) and Ni(II) ions.

The FTIR spectroscopy was used to provide the evidence of comparable differences between the fresh CSDE beads and loaded by Pb(II) or Ni(II) as displayed in Figure 5-3. The FTIR-spectra of fresh CSDE beads showed peaks at 1640 cm^{-1}, which was assigned to the N-H deformation vibrations of the NH_2 group, at 3298 - 3384 cm^{-1} range for -OH and -NH stretching, and that at 2902 cm^{-1} was attributed to C-H stretching vibration. The stretching bands of the Si-O, Si-O-Si and Al-O-Si groups and the deformation bands for these bands corresponded to1355, 1095, 794 and 472 cm^{-1} respectively [122,32]. In addition, a peak appeared at 630 cm^{-1}, which indicated to stretching vibration of O-H stretching. On the other hand, after metal ions adsorption onto CSDE beads, the deformation vibrations of the NH_2 groups shifted

from 1640 cm^{-1} to 1618 and 1633 cm^{-1} range after being loaded by Pb(II) and Ni(II), respectively. However, the stretching of -OH and -NH groups shifted to 3211 and 3295 cm^{-1} after being loaded by Pb(II) and Ni(II), respectively. These observations indicate that the amine and hydroxide groups are present in the CSDE beads and successfully bonded with heavy metals, indicating that the metal ions are adsorbed onto CSDE beads. In addition, the above-mentioned shifts happened in the main active groups confirmed to the presence of the probable physical and chemical interactions between metal ions and the functional surface groups of the CSDE beads. These interactions can be characterized as electrostatic attractions, ion exchange and/or chemical complex reaction [116,138]. This indicated that the Pb(II) and Ni(II) ions were successfully adsorbed onto the surface of the CSDE beads.

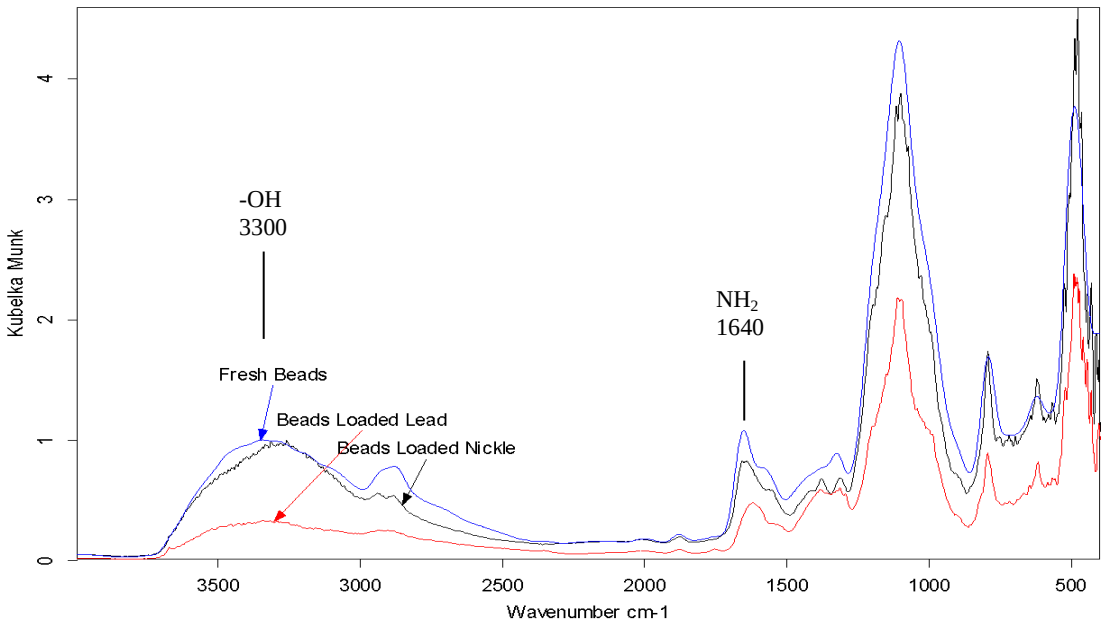

Figure 5-3 FT-IR spectra of fresh CSDE beads, CSDE beads loaded Pb(II) ions, and CSDE beads loaded Ni(II) ions.

Figure 5-4 shows the EDS analysis of fresh and loaded CSDE beads by Ni(II) and Pb(II). It can be seen that carbon, nitrogen, oxygen, silicon, chloride (comes from $NiCl_2$ - the salt that was used to prepare Ni(II) solution) and nickel were presented in

the loaded CSDE beads by Ni(II) (Figure 5-4a). However, they were also presented in the loaded CSDE beads by Pb(II) excluding chloride and nickel (Figure 5-4b). The quantitative elemental compositions of CSDE beads are summarized in the tables that located into Figure 5-4. The percentages of adsorbed Pb(II) and Ni(II) ions onto CSDE advocated the high content and equal to 9.42 and 7.97 %, respectively. The total elemental weight percentages of loaded CSDE beads by Pb(II) and Ni(II) were 96.50 and 97.79 %, respectively, the rest percentages were some impurities like Fe, Al, and Na. The higher percentage of O along with N enhances the interaction between chitosan beads and heavy metals. We coated the samples by platinum because they were experiencing charging, which can greatly affect the quality of EDS results, a charged surface interacts with the incoming beam, which can alter the incident energy and/or deflect the beam to a different region.

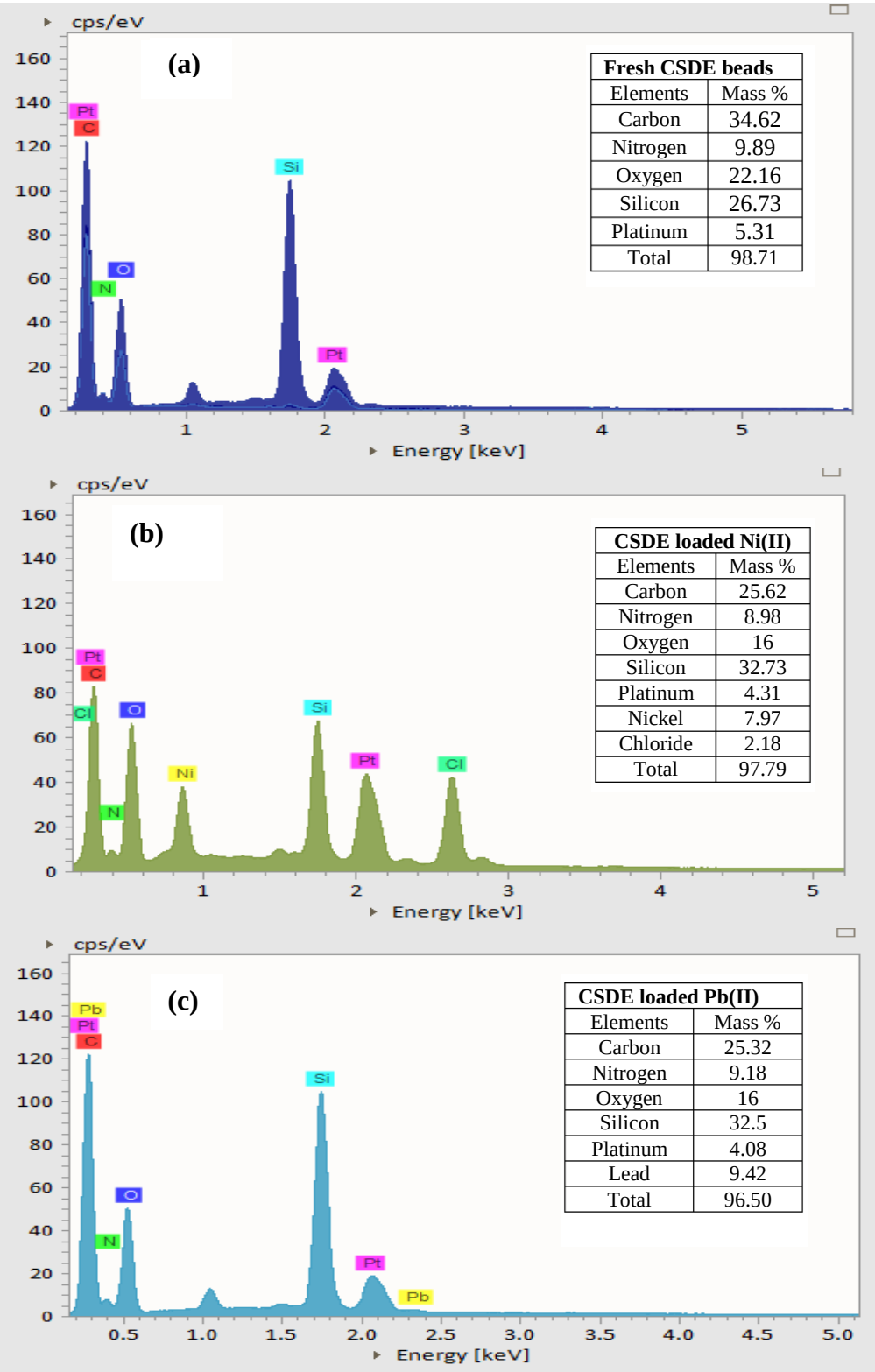

Fresh CSDE beads	
Elements	Mass %
Carbon	34.62
Nitrogen	9.89
Oxygen	22.16
Silicon	26.73
Platinum	5.31
Total	98.71

CSDE loaded Ni(II)	
Elements	Mass %
Carbon	25.62
Nitrogen	8.98
Oxygen	16
Silicon	32.73
Platinum	4.31
Nickel	7.97
Chloride	2.18
Total	97.79

CSDE loaded Pb(II)	
Elements	Mass %
Carbon	25.32
Nitrogen	9.18
Oxygen	16
Silicon	32.5
Platinum	4.08
Lead	9.42
Total	96.50

Figure 5-4 EDS analysis of (a) Fresh CCDE beads; (b) Loaded CSDE beads by Ni(II); (c) Loaded CSDE beads by Pb(II).

The zeta potentials over a range of pH values of CS and CSDE beads were carried out by using photon correlation spectroscopy and electrophoretic light scattering. As shown in Figure 5-5, the pH - point of zero charge (pH_{PZC}) of CS and CSDE beads was 6.63 and 5.8, respectively, indicating that the surface charge of prepared CSDE beads is positive at pH < 5.8, which is unfavorable for the adsorption of Pb(II) and Ni(II) via electrostatic interaction. The positive zeta potentials at low pH (less than 5.8) created by the protonation of amine groups in chitosan to NH_3^+. At pH > 5.8, a rapid rise of surface negative charge was observed due to the deprotonation of amine groups and increasing the hydroxyl groups (OH^-), indicated to the plentiful protonated amino groups on the surface which makes the CSDE structure more suitable for selective adsorption.

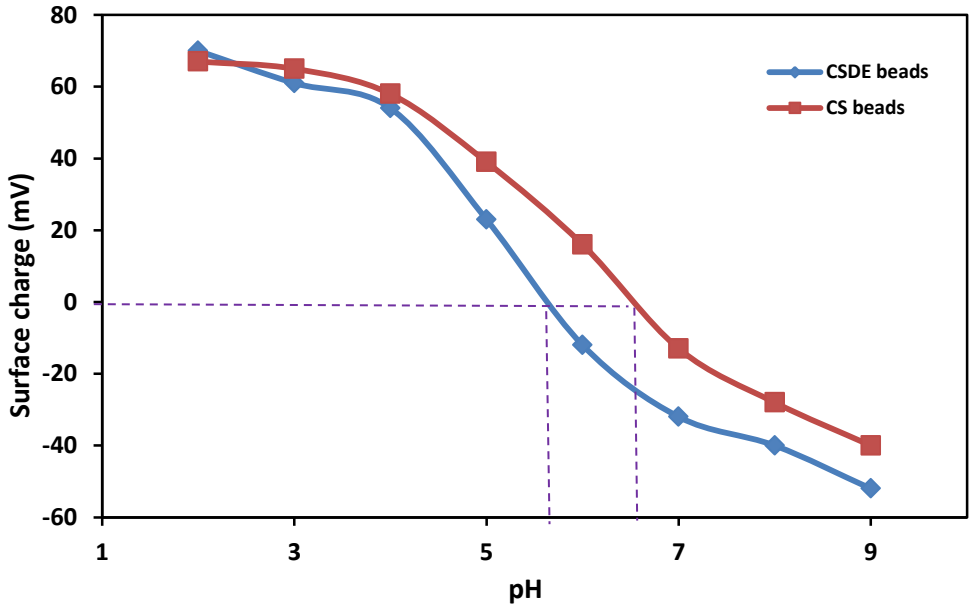

Figure 5-5 Surface charge of CS and CSDE beads at different solution-pH.

5.4.2 Adsorption properties of the CSDE beads

5.4.2.1 Effect of pH on adsorption

The initial pH of aqueous solutions plays a very vital role and significantly affects the liquid-solid adsorption phenomena. It can impact not only on the surface charge and states of the binding sites of adsorbent, but also on the interactions between metal ions and adsorbents [2]. Heavy metals uptake onto chitosan composite adsorbent is mostly happened by NH_2 groups due to the presence of electron pairs on nitrogen atom in chitosan. Hence, the Pb(II) and Ni(II) adsorption features at various pH values onto CSDE beads were studied at the range from 2 to 8, whereas the initial concentration of both metal ions was kept at 400 mg/L. The adsorption capacities of both metal ions displayed a similar pH-dependence as represented in Figure 5-6. It could be seen that the adsorption capacity of both metals had an approximately similar variation behavior and was significantly affected by the solution-pH because they exist in cation form in the solution. At pH 6 and 7, the adsorption capacities of Ni(II) and Pb(II) reached maximum values, 138 and 164 mg/g, respectively. For Pb(II), it was sharply increased with increasing the solution-pH from 2 to 6 and slightly increased from 6 to reach its maximum (164 mg/g) at pH 7, and then decreased to 148 mg/g at pH 8. It was noticed that at pH 8, the lead hydroxide started to participate in the solution leading to reduce the adsorption capacity of Pb(II). The Ni(II) adsorption behaved similarly to Pb(II) adsorption except that the maximum removal capacity happened at pH 6 (138 mg/g) and decreases at pH 7 and 8 due to the precipitation of nickel hydroxide in the solution. This phenomenon could be attributed to the protonation of chitosan amine groups ($-NH_2$) at highly acidic media (lower pH) to the NH_4^+ making the surface of CSDE beads positively charged (as reported in Figure 5-5), which causes an electrostatic repulsion between the positive Pb(II) and

Ni(II) ions and the protonated amino group on the surface of the CSDE beads. Consequently the adsorption capacities of both metal ions were inhibited. Moreover, under acidic conditions, the surface of CSDE beads was covered with H^+ ions which compete with the Pb(II) and Ni(II) ions adsorption on the surface of CSDE beads [139]. But at pH 6 - 7 (above pH_{PZC}, 5.8) the amine groups are completely deprotonated from NH_4^+ to $-NH_2$ and then a large mass of active adsorption sites are available for the adsorption of metal ions by electrostatic attraction and they become ready to bond and/or coordinate with the metal ions to make metal-resin complex. Hence, the adsorption process onto CSDE beads is mainly controlled by electrostatic attraction between the positive charge of both heavy metals and the electron pairs on the nitrogen atom ($-NH_2$) [32,140].

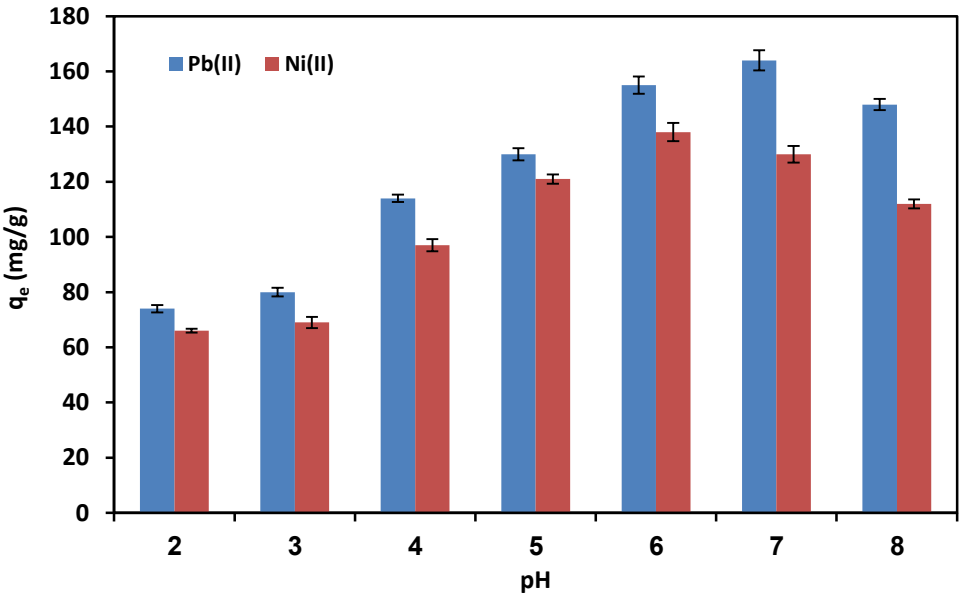

Figure 5-6 Effect of solution-pH on adsorption behavior of Pb(II) and Ni(II) onto CSDE beads (C_0 = 400 mg/L, T = 25 ^oC, contact time = 300 min).

5.4.2.2 Effect of foreign ions and ionic concentration

Industrial wastewater commonly contains foreign ions such as Na^{+}, Mg^{2+}, and Ca^{2+}, which change the ionic strength of the wastewater and effect the heavy metal removal [5,6]. Consequently, the equilibrium adsorption capacity of Pb(II) and Ni(II) onto CSDE beads was investigated in the presence of these ions. Figure 5-7 shows the effect of foreign ions on the Pb(II) and Ni(II) adsorption performance at different ionic concentrations (0.01, 0.025, 0.05, 0.075, and 0.1 mol/L). One can observe that the adsorption of Pb(II) onto CSDE beads was not affected by the presence of Na^{+} ions in all used ionic concentrations, but it was slightly affected in the presence of Mg^{2+} ions and more in Ca^{2+} ions especially at high ionic concentration (0.1 mol/L). The hydrated radii of Mg^{2+}, Na^{+} and Ca^{2+} is larger than the Pb(II) ions, and therefore the adsorption of Pb(II) onto CSDE beads was weakly affected by these cations in the solution [140]. On the other hand, the Ni(II) adsorption onto CSDE beads was largely affected by the presence of the Ca^{2+} and Mg^{2+} ions and that effect increased with increasing the ionic concentration from 0.01 to 0.1 mol/L, which reduced the Ni(II) adsorption capacity by 46.4% at 0.1mol/L of Mg^{2+} and 34.8% at the 0.1mol/L Ca^{2+} ions, but it was not affected by the presence of the Na^{+} ions. This phenomena might be happened due to the fact that the radii of Ca^{2+} and Mg^{2+} ions is smaller than that Na^{+} and Ni(II) ions. Therefore, the Ca^{2+} and Mg^{2+} had the highest affinity to the surface of the CSDE beads and highest tendency for ion exchange with the active surface groups of CSDE beads, which reduced the ionic interaction sites between the surface of CSDE beads and Ni(II) ions. The smaller hydrated radius takes up more ionic exchange sites and leads to decrease the Ni(II) adsorption onto adsorbents [141].

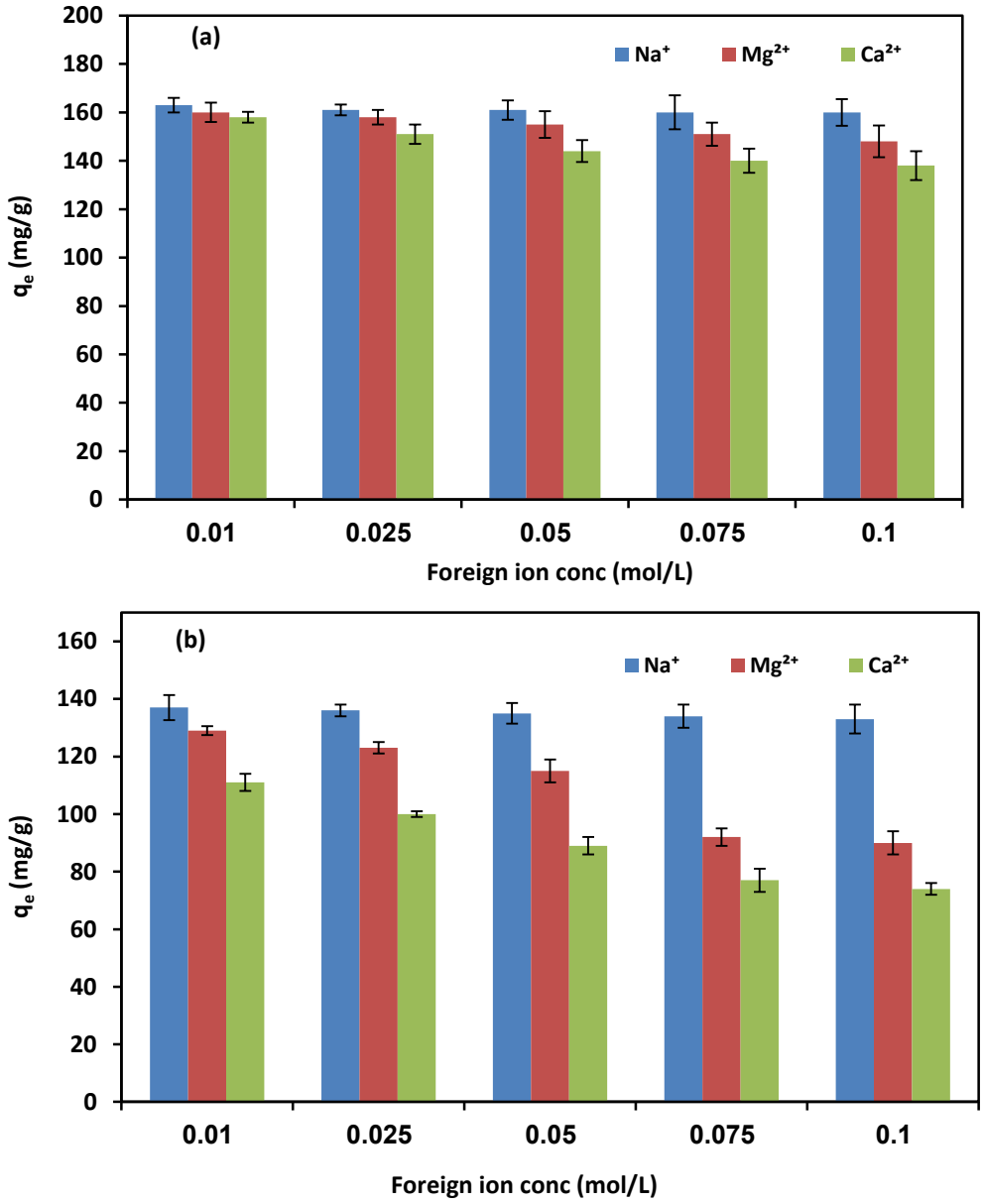

Figure 5-7 Effect of ionic concentrations and foreign ions on (a) Pb(II) adsorption; (b) Ni(II) adsorption onto CSDE beads (C_0 = 400 mg/L, pH = 7(for Pb(II)), pH = 6 (for Ni(II)), contact time = 300 min).

5.4.2.3 Selective and competitive adsorption

Pb(II) and Ni(II) usually coexist in some wastewaters. Therefore, the competitive adsorption of these metal ions onto CSDE beads was performed at concentration 400 mg/L for each kind of metal ion and initial pH 6. The results are represented in Figure

5-8. The order of adsorption capacity matched the noncompetitive adsorption results (Pb(II) > Ni(II)). The results showed that the CSDE beads had an excellent adsorption selectivity and a high affinity for Pb(II) adsorption followed by Ni(II). This could be attributed to the hydrated ionic radius of Pb(II) which is smaller than Ni(II) ions, that created more distorted structure between CSDE chelates and Pb(II) ions [119,11]. The maximal Pb(II) and Ni(II) removal dropped only about 20.6 % and 37.23 %, respectively as compared to non-competitive removal onto CSDE beads. That was due to the competition between coexisting ions onto the active group adsorption sites. It is important to mention here that the adsorption capacity of Pb(II) and Ni(II) together onto CSDE beads was about 234.8 mg/g which was higher than noncompetitive adsorption of each metal ions.

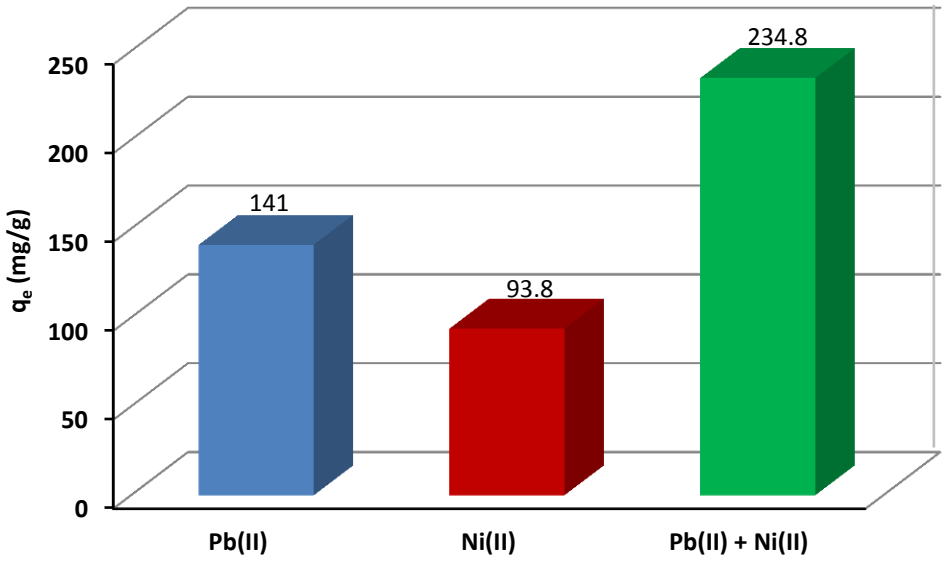

Figure 5-8 Competitive adsorption of Pb(II) and Ni(II) onto CSDE beads (C_0= 400 mg/L for each metal ions, pH = 6, contact time = 300 min).

5.4.2.4 Effect of initial concentration and adsorption isotherm

Establishing an appropriate relationship of liquid - solid adsorption at equilibrium is helpful to optimize the adsorption mechanism and to predict the adsorption capacities of the prepared CSDE beads. The adsorption isotherms were studied at 50 - 400 mg/L initial ion concentrations, 0.1 g dosage adsorbent, pH 6, 300 min contact time, and 25 ^{o}C temperature. As shown in Figure 5-9 a, the results displayed that the CSDE beads were more efficient for Pb(II) removal rather than Ni(II) and reached the saturation at 300 mg/L initial concentration. Two widely used adsorption isothermal models (Langmuir and Freundlich) were applied to Pb(II) and Ni(II) adsorption onto CCDE beads. The Langmuir isotherm theory assumes that the adsorption takes place on the specific homogeneous sites of the adsorbent, that is, the surface sites are identical [121], The equation is,

$$q_e = \frac{\alpha q_m C_e}{1 + \alpha C_e} \qquad (5-2)$$

Where α is an adsorption constant related to binding energy (L/mg), q_m is the maximal adsorption capacity (mg/g), and C_e is the equilibrium concentration of metal ions. On the other hand, the Freundlich model assumes a heterogeneous adsorption on the surface sites with different energies [123]. The equation is,

$$q_e = \beta (C_e)^{\frac{1}{n}} \qquad (5-3)$$

where β and n are constants.

The results showed that the Langmuir isotherm was more fitted to the experimental data than Freundlich model as shown in Figure 5-10 a and b. The parameter values of both models are summarized in Table 5-3. The maximal adsorption capacities of Pb(II) and Ni(II), calculated on the basis of the Langmuir model, were 175.22 mg/g and 149.64 mg/g, respectively. The comparative adsorption

capacities of Pb(II) and Ni(II) onto various adsorbents that were previously reported by studies are displayed in Table 5-1. The results showed that the CSDE beads present a higher adsorption capacity compared with other adsorbents.

To better understanding the adsorption results, the separation factor (R_L) which was determined by using Equation (5-4) based on the Langmuir model. It was determined for the adsorption of Pb(II) and Ni(II) onto CSDE beads over the range of adsorption studies, and plotted against the initial metal concentrations (Figure 5-11). The comparatively low values of R_L ($0 < R_L < 1$) that obtained for prepared adsorbent are support that CSDE beads were being very favorable adsorbent for both metals because lower R_L values indicate more favorable adsorption [142].

$$R_L = \frac{1}{1 + \alpha C_0} \qquad (5-4)$$

where C_0 (mg/L) is the initia concentration of metal ions, α (L /mg) is Langmuir constant.

Table 5-3. Isotherm model parameters of Pb(II) and Ni(II) adsorption onto CSDE beads.

Isotherm model	Parameter	Pb(II)	Ni(II)
Langmuir model	q_m (mg/g)	175.22	149.64
	α (L/mg)	0.0276	0.0123
	R^2	0.9529	0.9157
Freundlich model	n	3.56	2.87
	β ($mg^{1-1/n}. L^{1/n}$ /g)	40.94	23.21
	R^2	0.9042	0.8367

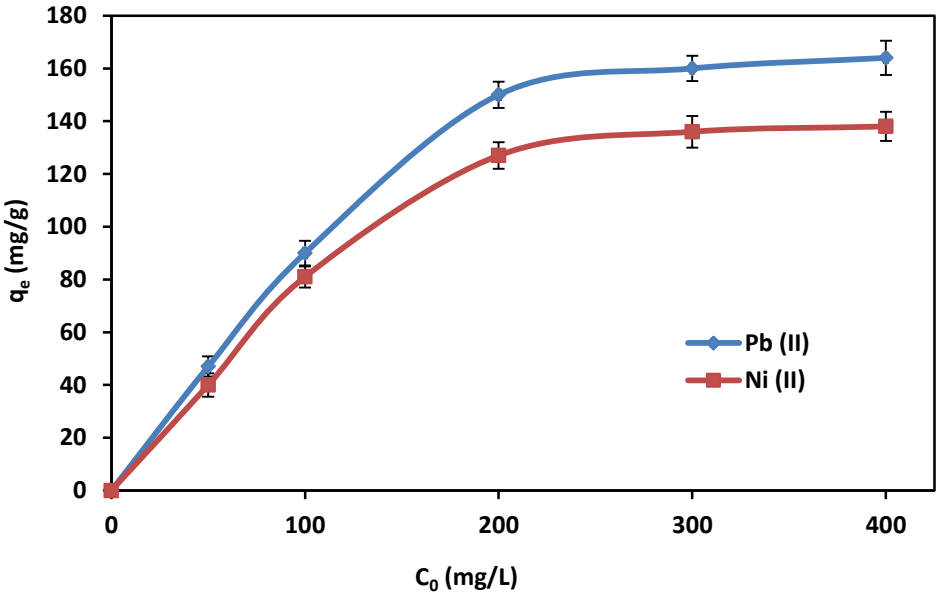

Figure 5-9 Adsorption isotherms for the adsorption of Pb(II) and Ni(II) onto CSDE beads (pH = 6, contact time = 300 min).

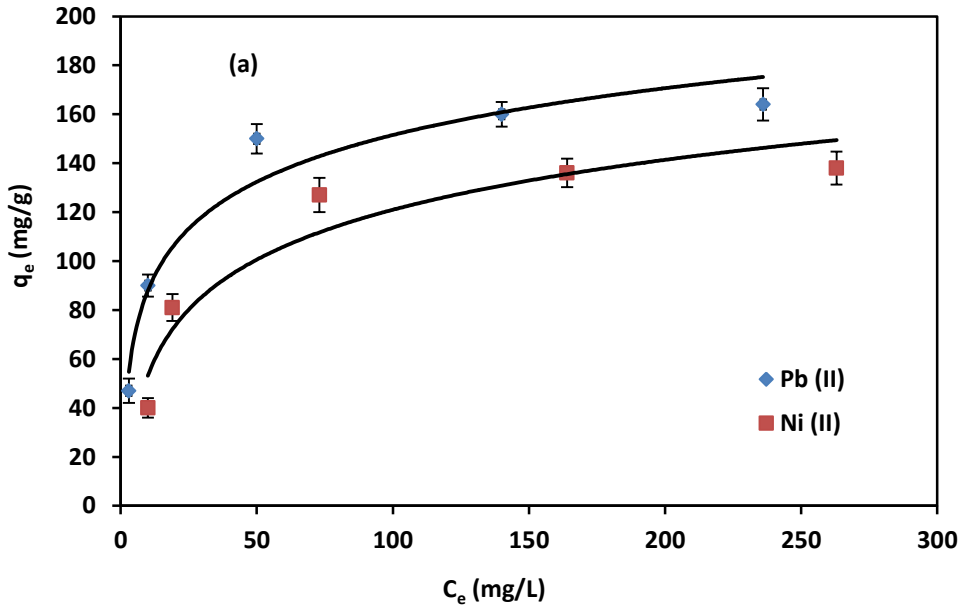

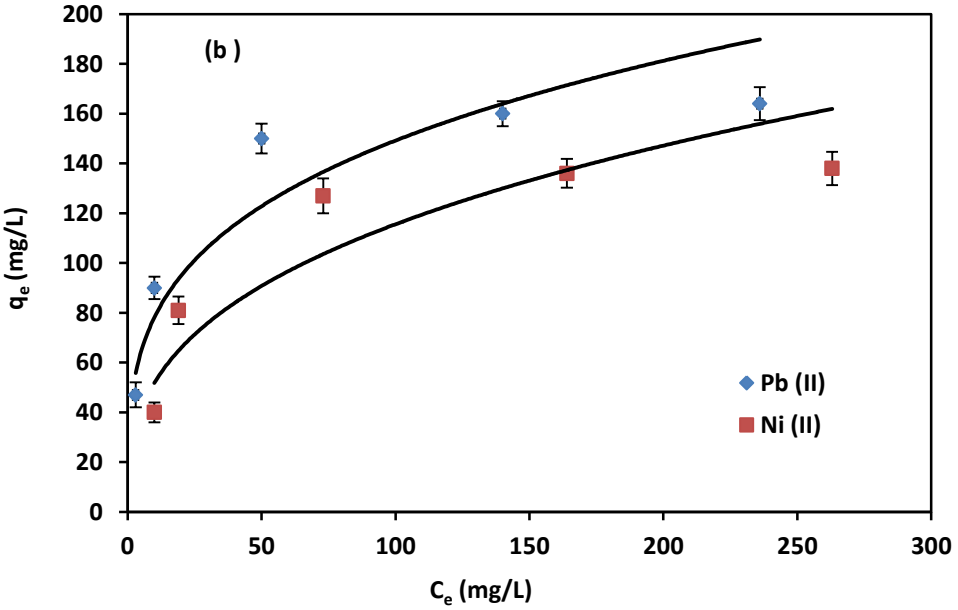

Figure 5-10 (a) Langmuir Model, (b) Freundlich model for the adsorption of Pb(II) and Ni(II) onto CSDE beads (pH = 6, contact time = 300 min).

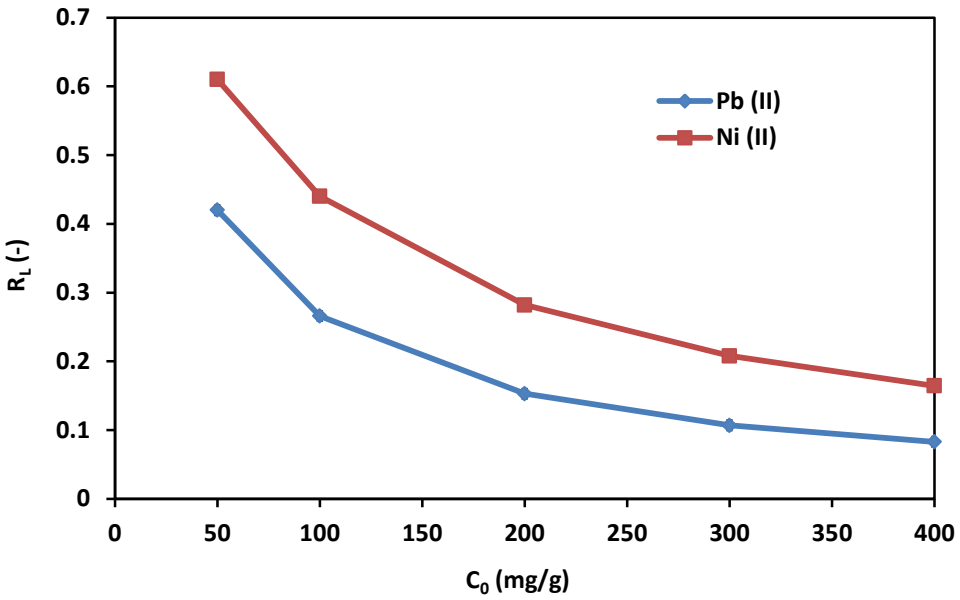

Figure 5-11 Effect of initial concentrations on R_L values for the adsorption of Pb(II) and Ni(II) onto CSDE beads (pH = 6, contact time = 300 min).

5.4.2.5 Effect of contact time and kinetic studies

The residence time of metal ions removal at the solid-liquid interface determines the adsorption rate of adsorbates. Hence, in general, it is important to understand and describe the adsorption kinetics data. In this study, the kinetic experiments were carried out at initial concentration 400 mg/L for each metal ion, pH 6, and contact time 15 - 300 min. The effect of contact time on the adsorption behavior of Pb(II) and Ni(II) onto CSDE beads are shown in Figure 5-12. The adsorption capacity of both metals increased significantly in the first 120 min and then slowed down until it reached the equilibrium in about 180 min. The reason of this phenomenon could be attributed to the strong attractive forces between metal ions and the active sites in CSDE beads, which caused a fast diffusion of Pb(II) and Ni(II) ions into the interlayer space of the adsorbents.

A commonly used kinetic models are the pseudo-first-order (Equation 5-5), which assumes the rate change of metal ions removal with time is directly proportional to the

difference in saturation concentration, and the pseudo-second-order model (Equation 5-6), which assumes the rate determining step of adsorption could be through electron exchange between metal ions and the adsorbent [143]. They were employed to decipher the mechanism of both metals adsorption onto CSDE beads and to analyze the rate-controlling step.

$$\ln(q_e - q_t) = \ln q_e - k_1 t \qquad (5-5)$$

$$\frac{t}{q_t} = \frac{1}{k_2 q_e^2} + \frac{t}{q_e} \qquad (5-6)$$

Where q_e (mg/g) and q_t (mg/g) are the amounts of metal ions adsorbed per unit mass of the adsorbent at equilibrium and at any time (t), respectively. The k_1 (min^{-1}) and k_2 (g/(mg.min)) are constants. The adsorption kinetics were described very well with pseudo-second-order model, where the chemical adsorption is the main controlling factor, and the adsorption capacity scales with the number of active sites [144,145]. The equilibrium adsorption capacities obtained from the pseudo-second-order model were 169.44 and 141.89 mg/g for Pb(II) and Ni(II), respectively, which were close far to the experimental adsorption capacities than those obtained from pseudo-first-order model. That means that the adsorption rates of both metal ions onto CSDE beads were controlled by the chemical adsorption. The results of both kinetic models are summarized in Table 5-4.

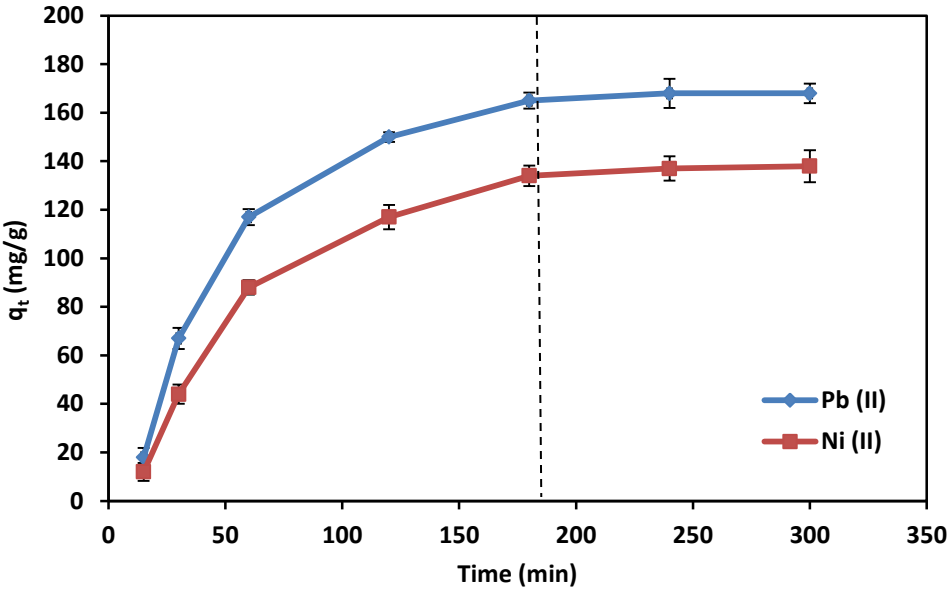

Figure 5-12 Effect of contact time on Pb(II) and Ni(II) adsorption onto CSDE beads (pH = 6, C_0 = 400 mg/L).

Table 5-4 Kinetic model parameters for Pb(II) and Ni(II) adsorption onto CSDE beads.

	Pseudo-first-order model			Pseudo-second-order model			
Metal ions	k_1 (min^{-1})	q_e (mg/g)	R^2	k_2 (g/mg.min)	q_e (mg/g)	R^2	q_e (Exp.) (mg/g)
Pb(II)	0.146	157.76	0.9798	0.0381	169.44	0.9989	164
Ni(II)	0.121	132.21	0.9801	0.0292	141.89	0.9967	138

5.4.2.6 Desorption and reusability

The performance of any adsorbent should not only depend on its adsorption capacity, but also on its regeneration and potential reuse to provide economic benefits and to allow using them in practical application. For this purpose, the prepared CSDE beads that loaded by Pb(II) or Ni(II) were regenerated and reused for adsorption process in ten adsorption-desorption successive cycles. The CSDE beads contain a

mass of amine groups and hydroxyl groups which are sensitive to H^+ ions. In the present investigation, the regeneration of the CSDE beads were accomplished via exposure to different solutions, 0.1 mol/L of ethylene diamine tetra acetic acid (EDTA), sodium hydroxide (NaOH), and hydrochloric acid (HCl) which are well known as strong chelating agents for heavy metal ions [125]. The results of ten adsorption-desorption cycles are illustrated in Figure 5-13. The reduction in Pb(II) adsorption capacity until 10^{th} cycle onto CSDE beads was still maintained above 92%, 87% and 85.4 %, whereas the reduction in Ni(II) adsorption was 89%, 85%, and 83% from initial removal by using NaOH, EDTA, and HCl, respectively. This may be attributed to the different mechanisms of the used reagents. NaOH can form steady electrostatic and chelation complexes with metal ions, while the desorption takes place in the HCl and EDTA solution mainly due to the ion exchange [146, 147]. It was concluded from these experiments that the loaded CSDE beads by Pb(II) or Ni(II) were successfully regenerated without losing their adsorption capacity until ten repeated uses, and they were efficient and stable adsorbent for the removal of Pb(II) and Ni(II) ions from wastewater.

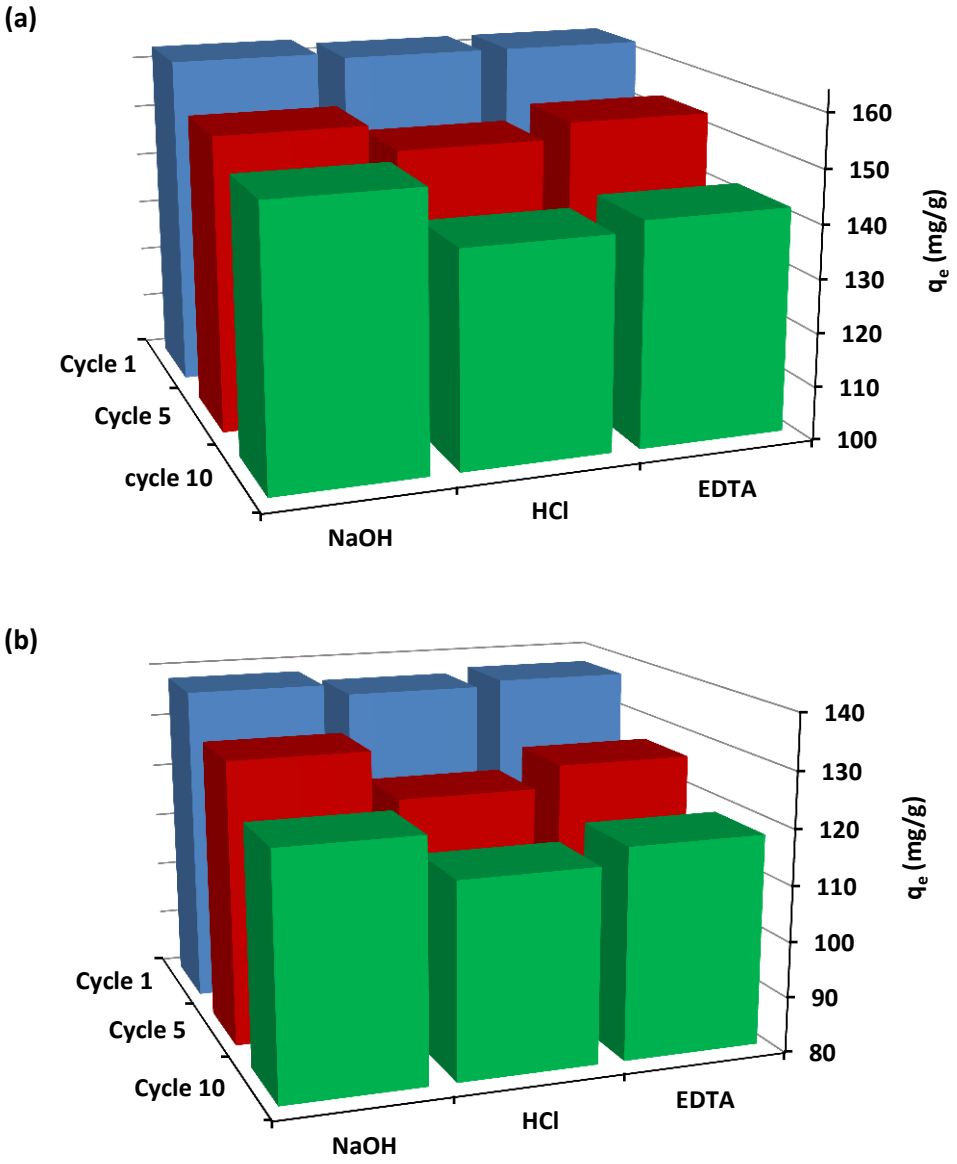

Figure 5-13 Adsorption-desorption cycles of the prepared CSDE beads for (a) Pb(II) adsorption, (b) Ni(II) adsorption (C_0 = 400 mg/L, T = 25 ^oC , contact time = 300 min, pH = 7 for Pb(II), pH = 6 for Ni(II)).

5.5 Conclusions

In this study, we have successfully prepared chitosan- diatomaceous earth (CSDE) beads as alternative adsorbent for heavy metals removal from aqueous solution. Adsorption attained equilibrium in about 200 min and it was highly depended on the

initial metal concentration and solution-pH. The optimum pH values after pH-affected experiments were found 7 for Pb(II) and 6 for Ni(II) adsorption. Langmuir isotherm model was found to be the best fit of the experimental data and the maximum saturation monolayer adsorption capacities were 175.22 mg Pb(II)/g and 149.64 mg Ni(II)/g onto CSDE beads. The adsorption kinetics followed the pseudo-second-order equation for both metal ions. NaOH was found to be the best solution for the regeneration of the CSDE beads with more than 92% for Pb(II) and 89% for Ni(II) in tenth adsorption-desorption cycle. The foreign ions in the solution affected on Ni(II) greater than Pb(II) adsorption capacity. According to the competitive adsorption studies, the CSDE beads had the highest affinity for Pb(II) ions and the lowest affinities for Ni(II) ions. The aforementioned results established that the prepared CSDE beads can be used confidently as the promising and cost-effective adsorbent for selectively heavy metals removal from the wastewater.

CHAPTER 6. CONCLUSIONS AND FUTURE WORK

6.1 Conclusions of the Present Research

Chitosan and diatomaceous earth are highly abundant, non-toxic, and biocompatible in nature. In this work, chitosan was coated successfully with diatomaceous earth and prepared as spherical beads of average diameter approximately 2 mm. The chitosan-coated diatomaceous earth beads were examined to study the aqueous phase adsorption of zinc, chromium, lead, and nickel in both competitive and non-competitive mode.

The BET data showed that the prepared CSDE beads have a high surface area, 14.4 m^2/g compared to the pristine chitosan, 1.9 m^2/g. The SEM and EDS analysis showed that the CSDE beads were highly porous and the exposed adsorbents to the heavy metals solution have relatively high percentages, 7.73% for Zn(II), 7.53% for Cr(VI), 9.42 for Pb(II), and 7.97% for Ni(II), which indicates a high adsorption capacity of prepared adsorbent. The FTIR results indicated that the adsorption mechanism could mainly be the inner sphere complexation between the active site groups (amine and hydroxyl), and the heavy metal ions.

The chitosan-coated diatomaceous earth (CSDE) beads had the strongest affinity to Pb(II) and Ni(II) ions superior to Cr(VI) and Zn(II) ions. According to the analysis of adsorbent surface properties at different solution-pH, the prepared adsorbents have zero potential charge (pH_{ZPC}) at 5.8 and negative surface charge at pH greater than the pH_{ZPC}, due to the deprotonation of amine groups. That means the cations heavy metals are preferably adsorbed at pH greater than 5.8. In the batch mode, after parameters were optimized, the results of isotherm and kinetic studies showed that the Langmuir isotherm (monolayer coverage of heavy metal ions onto prepared adsorbent) and pseudo-second-order kinetic model (the adsorption purely takes place

on external diffusion controlled mechanism) have a good correlation with all studied heavy metals adsorption onto CSDE beads. The negative thermodynamic parameter values (ΔH°, ΔS°, and ΔG°) indicated that the adsorption process of all heavy metals onto prepared adsorbents was spontaneous, exothermic, suitable, random, and the beads surface was energetically homogeneous, that means the metal ion removal decreased with increasing in the temperature.

Ten consecutive adsorption-desorption processes demonstrated that the prepared CSDE beads show excellent desorption performance and reusability, through a reduction in adsorption capacity of 8 % for Pb(II) and 11 % for Ni(II) in the tenth cycle, 13 % for Zn(II) in the fourth cycle, and 14.3 % for Cr(VI) in the fifth cycle using NaOH solution as a reagent. The coexisting anions/cations effect of wastewater on the removal efficiency of heavy metals was significant, the adsorption capacity was reduced by about 46.4 %, 7 % and 19.27 % for Ni(II), Zn(II), and Cr(VI), respectively, in the presence of these ions. The initial metal concentration and solution-pH had a significant impact on the adsorption capacity of prepared CSDE beads. A high removal capacity was observed and it was increased with increasing the initial metal concentration and contact times, but it was decreased by increasing the temperature and solution-pH at pH greater than 7 for Pb(II), Ni(II), and Zn(II). The highest Zn(II) ion uptake capacity onto prepared CCDE beads was 127.23 mg Zn(II)/g at pH 6, initial concentration 500 mg/L, contact time 130 min, and temperature 10 °C. The highest Cr(VI) uptake capacity was 84 mg Cr(VI)/g at pH 3, initial concentration 500 mg/L, contact time 210 min, and temperature 10 °C. The highest uptake capacities of Pb(II) and NI(II) were 175.22 mg Pb(II)/g at pH 7 and 149.64 mg Ni(II)/g at pH 6, temperature 25 °C, initial concentration 1000 mg/L, and contact time 180 min onto CSDE beads. Breakthrough data from contentious bed

column showed that the flow rate of solution had a significant effect on adsorption capacity of Zn(II) ions and exhausted time of adsorbent, the exhausted time was decreased from 335 to 115 min when the flow rate of solution increased from 3 to 6 ml/min, respectively. Finally, this study indicates that the modified chitosan by diatomaceous earth could serve as a viable low-cost potential adsorbent for the removal of heavy metal ions from aqueous solution in batch and continuous column mode.

6.2 Recommendations for Further Research

The knowledge and insights gained from the adsorption of heavy metals onto a new prepared sustainable adsorbent in this research paved the way further studies by providing a better understanding of adsorbent characterization and adsorption process. First, studying the adsorption of other types of pollutants such as dyes and phenols, using the same prepared CSDE beads. Second, using the prepared CSDE beads in real industrial wastewater adsorption to evaluate the feasibility of new adsorbent for practical applications. Third, modified chitosan chemically beside the physical modification to enhance some of the other properties of prepared CSDE beads such as enhancing the stability in highly acidic media and reducing the gel formation. Fourth, using the X-ray photoelectron spectroscopy (XPS) technique to characterize the prepared CSDE beads, which could give more useful information about the mechanism of blending chitosan/diatomaceous earth composite, and about the interacting mechanism of adsorbing metals onto active site groups. Fifth, evaluating the impact of increasing the adsorbent dose, agitator speed, and ionic strength on the adsorption behavior of heavy metals onto CSDE beads. Sixth, predicting some of the final properties of the prepared CSDE beads such as the mechanical strength,

swelling, and agglomeration and finally developing mathematical models for simulating the adsorption process.

BIBLIOGRAPHY

[1] Chintana, S., Removal of heavy metals from waste water by adsorption using chitosan. Master thesis, Suranaree University of Technology, 2002.

[2] Zhang, H., Dang, Q., Liu, C., Cha, D., Yu, Z., Zhu, W., Fan, B., Uptake of Pb(II) and Cd(II) on chitosan microsphere surface successively grafted by methyl acrylate and diethylenetriamine. ACS Applied Materials & Interfaces. 2017, 9(12), 11144-11155.

[3] Patterson, J.W., Industrial wastewater treatment technology. Second edition, Butterworth Publishers, Massachusetts, USA. 1985.

[4] Lu, S., Gibb, S. W., Cochrane, E., Effective removal of zinc ions from aqueous solutions using crab carapace biosorbent. Journal of Hazardous Materials. 2007, 149(1), 208-217.

[5] Li, N., Bai, R., Highly enhanced adsorption of lead ions on chitosan granules functionalized with poly (acrylic acid). Industrial & Engineering Chemistry Research. 2006, 45(23), 7897-7904.

[6] Nuhoglu, Y., Malkoc, E., Thermodynamic and kinetic studies for environmentally friendly Ni(II) biosorption using waste pomace of olive oil factory. Bioresource Technology. 2009, 100(8), 2375-2380.

[7] Bhowmik, D., Chiranjib, K. P., Kumar, S., A potential medicinal importance of zinc in human health and chronic. Journal of Pharmaceutical and Biomedical Sciences. 2010, 1(1), 05-11.

[8] Zhang, L., Zeng, Y., Cheng, Z., Removal of heavy metal ions using chitosan and modified chitosan: A review. Journal of Molecular Liquids. 2016, 214, 175-191.

[9] Gerente, C., Lee, V. K. C., Cloirec, P. L., McKay, G., Application of chitosan for the removal of metals from wastewaters by adsorption-mechanisms and models

review. Critical Reviews in Environmental Science and Technology. 2007, 37(1), 41-127.

[10] Fields, P., Allen, S., Korunic, Z., McLaughlin, A., Stathers, T., Standardised testing for diatomaceous earth. In Advances in stored products protection. Proceedings of the eighth international working conference on stored product protection. CABI International, Wallingford. 2003, 779-784.

[11] Caner, N., Sarı, A., Tüzen, M., Adsorption characteristics of mercury (II) ions from aqueous solution onto chitosan-coated diatomite. Industrial & Engineering Chemistry Research. 2015, 54(30), 7524-7533.

[12] Bailey, S. E., Olin, T. J., Bricka, R. M., Adrian, D. D., A review of potentially low-cost sorbents for heavy metals. Water Research. 1999, 33(11), 2469-2479.

[13] Förstner, U., Wittmann, G. T., Metal pollution in the aquatic environment. Springer Science & Business Media. 2012.

[14] Fu, F., Wang, Q., Removal of heavy metal ions from wastewaters: a review. Journal of Environmental Management. 2011, 92(3), 407-418.

[15] Ko, D., Lee, J.S., Patel, H.A., Jakobsen, M.H., Hwang, Y., Yavuz, C.T., Hansen, H.C.B., Andersen, H.R., Selective removal of heavy metal ions by disulfide linked polymer networks. Journal of Hazardous Materials. 2017, 332, 140-148.

[16] Shen, F., Su, J., Zhang, X., Zhang, K., Qi, X., Chitosan-derived carbonaceous material for highly efficient adsorption of chromium (VI) from aqueous solution. International Journal of Biological Macromolecules. 2016, 91, 443-449.

[17] Li, L., Li, Y., Cao, L., Yang, C., Enhanced chromium (VI) adsorption using nanosized chitosan fibers tailored by electrospinning. Carbohydrate Polymers. 2015, 125, 206-213.

[18] Shrestha, S., Son, G., Lee, S. H., Lee, T. G., Isotherm and thermodynamic studies of Zn(II) adsorption on lignite and coconut shell-based activated carbon fiber. Chemosphere. 2013, 92(8), 1053-1061.

[19] Anitha, T., Senthil Kumar, P., Sathish Kumar, K., Binding of Zn(II) ions to chitosan–PVA blend in aqueous environment: adsorption kinetics and equilibrium studies. Environmental Progress & Sustainable Energy. 2015, 34(1), 15-22.

[20] Al Akeel, K., Empirical investigation of water pollution control through use of phragmites australis. Doctoral dissertation, Brunel University School of Engineering and Design, PhD Theses. 2013.

[21] Moazeni, M., Ebrahimi, A., Rafiei, N., Pourzamani, H. R., Removal of lead ions from aqueous solution by nano zero-valent iron (nZVI). Health Scope. 2017, 6(2).

[22] Ceballos Quintana, J., Bio-sorption of heavy metals from wastewater by using marine biomass wastes. Doctoral dissertation, Memorial University of Newfoundland. 2014.

[23] Congeevaram, S., Dhanarani, S., Park, J., Dexilin, M., Thamaraiselvi, K., Biosorption of chromium and nickel by heavy metal resistant fungal and bacterial isolates. Journal of Hazardous Materials. 2007, 146(1-2), 270-277.

[24] https://www.lenntech.com/periodic/elements/ni.htm#ixzz54f2s0eO1.

[25] Muzzarelli, R. A., Natural chelating polymers; alginic acid, chitin and chitosan. In natural chelating polymers; alginic acid, chitin and chitosan. Pergamon Press. 1973.

[26] Hasan, M., Development of materials for the removal of metal ions from radioactive and non-radioactive waste streams. 2005.

[27] NAN, L., Study of chitosan-based biopolymer adsorbents and their applications in heavy metal removal. Doctoral dissertation. 2007.

[28] Khairkar, S. R., Raut, A. R., Adsorption studies for the removal heavy metal by chitosan-g-poly (acrylicacid-co-acrylamide) composite. Science. 2014, 2(6), 67-70.

[29] Wang, X., Deng, W., Xie, Y., Wang, C., Selective removal of mercury ions using a chitosan–poly (vinyl alcohol) hydrogel adsorbent with three-dimensional network structure. Chemical Engineering Journal. 2013, 228, 232-242.

[30] Wan, M. W., Kan, C. C., Rogel, B. D., Dalida, M. L. P., Adsorption of copper (II) and lead (II) ions from aqueous solution on chitosan-coated sand. Carbohydrate Polymers. 2010, 80(3), 891-899.

[31] Hasan, S., Ghosh, T. K., Viswanath, D. S., Boddu, V. M., Dispersion of chitosan on perlite for enhancement of copper (II) adsorption capacity. Journal of Hazardous Materials. 2008, 152(2), 826-837.

[32] Tirtom, V. N., Dinçer, A., Becerik, S., Aydemir, T., Çelik, A., Comparative adsorption of Ni(II) and Cd(II) ions on epichlorohydrin crosslinked chitosan–clay composite beads in aqueous solution. Chemical Engineering Journal. 2012, 197, 379-386.

[33] Futalan, C. M., Kan, C. C., Dalida, M. L., Hsien, K. J., Pascua, C., Wan, M. W., Comparative and competitive adsorption of copper, lead, and nickel using chitosan immobilized on bentonite. Carbohydrate Polymers. 2011, 83(2), 528-536.

[34] Wan, M. W., Kan, C. C., Rogel, B. D., & Dalida, M. L. P., Adsorption of copper (II) and lead (II) ions from aqueous solution on the chitosan-coated sand. Carbohydrate Polymers. 2010, 80(3), 891-899.

[35] Futalan, C. M., Kan, C. C., Dalida, M. L., Hsien, K. J., Pascua, C., & Wan, M. W., Comparative and competitive adsorption of copper, lead, and nickel using chitosan immobilized on bentonite. Carbohydrate Polymers. 2011, 83(2), 528-536.

[36] Paulino, A. T., Belfiore, L. A., Kubota, L. T., Muniz, E. C., Almeida, V. C., & Tambourgi, E. B., Effect of magnetite on the adsorption behavior of Pb (II), Cd (II), and Cu (II) in chitosan-based hydrogels. Desalination. 2011, 275(1-3), 187-196.

[37] Sargın, İ., & Arslan, G., Chitosan/sporopollenin microcapsules: Preparation, characterisation and application in heavy metal removal. International journal of biological macromolecules. 2015, 75, 230-238.

[38] Min, L. L., Yuan, Z. H., Zhong, L. B., Liu, Q., Wu, R. X., & Zheng, Y. M., Preparation of chitosan-based electrospun nanofiber membrane and its adsorptive removal of arsenate from aqueous solution. Chemical Engineering Journal. 2015, 267, 132-141.

[39] Nithya, R., Gomathi, T., Sudha, P. N., Venkatesan, J., Anil, S., & Kim, S. K., Removal of Cr(VI) from aqueous solution using chitosan-g-poly (butyl acrylate)/silica gel nanocomposite. International journal of biological macromolecules. 2016, 87, 545-554.

[40] Tsai, W. T., Lai, C. W., Hsien, K. J., Characterization and adsorption properties of diatomaceous earth modified by hydrofluoric acid etching. Journal of Colloid and Interface Science. 2006, 297(2), 749-754.

[41] Min, L. L., Yuan, Z. H., Zhong, L. B., Liu, Q., Wu, R. X, Zheng, Y. M., Preparation of chitosan-based electrospun nanofiber membrane and its adsorptive removal of arsenate from aqueous solution. Chemical Engineering Journal. 2015, 267, 132-141.

[42] Sakti, S. C. W., Development of magnetic separation using modified magnetic chitosan for removal of pollutants in solution. 2015.

[43] Jain, C. K., Singhal, D. C., Sharma, M. K., Adsorption of zinc on bed sediment of River Hindon: adsorption models and kinetics. Journal of Hazardous Materials. 2004, 114(1), 231-239.

[44] Hua, M., Zhang, S., Pan, B., Zhang, W., Lv, L., Zhang, Q., Heavy metal removal from water/wastewater by nanosized metal oxides: a review. Journal of Hazardous Materials. 2012, 211, 317-331.

[45] Babel, S., Kurniawan, T. A., Low-cost adsorbents for heavy metals uptake from contaminated water: a review. Journal of Hazardous Materials. 2003, 97(1), 219-243.

[46] Pandey, A., Bera, D., Shukla, A., Ray, L., Studies on Cr(VI), Pb(II) and Cu(II) adsorption-desorption using calcium alginate as biopolymer. Chemical Speciation & Bioavailability. 2007, 19(1), 17-24.

[47] Ghimire, K. N., Inoue, K., Ohto, K, Hayashida, T., Adsorption study of metal ions onto cross-linked seaweed Laminaria japonica. Bioresource technology. 2008, 99(1), 32-37.

[48] Ricordel, S., Taha, S., Cisse, I., Dorange, G., Heavy metals removal by adsorption onto peanut husks carbon: characterization, kinetic study, and modeling. Separation and Purification Technology. 2001, 24(3), 389-401.

[49] Ozer, A., Tumen, F., Cu(II) adsorption from aqueous solutions on sugar beet pulp carbon. The European Journal of Mineral Processing and Environmental Protection. 2005, 5(1), 26-34.

[50] Zhao, F., Repo, E., Yin, D., Sillanpää, M. E., Adsorption of Cd(II) and Pb(II) by a novel EGTA-modified chitosan material: Kinetics and isotherms. Journal of Colloid and Interface Science. 2013, 409, 174-182.

[51] Ngah, W. W., Ab Ghani, S., Kamari, A., Adsorption behavior of Fe(II) and Fe(III) ions in aqueous solution on chitosan and cross-linked chitosan beads. Bioresource Technology. 2005, 96(4), 443-450.

[52] Jagtap, S., Thakre, D., Wanjari, S., Kamble, S., Labhsetwar, N., Rayalu, S., New modified chitosan-based adsorbent for defluoridation of water. Journal of Colloid and Interface Science. 2009, 332(2). 280-290.

[53] Annaduzzaman, M., Chitosan biopolymer as an adsorbent for drinking water treatment: Investigation on Arsenic and Uranium. Doctoral dissertation, KTH Royal Institute of Technology. 2015.

[54] Toledo, T. V., Bellato, C. R., Souza, C. H., Domingues, J. T., Silva, D. D. C., Reis, C., Fontes, M. P. F., Preparation and evaluation of magnetic chitosan particles modified with ethylenediamine and Fe(III) for the removal of Cr(VI) from aqueous solutions. Química Nova. 2014, 37(10), 1610-1617.

[55] Sofiane, B., Sofia, K. S., Biosorption of heavy metals by chitin and the chitosan. Der Pharma Chemica. 2015, 7: 54-63.

[56] Qudsieh, I. Y., Mirghani, E. S., Kabbashi, N. A., Muyibi, S. A., Central composite design of zinc removal from model water using chitosan biopolymer. Advances in Environmental Biology. 2014, 658-667.

[57] Zhou, T., Li, C., Jin, H., Lian, Y., Han, W. (2017). Effective adsorption/reduction of Cr(VI) oxyanion by halloysite@ polyaniline hybrid nanotubes. ACS Applied Materials & Interfaces. 2017, 9(7), 6030-6043.

[58] Nieto, J. M., Peniche Covas, C., Padro, G., Characterization of chitosan by pyrolysis-mass spectrometry, thermal analysis, and differential scanning calorimetry. Thermochimica Acta. 1991, 176, 63-68.

[59] Neto, C. D. T., Giacometti, J. A., Job, A. E., Ferreira, F. C., Fonseca, J. L. C., Pereira, M. R., Thermal analysis of chitosan-based networks. Carbohydrate Polymers. 2005, 62(2), 97-103.

[60] Qi, L, Xu, Z., Jiang, X., Hu, C., Zou, X., Preparation and antibacterial activity of chitosan nanoparticles. Carbohydrate Research. 2004, 339(16), 2693-2700.

[61] Arvand, M., Pakseresht, M. A., Cadmium adsorption on modified chitosan-coated bentonite: batch experimental studies. Journal of Chemical Technology and Biotechnology. 2013, 88(4), 572-578.

[62] Hu, X. J., Wang, J. S., Liu, Y. G., Li, X., Zeng, G. M., Bao, Z. L., Long, F., Adsorption of chromium (VI) by ethylenediamine-modified cross-linked magnetic chitosan resin: isotherms, kinetics, and thermodynamics. Journal of Hazardous Materials. 2011, 185(1), 306-314.

[63] Malkoc, E., Nuhoglu, Y., Dundar, M., Adsorption of chromium (VI) on panacea olive oil industry waste: batch and column studies. Journal of Hazardous Materials. 2006, 138(1), 142-151.

[64] Karthikeyan, G., Anbalagan, K., Andal, N. M., Adsorption dynamics and equilibrium studies of Zn(II) onto chitosan. Journal of Chemical Sciences. 2004, 116(2), 119-127.

[65] Saha, P., Chowdhury, S., Insight into adsorption thermodynamics. INTECH Open Access Publisher. 2011.

[66] Tellinghuisen, J., Van't Hoff analysis of K°(T): How good… or bad?. Biophysical Chemistry. 2006, 120(2), 114-120.

[67] Salih, S. S., Ghosh, T. K., Adsorption of Zn(II) ions by chitosan coated diatomaceous earth. International Journal of Biological Macromolecules. 2018, 106, 602-610.

[68] Aydın, Y. A., Aksoy, N. D., Adsorption of chromium on chitosan: Optimization, kinetics, and thermodynamics. Chemical Engineering Journal. 2009, 151(1), 188-194.

[69] Hawari, A., Rawajfih, Z., Nsour, N., Equilibrium and thermodynamic analysis of zinc ions adsorption by olive oil mill solid residues. Journal of Hazardous Materials. 2009, 168(2), 1284-1289.

[70] Doke, K. M., Khan, E. M., Adsorption thermodynamics to clean up wastewater; a critical review. Reviews in Environmental Science and Bio/Technology. 2013, 12(1), 25-44.

[71] Ho, Y. S., McKay, G., Sorption of dye from aqueous solution by peat. Chemical Engineering Journal. 1998, 70(2), 115-124.

[72] Ho, Y. S., McKay, G., Pseudo-second order model for sorption processes. Process Biochemistry. 1999, 34(5), 451-465.

[73] Chou W. L., Wang C. T., Chang W. C., Chang S. Y., Adsorption treatment of oxide chemical mechanical polishing wastewater from a semiconductor manufacturing plant by electrocoagulation. Journal of Hazardous Material. 2010, 180(1), 217-224.

[74] Vaz, M.G., Pereira, A.G., Fajardo, A.R., Azevedo, A.C., Rodrigues, F.H., Methylene blue adsorption on chitosan-g-poly (acrylic acid)/rice husk ash superabsorbent composite: kinetics, equilibrium, and thermodynamics. Water, Air, & Soil Pollution. 2017, 228(1), 14.

[75] Ennigrou, D. J., Ali, M. B. S., Dhahbi, M., Copper and zinc removal from aqueous solutions by polyacrylic acid assisted-ultrafiltration. Desalination. 2014, 343, 82-87.

[76] Charerntanyarak, L., Heavy metals removal by chemical coagulation and precipitation. Water Science and Technology. 1999, 39(10-11), 135-138.

[77] Rengaraj, S., Yeon, K. H., Moon, S. H., Removal of chromium from water and wastewater by ion exchange resins. Journal of Hazardous Materials. 2001, 87 (1-3), 273-287.

[78] Malaeb, L., Ayoub, G. M., Reverse osmosis technology for water treatment: state of the art review. Desalination. 2011, 267(1), 1-8.

[79] Tang, X., Zheng, H., Teng, H., Sun, Y., Guo, J., Xie, W., Yang, Q., Chen, W., Chemical coagulation process for the removal of heavy metals from water: a review. Desalination and Water Treatment. 2016, 57(4),1733-1748.

[80] Trivunac, K., Stevanovic, S., Removal of heavy metal ions from water by complexation-assisted ultrafiltration. Chemosphere. 2006, 64(3), 486-491.

[81] Ferhat, M., Kadouche, S., Drouiche, N., Messaoudi, K., Messaoudi, B., Lounici, H., Competitive adsorption of toxic metals on bentonite and use of chitosan as flocculent coagulant to speed up the settling of generated clay suspensions. Chemosphere. 2016, 165, 87-93.

[82] Baran, A., Bıçak, E., Baysal, Ş. H., Önal, S., Comparative studies on the adsorption of Cr(VI) ions on to various sorbents. Bioresource technology. 2007, 98(3), 661-665.

[83] Mishra, V., Biosorption of zinc ion: a deep comprehension. Applied Water Science. 2014, 4(4), 311-332.

[84] Xie, J., Li, C., Chi, L., Wu, D., Chitosan modified zeolite as a versatile adsorbent for the removal of different pollutants from water. Fuel. 2013, 103, 480-485.

[85] Li, Z., Li, T., An, L., Fu, P., Gao, C., Zhang, Z., Highly efficient chromium (VI) adsorption with nanofibrous filter paper prepared through electrospinning chitosan/polymethylmethacrylate composite. Carbohydrate polymers. 2016, 137, 119-126.

[86] Chauhan, D., Jaiswal, M., Sankararamakrishnan, N., Removal of cadmium and hexavalent chromium from electroplating waste water using thiocarbamoyl chitosan. Carbohydrate Polymers. 2012, 88(2), 670-675.

[87] Ge, H., Ma, Z., Microwave preparation of triethylenetetramine modified graphene oxide/chitosan composite for adsorption of Cr(VI). Carbohydrate Polymers. 2015, 131, 280-287.

[88] Ngah, W. W., Teong, L. C., Hanafiah, M. A. K. M., Adsorption of dyes and heavy metal ions by chitosan composites: A review. Carbohydrate Polymers. 2011, 83(4), 1446-1456.

[89] Kyzas, G. Z., Bikiaris, D. N., Recent modifications of chitosan for adsorption applications: a critical and systematic review. Marine Drugs. 2015, 13(1), 312-337.

[90] Sargın, İ., Arslan, G., Chitosan/sporopollenin microcapsules: Preparation, characterisation and application in heavy metal removal. International Journal of Biological Macromolecules. 2015, 75, 230-238.

[91] Vieira, R.S., Meneghetti, E., Baroni, P., Guibal, E., de la Cruz, V.M.G., Caballero, A., Rodríguez-Castellón, E., Beppu, M.M., Chromium removal on chitosan-based sorbents–An EXAFS/XANES investigation of mechanism. Materials Chemistry and Physics. 201, 146(3) 412-417.

[92] Ramnani, S. P., Sabharwal, S., Adsorption behavior of Cr(VI) onto radiation crosslinked chitosan and its possible application for the treatment of wastewater containing Cr(VI). Reactive and Functional Polymers. 2006, 66(9), 902-909.

[93] Kyzas, G. Z., Siafaka, P. I., Pavlidou, E. G., Chrissafis, K. J., Bikiaris, D. N., Synthesis and adsorption application of succinyl-grafted chitosan for the simultaneous removal of zinc and cationic dye from binary hazardous mixtures. Chemical Engineering Journal. 2015, (259) 438-448.

[94] Ahmad, M. F., Haydar, S., Quraishi, T. A., Enhancement of biosorption of zinc ions from aqueous solution by immobilized Candida utilis and Candida tropicalis cells. International Biodeterioration & Biodegradation. 2013,(83) 119-128.

[95] Adamczuk, A., Kołodyńska, D., Equilibrium, thermodynamic and kinetic studies on removal of chromium, copper, zinc and arsenic from aqueous solutions onto fly ash coated by chitosan. Chemical Engineering Journal. 2015, (274) 200-212.

[96] Calagui, M. J. C., Senoro, D. B., Kan, C. C., Salvacion, J. W., Futalan, C. M., Wan, M. W., Adsorption of indium (III) ions from aqueous solution using chitosan-coated bentonite beads. Journal of Hazardous Materials. 2014, (277) 120-126.

[97] Vaiopoulou, E., Gikas, P., Effects of chromium on activated sludge and on the performance of wastewater treatment plants: a review. Water Research. 2012, 46(3) 549-570.

[98] Rouquerol J, Rouquerol F, Llewellyn P, Maurin G, Sing KS., Adsorption by powders and porous solids: principles, methodology, and applications, 2nd edition, Academic press, 2012. eBook ISBN: 9780080970363.

[99] Han, X., Wong, Y. S., Wong, M. H., Tam, N. F. Y., Effects of anion species and concentration on the removal of Cr(VI) by a microalgal isolate, Chlorella miniata. Journal of Hazardous Materials. 2008, 158(2-3), 615-620.

[100] Salih S.S., Ghosh T.K., Preparation and characterization of bioadsorbent beads for chromium and zinc ions adsorption. Cogent Environmental Science. 2017, 3: 1401577.

[101] Jung, C., Heo, J., Han, J., Her, N., Lee, S.J., Oh, J., Ryu, J., Yoon, Y., Hexavalent chromium removal by various adsorbents: powdered activated carbon, chitosan, and single/multi-walled carbon nanotubes. Separation and Purification Technology. 2013, (106) 63-71.

[102] Zhao, F., Repo, E., Yin, D., Chen, L., Kalliola, S., Tang, J., Iakovleva, E., Tam, K.C., Sillanpää, M., One-pot synthesis of trifunctional chitosan-EDTA-β-cyclodextrin polymer for simultaneous removal of metals and organic micropollutants. Scientific Reports. 2017, 7(1) 15811.

[103] Muzzarelli, R. A., Chitosan composites with inorganics, morphogenetic proteins and stem cells, for bone regeneration. Carbohydrate Polymers. 2011, 83(4), 1433-1445.

[104] Salih, S. S., Ghosh, T. K., Highly efficient competitive removal of Pb(II) and Ni(II) by chitosan/diatomaceous earth composite. Journal of Environmental Chemical Engineering. 2018, 6(1), 435-443.

[105] Hu, P., Wang, J., Huang, R., Simultaneous removal of Cr(VI) and Amido black 10B (AB10B) from aqueous solutions using quaternized chitosan coated bentonite. International Journal of Biological Macromolecules. 2016, (92) 694-701.

[106] Boddu, V. M., Abburi, K., Talbott, J. L., Smith, E. D., Removal of hexavalent chromium from wastewater using a new composite chitosan biosorbent. Environmental Science & Technology. 2003, 37(19) 4449-4456.

[107] Chen, D., Li, W., Wu, Y., Zhu, Q., Lu, Z., Du, G., Preparation and characterization of chitosan/montmorillonite magnetic microspheres and its application for the removal of Cr(VI). Chemical Engineering Journal. 2013, (221) 8-15.

[108] Hasan, S., Krishnaiah, A., Ghosh, T. K., Viswanath, D. S., Boddu, V. M., Smith, E. D., Adsorption of chromium (VI) on chitosan-coated perlite. Separation Science and Technology. 2003, 38(15) 3775-3793.

[109] de Almeida, F. T. R., Ferreira, B. C. S., Moreira, A. L. D. S. L., de Freitas, R. P., Gil, L. F., Gurgel, L. V. A. (2016). Application of a new bifunctionalized chitosan derivative with zwitterionic characteristics for the adsorption of Cu^{2+}, Co^{2+}, Ni^{2+}, and oxyanions of Cr^{6+} from aqueous solutions: Kinetic and equilibrium aspects. Journal of Colloid and Interface Science. 2016, (466) 297-309.

[110] Dash, S., Chaudhuri, H., Gupta, R., Nair, U. G., Sarkar, A., Fabrication and application of low-cost thiol functionalized coal fly ash for selective adsorption of heavy toxic metal ions from water. Industrial & Engineering Chemistry Research. 2017, 56(6) 1461-1470.

[111] Zhao, F., Repo, E., Meng, Y., Wang, X., Yin, D., Sillanpää, M., An EDTA-β-cyclodextrin material for the adsorption of rare earth elements and its application in preconcentration of rare earth elements in seawater. Journal of Colloid and Interface Science. 2016, (465) 215-224.

[112] Xiong, Y., Cui, X., Zhang, P., Wang, Y., Lou, Z., Shan, W., Improving Re(VII) adsorption on diisobutylamine-functionalized graphene oxide. ACS Sustainable Chemistry & Engineering. 2016, 5(1) 1010-1018.

[113] Wang, W., Zhou, J., Achari, G., Yu, J., Cai, W., Cr(VI) removal from aqueous solutions by hydrothermal synthetic layered double hydroxides: adsorption performance, coexisting anions and regeneration studies. Colloids and Surfaces A: Physicochemical and Engineering Aspects. 2014, (457) 33-40.

[114] Jorgetto, A.D.O., da Silva, A.C., Wondracek, M.H., Silva, R.I., Velini, E.D., Saeki, M.J., Pedrosa, V.A., Castro, G.R., Multilayer adsorption of Cu(II) and Cd(II) over Brazilian Orchid Tree (Pata-de-vaca) and its adsorptive properties. Applied Surface Science. 2015, (345) 81-89.

[115] d'Halluin, M., Rull-Barrull, J., Bretel, G., Labrugère, C., Le Grognec, E., Felpin, F. X., Chemically modified cellulose filter paper for heavy metal remediation in water. ACS Sustainable Chemistry & Engineering. 2017, 5(2), 1965-1973.

[116] Ronteltap, M., Maurer, M., Gujer, W., The behaviour of pharmaceuticals and heavy metals during struvite precipitation in urine. Water Research. 2007, 41(9), 1859-1868.

[117] Chen, C., Huang, D., Liu, J. (2009). Functions and toxicity of nickel in plants: recent advances and future prospects. CLEAN-Soil, Air, Water. 2009, 37(4-5), 304-313.

[118] Mahmoud, M. E., Amira, M. F., Seleim, S. M., Mohamed, A. K., Adsorption isotherm models, kinetics study, and thermodynamic parameters of Ni(II) and Zn(II) removal from water using the LbL technique. Journal of Chemical & Engineering Data. 2017, 62(2), 839-850.

[119] Alomá, I., Martín-Lara, M. A., Rodríguez, I. L., Blázquez, G., Calero, M., Removal of nickel (II) ions from aqueous solutions by biosorption on sugarcane bagasse. Journal of the Taiwan Institute of Chemical Engineers. 2012, 43(2), 275-281.

[120] Guo, Z., Zhang, X., Kang, Y., Zhang, J., Biomass-derived carbon sorbents for Cd (II) removal: activation and adsorption mechanism. ACS Sustainable Chemistry & Engineering. 2017, 5(5), 4103-4109.

[121] Bée, A., Obeid, L., Mbolantenaina, R., Welschbillig, M., Talbot, D., Magnetic chitosan/clay beads: A magsorbent for the removal of cationic dye from water. Journal of Magnetism and Magnetic Materials. 2017, 421, 59-64.

[122] Ramaraju, B., Manoj Kumar Reddy, P., Subrahmanyam, C., Low cost adsorbents from agricultural waste for removal of dyes. Environmental Progress & Sustainable Energy. 2014, 33(1), 38-46.

[123] Pham, T. D., Kobayashi, M., Adachi, Y., Adsorption characteristics of anionic azo dye onto large α-alumina beads. Colloid and Polymer Science. 2015, 293(7), 1877-1886.

[124] Pham, T. D., Kobayashi, M., Adachi, Y., Adsorption of polyanion onto large alpha alumina beads with variably charged surface. Advances in Physical Chemistry. 2014, 2014.

[125] Pham, T. D., Kobayashi, M., Adachi, Y., Adsorption of anionic surfactant sodium dodecyl sulfate onto alpha alumina with small surface area. Colloid and Polymer Science. 2015, 293(1) 217-227.

[126] Kumari, H. J., Krishnamoorthy, P., Arumugam, T. K., Radhakrishnan, S., Vasudevan, D., An efficient removal of crystal violet dye from waste water by adsorption onto TLAC/Chitosan composite: A novel low cost

adsorbent. International Journal of Biological Macromolecules. 2017, 96, 324-333.

[127] Shaker, M. A., Equilibrium, kinetics and thermodynamics studies of chitosan-based solid phase nanoparticles as sorbent for lead (II) cations from aqueous solution. Materials Chemistry and Physics. 2015, (162) 580-591.

[128] Zhu, Y., Hu, J., Wang, J., Competitive adsorption of Pb(II), Cu(II) and Zn(II) onto xanthate-modified magnetic chitosan. Journal of Hazardous Materials. 2012, (221) 155-161.

[129] Wang, N., Xu, X., Li, H., Yuan, L., Yu, H., Enhanced selective adsorption of Pb(II) from aqueous solutions by one-pot synthesis of xanthate-modified chitosan sponge: behaviors and mechanisms. Industrial & Engineering Chemistry Research. 2016, 55(47), 12222-12231.

[130] Anitha, T., Kumar, P. S., Kumar, K. S., Ramkumar, B., Ramalingam, S., Adsorptive removal of Pb(II) ions from polluted water by newly synthesized chitosan–polyacrylonitrile blend: equilibrium, kinetic, mechanism and thermodynamic approach. Process Safety and Environmental Protection. 2015, (98) 187-197.

[131] Wang, Y., Li, L., Luo, C., Wang, X., Duan, H., Removal of Pb^{2+} from water environment using a novel magnetic chitosan/graphene oxide imprinted Pb^{2+}. International Journal of Biological Macromolecules. 2016, (86) 505-511.

[132] Liu, B., Chen, W., Peng, X., Cao, Q., Wang, Q., Wang, D., Meng, X., Yu, G., Biosorption of lead from aqueous solutions by ion-imprinted tetraethylenepentamine modified chitosan beads. International Journal of Biological Macromolecules. 2016, (86) 562-569.

[133] Ngah, W. W., Fatinathan, S., Adsorption characterization of Pb(II) and Cu(II) ions onto chitosan-tripolyphosphate beads: kinetic, equilibrium and thermodynamic studies. Journal of Environmental Management. 2010, 91(4), 958-969.

[134] Monier, M., Ayad, D. M., Wei, Y., Sarhan, A. A., Adsorption of Cu(II), Co(II), and Ni(II) ions by modified magnetic chitosan chelating resin. Journal of Hazardous Materials. 2010, 177(1-3), 962-970.

[135] Zhou, L., Wang, Y., Liu, Z., Huang, Q. (2009). Characteristics of equilibrium, kinetics studies for adsorption of Hg(II), Cu(II), and Ni(II) ions by thiourea-modified magnetic chitosan microspheres. Journal of Hazardous Materials. 2009, 161(2-3), 995-1002.

[136] Nguyen, M. L., Huang, C., Juang, R. S., Synergistic biosorption between phenol and nickel (II) from Binary mixtures on chemically and biologically modified chitosan beads. Chemical Engineering Journal. 2016, (286) 68-75.

[137] Popuri, S. R., Vijaya, Y., Boddu, V. M., Abburi, K., Adsorptive removal of copper and nickel ions from water using chitosan coated PVC beads. Bioresource technology. 2009, 100(1) 194-199.

[138] Eser, A., Tirtom, V. N., Aydemir, T., Becerik, S., Dinçer, A., Removal of nickel (II) ions by histidine modified chitosan beads. Chemical Engineering Journal. 2012, (210) 590-596.

[139] Vijaya, Y., Popuri, S. R., Boddu, V. M., Krishnaiah, A., Modified chitosan and calcium alginate biopolymer sorbents for removal of nickel (II) through adsorption. Carbohydrate Polymers. 2008, 72(2), 261-271.

[140] Salih, S. S., Ghosh, T. K., Adsorption of Zn(II) ions by chitosan coated diatomaceous earth. International Journal of Biological Macromolecules. 2018, (106) 602-610.

[141] Kuang, S. P., Wang, Z. Z., Liu, J., Wu, Z. C., Preparation of triethylene-tetramine grafted magnetic chitosan for adsorption of Pb(II) ion from aqueous solutions. Journal of Hazardous Materials. 2013, (260) 210-219.

[142] Pham, T. D., Do, T. T., Doan, T. H. Y., Nguyen, T. A. H., Mai, T. D., Kobayashi, M., Adachi, Y., Adsorptive removal of ammonium ion from aqueous solution using surfactant-modified alumina. Environmental Chemistry. 2017, 14(5) 327-337.

[143] Pham, T.D., Nguyen, H.H., Nguyen, N.V., Vu, T.T., Pham, T.N.M., Doan, T.H.Y., Nguyen, M.H., Ngo, T.M.V., Adsorptive removal of copper by using surfactant modified laterite soil. Journal of Chemistry. 2017, 2017.

[144] Xu, D., Tan, X. L., Chen, C. L., Wang, X. K., Adsorption of Pb(II) from aqueous solution to MX-80 bentonite: effect of pH, ionic strength, foreign ions and temperature. Applied Clay Science. 2008, 41(1-2) 37-46.

[145] Yang, S., Li, J., Shao, D., Hu, J., Wang, X., Adsorption of Ni(II) on oxidized multi-walled carbon nanotubes: effect of contact time, pH, foreign ions and PAA. Journal of Hazardous Materials. 2009, 166(1) 109-116.

[146] Li, X., Wang, S., Liu, Y., Jiang, L., Song, B., Li, M., Zeng, G., Tan, X., Cai, X., Ding, Y., Adsorption of Cu(II), Pb(II), and Cd(II) ions from acidic aqueous solutions by diethylenetriaminepentaacetic acid-modified magnetic graphene oxide. Journal of Chemical & Engineering Data. 2016, 62(1) 407-416.

[147] Salih, S.S. and Ghosh, T.K., Preparation and characterization of chitosan-coated diatomaceous earth for hexavalent chromium removal. Environmental Processes. 2017, 1-17.

LIST OF PUBLICATIONS

Salih, Suhaib S., and Tushar K. Ghosh. "Preparation and characterization of bioadsorbent beads for chromium and zinc ions adsorption" Cogent Environmental Science 3.1 (2017): 1401577.

Salih, Suhaib S., and Tushar K. Ghosh. "Adsorption of Zn(II) ions by chitosan coated diatomaceous earth" International journal of biological macromolecules 106 (2018): 602-610.

Salih, Suhaib S., and Tushar K. Ghosh. "Preparation and characterization of chitosan-coated diatomaceous earth for hexavalent chromium removal" Environmental Processes (2017): 1-17.

Salih, Suhaib S., and Tushar K. Ghosh. "Highly efficient competitive removal of Pb(II) and Ni(II) by chitosan/diatomaceous earth composite" Journal of Environmental Chemical Engineering 6.1 (2018): 435-443.

VITA

Suhaib S. Salih was born in Diyala, Iraq. He received his B.S. and M.S. in Chemical Engineering from the University of Tikrit, Iraq. During his Ph.D. study, he published four peer-review journal papers as the first author. Suhaib's research has primarily focused on the experimental study of removing some heavy metals from wastewater streams, using sustainable and low-cost adsorbents.